

อิทธิพลของปัจจัยในการบ่มต่อสมบัติเชิงกลของอีพอกซีเรซินเสริมเส้นใยแก้ว
สำหรับเคลือบคอนกรีตและมอร์ตาร์



นางสาว วิชญา วิชยาภัย นุนนาค

สถาบันวิทยบริการ
จุฬาลงกรณ์มหาวิทยาลัย

วิทยานิพนธ์นี้เป็นส่วนหนึ่งของการศึกษาตามหลักสูตรปริญญาวิศวกรรมศาสตรมหาบัณฑิต

สาขาวิชาวิศวกรรมเคมี ภาควิชาวิศวกรรมเคมี

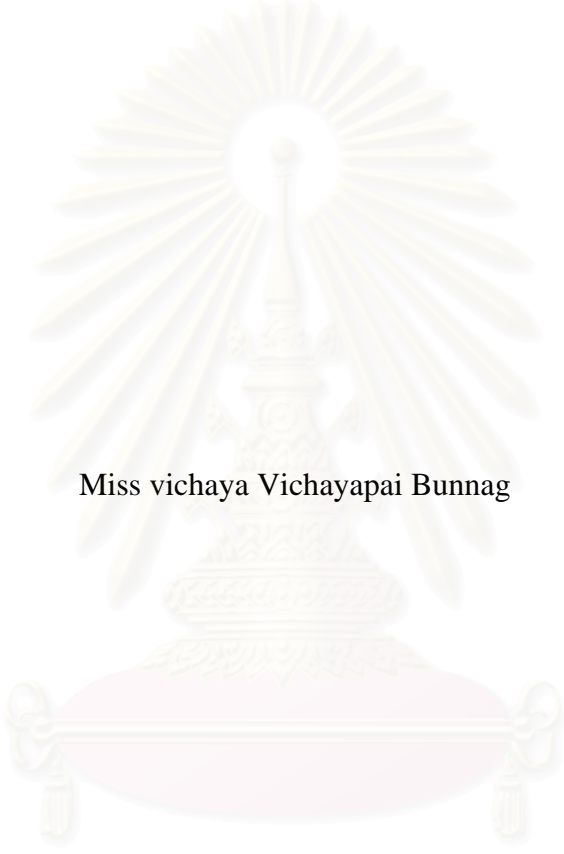
คณะวิศวกรรมศาสตร์ จุฬาลงกรณ์มหาวิทยาลัย

ปีการศึกษา 2543

ISBN 974-13-0197-9

ลิขสิทธิ์ของจุฬาลงกรณ์มหาวิทยาลัย

INFLUENCES OF CURING FACTORS ON MECHANICAL PROPERTIES OF GLASS FIBER-
REINFORCED EPOXY COMPOSITE FOR COATING CONCRETE AND MORTAR



Miss vichaya Vichayapai Bunnag

สถาบันวิทยบริการ
จุฬาลงกรณ์มหาวิทยาลัย

A Thesis Submitted in Partial Fulfillment of the Requirements
For the Degree of Master of Engineering in Chemical Engineering
Department of Chemical Engineering
Faculty of Engineering
Chulalongkorn University
Academic Year 2000
ISBN 974-13-0197-9

Thesis Title Influences of Curing Factors on Mechanical properties of Glass
Fiber-Reinforced Epoxy Composite for Coating Concrete and
Mortar
By Miss Vichaya Vichayapai Bunnag
Department Chemical Engineering
Thesis Advisor Dr. Sirijutaratana Covavisaruch, Ph.D.

Accepted by the Faculty of Engineering, Chulalongkorn University in Partial
Fulfillment of the Requirements for the Master's Degree

.....Dean of Faculty of Engineering
(Professor Somsak Punyakaew, Dr. Eng)

THESIS COMMITTEE

.....Chairman
(Assistant Professor Sasithorn Boon-Long, Dr. 3ieme Cycle)

.....Thesis Advisor
(Dr. Sirijutaratana Covavisaruch, Ph.D.)

.....Member
(Dr. Chadchart Sittiphan, Ph.D.)

.....Member
(Dr. Sarawut Rimdusit, Ph.D.)

ชื่อผู้ทำวิทยานิพนธ์ : วิชญา วิชยาภย์ บุนนาค. (INFLUENCES OF CURING FACTORS ON MECHANICAL PROPERTIES OF GLASS FIBER-REINFORCED EPOXY COMPOSITE FOR COATING CONCRETE AND MORTAR)

ขอปรึกษา : ดร.สิริจุฑารัตน์ โควาริสารัช, 149 หน้า.

ISBN 974-13-0197-9.

งานวิจัยนี้เน้นการศึกษาผลของปัจจัยในการบ่มต่อสมบัติเชิงกลของผลิตภัณฑ์ประกอบแต่งอีพอกซีสำหรับเคลือบพื้นโรงงานอุตสาหกรรม ผลิตภัณฑ์ประกอบแต่งนี้ประกอบด้วย อีพอกซีเรซิน (diglycidyl ether of bisphenol A (DGEBA)) สารบ่ม diethylene triamine (DETA) เส้นใยแก้ว และทราย งานวิจัยนี้ได้ศึกษาผลิตภัณฑ์ประกอบแต่งอีพอกซีเรซินทั้งในรูปแบบของสารเคลือบที่ยังไม่ได้นำไปเคลือบผิว และแบบที่เคลือบแล้ว โดยจำลองขึ้นจากการเคลือบผลิตภัณฑ์ประกอบแต่งอีพอกซีเรซินลงบนคอนกรีตหรือมอร์ตาร์ งานวิจัยนี้มีการออกแบบการทดลองแปรสภาวะในการบ่มสารเคลือบผิวโดยประยุกต์ใช้หลักการออกแบบเซ็นทรัลคอมโพสิทโรเททาเบิล (Central Composite Rotatable, CCR) และเลือกใช้การวิเคราะห์ผลโดยวิธีพื้นผิวตอบสนอง (Response Surface Methodology, RSM) ทำให้ได้ผลการพื้นผิวตอบสนองแสดงความสัมพันธ์ระหว่างปัจจัยในการบ่มกับสมบัติเชิงกลตอบสนองของผลิตภัณฑ์ประกอบแต่งอีพอกซีเรซิน ผลจากการศึกษาอิทธิพลของปัจจัยในการบ่มซึ่งได้แก่ อุณหภูมิการบ่ม ระยะเวลาในการบ่ม และปริมาณทรายที่ใช้เป็นสารเติมแต่งที่มีต่อสมบัติเชิงกล พบว่าของผลิตภัณฑ์ประกอบแต่งอีพอกซีเรซินที่บ่ม ณ อุณหภูมิห้อง (31°C) จะมีความสามารถในการรับแรงกระแทก (impact strength) และค่าความเหนียวเมื่อแตก (fracture toughness) สูง ในขณะที่ความสามารถในการรับแรงกด (compressive strength) ต่ำกว่าเมื่อเทียบกับการเมื่อเทียบกับการรับแรงกดตันของผลิตภัณฑ์ประกอบแต่ง ที่บ่ม ณ อุณหภูมิสูง (99°C) การเพิ่มเวลาในการบ่มจะช่วยให้คุณสมบัติในการรับแรงกดดีขึ้น ส่วนการใส่ทรายเพื่อเป็นสารเติมแต่งไม่ได้มีผลต่อการรับแรงกดเท่าใดนัก แต่กลับช่วยให้พลังงานการแตก (fracture energy) ของผลิตภัณฑ์ประกอบแต่งอีพอกซีเรซินสูงขึ้นมากแต่ขณะเดียวกันก็ทำให้สมบัติในการรับแรงกดและแรงกระแทกลดลงเล็กน้อย ผลจากการวิเคราะห์แสดงให้เห็นว่า แต่ละสมบัติเชิงกลจะมีสภาวะที่เหมาะสมในการบ่มจะแตกต่างกันออกไป ผลิตภัณฑ์ประกอบแต่งอีพอกซีเรซินจะมีคุณสมบัติเชิงกลโดยรวมดีที่สุดเมื่อบ่มที่ 31°C นาน 56.2 ชั่วโมง ซึ่งเป็นเวลาบ่มที่นานที่สุดในงานวิจัย โดยใส่ทราย 23-25% สมบัติเชิงกลที่ลดลงมากที่สุด ณ สภาวะการบ่มนี้ ได้แก่ ความสามารถในการรับแรงกด ซึ่งลดลง 24.2% อย่างไรก็ตาม แนวโน้มของความสามารถในการรับแรงกดจะเพิ่มขึ้นอีกเมื่อเพิ่มเวลาในการบ่มออกไปอีก

ภาควิชา	วิศวกรรมเคมี	ลายมือชื่อนิสิต
สาขาวิชา	วิศวกรรมเคมี	ลายมือชื่ออาจารย์ที่ปรึกษา
ปีการศึกษา	2543	

4170516221 : MAJOR CHEMICAL ENGINEERING

KEY WORD: EPOXY RESIN / AMINE CURING AGENT / CURING FACTORS / INDUSTRIAL FLOORING

VICHAYA VICHAYAPAI BUNNAG : INFLUENCES OF CURING FACTORS ON MECHANICAL PROPERTIES OF GLASS FIBER-REINFORCED EPOXY COMPOSITE FOR COATING CONCRETE AND MORTAR. THESIS ADVISOR : SIRIJUTARATANA COVAVISARUCH, 149 pp.
ISBN 974-13-0197-9.

This experimental investigation aims to study the effects of curing factors on mechanical properties of epoxy composites for industrial floor coating. The epoxy composite system comprised of diglycidyl ether of bisphenol A (DGEBA) epoxy resin, diethylene triamine (DETA) curing agent, woven glass fiber reinforcement and sand filler. Both epoxy composite coating layer without any substrate and the epoxy composite coated concrete/mortar substrate, were investigated. An experimental design had been applied so that the results, obtained from a minimal number of experiments, would still be statistically conclusive by the technique of Central Composite Rotatable (CCR). Empirical models displaying the relationships between the curing factors and their corresponding response on mechanical properties were analyzed by the technique of Response Surface Methodology (RSM). The mechanical properties were analyzed as a function of the cure temperature, the cure time and the amount of added sand. Results studied showed that curing the epoxy composite at ambient temperature of 31°C gives better impact strength and fracture toughness, but less compressive strength than that of cured at a higher temperature of 99°C. The compressive strength can be improved by extending the cure time. Adding sand as a filler prominently improves the fracture toughness, but slightly decrease the compressive strength and the impact strength. Results drawn from this study illustrated that the most appropriate cure condition for each mechanical property varies. The optimum cure condition compromised from all mechanical properties is at the cure temperature of 31°C for 56.2 h, which is the longest cure time studied, with the amount of sand filler 29%. Curing at this condition minimize the reduction in mechanical property from the greatest achievable value. The highest reduction is 24.2% in the compressive strength of epoxy composite.

Department	Chemical Engineering	Student's signature.....
Field of study	Chemical Engineering	Advisor's signature.....
Academic year	2000	

ACKNOWLEDGEMENT

On my rocky road as a chemical engineering student, I have thought long and hard when I have an opportunity to write this page. I would like to sincerely express my deepest appreciation to Dr. Sirijutaratana Covavisaruch, my advisor. Without indefatigable support from her, I could never accomplish this thesis. She does not only guide me through every difficulty in this thesis, but also taught me how to face with all the problems in my life intellectually. I am indebted.

I would like to convey my sincere thankfulness to all members of my thesis committee, Assistant Professor Dr. Sasithorn Boon-Long, Dr. Chadchart Sittiphan, Dr. Sarawut Rimdusit, and Ms. Nattaporn Tonanon for their constructive guidance and invaluable recommendations. Indebtedness is also felt for Assistant Professor Dr. Boonchai Stitmannathum who gave his precious time to comment on my thesis. I am truly grateful for their aforementioned contribution.

I am very thankful for all organizations that had generously supported the testing facilities, namely the Department of Metallurgical Engineering and the Department of Civil Engineering, especially the National Metal and Materials Technology Center (MTEC).

I also appreciate Ms. Kittivan Setrkraisin and Mr. Praprut Songchitrukka for always being there through good and bad times. I am very thankful for every inspiration that they have made throughout my difficult years. They are more than my best friends. Thanks are also extended to Mr. Pichet Rojanapitayakorn, Mr. Mano Limvorapun, Mr. Montree Chandamnearnkij and every polymer engineering research laboratory member for every constructive discussion they contributed and all their help.

To the persons whom mean most in my life, I would like to dedicate this last small paragraph to my beloved family, especially my grandmother, for their eternal care and endless support. There is never even a single day without them standing by me. It is why I can journey this far. I am lifetime beholden.

CONTENTS

	PAGE
ABSTRACT (THAI).....	iv
ABSTRACT (ENGLISH).....	v
ACKNOWLEDGEMENT.....	vi
CONTENTS.....	vii
LIST OF TABLES.....	xi
LIST OF FIGURES.....	xiii
CHAPTER	
I INTRODUCTION.....	1
1.1 General Introduction.....	1
1.2 Objectives of the Present Study.....	2
1.3 Scope of the Present Study.....	3
1.4 Thesis Organization.....	4
II THEORY.....	6
2.1 Coating.....	6
2.1.1 Composition of Coatings.....	6
2.1.2 Surface Preparation.....	7
2.1.3 Film Formation.....	7
2.1.4 Industrial Floor Coating.....	8
2.2 Composites.....	8
2.3 Epoxy Resins.....	9
2.3.1 Types of Epoxy Resins.....	10
2.3.2 Preparation of Epoxy Resins.....	12
2.3.3 Basic Characteristics of Epoxy Resins.....	16
2.3.4 Applications of Epoxy Resins.....	18
2.4 Curing Agents.....	18
2.5 Curing Mechanism.....	19
2.6 Glass Fiber.....	22
2.6.1 Types of Glass Fiber.....	22
2.6.2 Glass Fiber Reinforced Composite.....	22

CONTENTS (CONTINUED)

CHAPTER	PAGE
2.7 Sand.....	23
2.8 Fracture of Polymers.....	24
2.8.1 Stress intensity factor.....	24
2.8.2 Fracture Energy.....	26
2.9 Statistical Approaches for Statistical Analysis.....	26
2.9.1 Response Surface Methodology.....	26
2.9.2 Central Composite Design.....	27
2.9.3 Regression Analysis.....	30
2.9.3.1 Linear Regression Model.....	30
2.9.3.2 Least Square Estimation.....	31
2.9.4 Analysis of Variance.....	35
2.9.4.1 Lack of Fit.....	37
2.9.4.2 Hypothesis of Multiple Linear Regression.....	38
2.9.4.3 Cross Validation.....	40
III LITERATURE REVIEWS.....	41
IV EXPERIMENTAL PROCEDURE.....	49
4.1 Materials.....	49
4.1.1 Epoxy Resins.....	49
4.1.2 Curing Agents.....	50
4.1.3 Glass Fiber.....	50
4.1.4 Sand.....	50
4.1.5 Concrete.....	51
4.1.6 Mortar.....	51
4.2 Experimental Design.....	52
4.3 Material Processing.....	54
4.3.1 Preparation of Epoxy Composite Specimens.....	54
4.3.1.1 Curing Epoxy and Curing Agent.....	54
4.3.2 Preparation of Concrete Specimens.....	57
4.3.2.1 Mixing of Concrete.....	57
4.3.2.2 Molding of Concrete.....	57

CONTENTS (CONTINUED)

CHAPTER	PAGE
4.3.2.3 Curing Concrete.....	57
4.3.3 Preparation of Mortar Specimens.....	58
4.3.3.1 Mixing of Mortar.....	58
4.3.3.2 Molding of Mortar.....	58
4.3.3.3 Curing Mortar.....	58
4.3.4 Preparation of Concrete and Mortar coated Specimens....	58
4.4 Mechanical Testing.....	59
4.4.1 Epoxy Composite Specimens.....	59
4.4.1.1 Compression Test.....	59
4.4.1.2 Impact Test.....	61
4.4.1.3 Double Torsion Test.....	61
4.4.2 Coated Concrete.....	63
4.4.3 Coated Mortar.....	63
4.5 Microscopic Observation.....	64
4.6 Sample Characterization.....	64
V RESULTS AND DISCUSSIONS.....	67
5.1 Regression Analysis.....	67
5.2 Analysis of Variance (ANOVA).....	70
5.3 Mechanical Properties of Epoxy Composites.....	73
5.3.1 Epoxy Composite Specimens.....	73
5.3.1.1 Compression Test.....	73
5.3.1.2 Impact Test.....	78
5.3.1.3 Double Torsion Test.....	82
5.3.2 Concrete Coated Specimens.....	89
5.3.3 Mortar Coated Specimens.....	93
5.4 Improvement in Mechanical Properties of the Epoxy Composites.....	100
5.5 Effects of Curing Factors on Mechanical Properties of the Epoxy Composite.....	101
5.6 Optimum Cure Condition.....	103

CONTENTS (CONTINUED)

x

	PAGE
CHAPTER	
5.7 Macroscopic Observation.....	104
5.8 Sample Characterization.....	112
VI CONCLUSIONS AND RECOMMENDATIONS.....	114
6.1 Conclusions.....	114
6.2 Recommendations for Further Studies.....	117
REFERENCES.....	118
APPENDICES	
A RESULTS OF THE MECHANICAL PROPERTIES FROM THE EXPERIMENTAL TESTS.....	123
B CALCULATION METHOD.....	128
C ANOVA TABLE AND REGRESSION COEFFICIENTS.....	136
D TABLE OF STATISTICAL t AND F DISTRIBUTION.....	142
VITA.....	149

สถาบันวิทยบริการ
จุฬาลงกรณ์มหาวิทยาลัย

LIST OF TABLES

TABLE		PAGE
2.1	Major applications of epoxy resins.....	18
2.2	Comparison between the number of experiments designed by factorial design and rotatable central composite design at 5 levels of variables.....	28
2.3	Rotatable central composite design for $k = 2$	29
2.4	Rotatable central composite design for $k = 3$	30
2.5	Data for multiple linear regression.....	31
2.6	ANOVA table for multiple regression.....	35
4.1	Central Composite Rotatable design for three dependent variables....	53
4.2	Appropriate curing condition at center point, cube point and star point.....	53
4.3	Most appropriate test condition from the experimental design.....	54
4.4	Cure Condition of epoxy composite.....	56
4.5	Amount of sand filler.....	56
5.1	Impact strength of epoxy composite.....	67
5.2	Experimental and calculated error for impact strength of epoxy Composite.....	68
5.3	Coefficients deriving from the second-order linear regression analysis for the properties of Epoxy Composites.....	69
5.4	ANOVA table for the multiple regression analysis of the interactions of cure temperature, cure time, and amount of sand on the impact strength of epoxy composite.....	70
5.5	Statistic- t_0 test of coefficients testing for interactions of cure temperature, cure time, and amount of sand on the impact strength of epoxy composite.....	70
5.6	Significant coefficients deriving from the second-order linear regression analysis for the properties of epoxy composites.....	72
5.7	Improvement in mechanical properties of the epoxy composites cured at 65 °C for 36 h.....	100

LIST OF TABLES (CONTINUED)

TABLE	PAGE
5.8	Improvement in compressive strength of the epoxy composites coated concrete cured at 65 °C for 36 h..... 101
5.9	Improvement in impact strength of the epoxy composites coated mortar cured at 65 °C for 36 h..... 101
5.10	Effects of the cure temperature on mechanical properties of the epoxy composites..... 102
5.11	Effects of the cure time on mechanical properties of the epoxy composites..... 102
5.12	Effects of the amount of sand on mechanical properties of the epoxy composites..... 103
5.13	The appropriate cure condition for each mechanical property..... 103
5.14	The mechanical properties of the epoxy composites, the composite coated on concrete and the mortar coated composite cured at 31°C for 56.2 h. The amount of sand filler added is 29%..... 104
5.15	Experimental results from dynamic mechanical analysis test for neat epoxy with different cure condition..... 113
6.1	Interaction between cure temperature (T) and the coded variables of cure time (t), amount of added sand (x) and the mechanical property (y). All equations are valid when the epoxy composites are cured with the cure temperature from 45 to 85 °C, the cure time from 24 to 48 h and the amount of sand from 27 to 34%..... 117

LIST OF FIGURES

FIGURE		PAGE
2.1	Continuous and discontinuous phase in a composite material.....	8
2.2	The structure of epoxide group.....	9
2.3	General structure of an epoxy resin.....	10
2.4	The chemical structure of bisphenol A.....	11
2.5	The chemical structure of novolac resins.....	11
2.6	The chemical structure of bisphenol F.....	11
2.7	Formation of epichlorohydrin.....	12
2.8	Formation of bisphenol A.....	12
2.9	The formation of diglycidyl ether of bisphenol A.....	13
2.10	Mechanism of reaction to form DGEBA.....	14
	(a) Substitution of Na atom in bisphenol A.....	14
	(b) Reaction between bisphenol A salt and epichlorohydrin.....	14
	(c) Reaction to form diglycidyl ether of bisphenol A.....	14
	(d) Reaction between three epichlorohydrin and two bisphenol A.....	15
	(e) Reaction between sodium salt and water.....	15
2.11	The structure of diethylene triamine (DETA).....	18
2.12	Bonding between carbon atom and nitrogen atom.....	20
2.13	Formation of alcohol group and amine group.....	20
2.14	Another epoxide end group is added to the same amine group.....	20
2.15	Two more epoxide groups reacts with amine at the other end.....	21
2.16	Crosslink network.....	21
2.17	Types of fiber-reinforced composites.....	23
2.18	The three modes of crack extension.....	24
2.19	Uniaxially stressed plate with a cracked hole (fracture in Mode I).....	25
2.20	Example of response surface.....	26
2.21	Rotatable central composite designs for $k = 2$ and $k = 3$	28
4.1	Chemical structure of diglycidyl ether of bisphenol-A (DGEBA).....	49
4.2	Chemical structure of diethylene triamine (DETA).....	50
4.3	Section through concrete showing aggregate.....	51

LIST OF FIGURES (CONTINUED)

FIGURE	PAGE
4.4	Laminae of the epoxy composite..... 55
4.5	Concrete tightens with a metal frame..... 59
4.6	Direction of applying load in compression test..... 60
4.7	Dimension of the compression test specimen..... 60
4.8	Specimen dimension and specimen arrangement for impact test..... 61
4.9	The shape and dimension of the double torsion specimen..... 62
4.10	Arrangement of specimen in the double torsion fixture..... 62
4.11	The arrangement and the dimensions of epoxy composite coated concrete..... 63
4.12	The arrangement and the dimensions of epoxy composite coated mortar..... 64
5.1	Epoxy composite test specimen from compression test perpendicular to the compression load..... 74
	(a) Before compression..... 74
	(b) After compression..... 74
5.2	Stress-strain curve from compression test of epoxy composite cured at 65°C for 36 h. The amount of added sand is 27% 74
5.3	Compressive strength of various neat epoxy composite, epoxy composite and sand-filled epoxy composite, all systems were cured at 65 °C for 36 h..... 75
5.4	Effects of cure temperature, cure time, and sand filler on the compressive strength of epoxy composites..... 77
5.5	Contour of the compressive strength for the epoxy composite between the amount of sand and the cure temperature at constant cure time 15.8 h..... 78
5.6	Epoxy composite broken in the impact test..... 79
	(a) Epoxy composite broke into 2 pieces upon impact..... 79
	(b) Glass fiber protruding from the fracture surface of epoxy composite..... 79

LIST OF FIGURES (CONTINUED)

FIGURE	PAGE
5.7	The impact strength of neat epoxy composite, epoxy composite and sand-filled epoxy composite, all systems were cured at 65 °C for 36 h.....79
5.8	Effects of cure temperature, cure time, and sand filler on the impact strength of epoxy composites..... 81
5.9	Contour of the impact strength for the epoxy composites between the amount of sand and the cure time at a constant cure temperature of 31°C..... 82
5.10	Schematic representation of the double torsion test 83 (a) The shape of the double torsion specimen..... 83 (b) Fracture surface from double torsion test..... 83
5.11	Epoxy composite specimen from double torsion test84 (a) Epoxy composite broke into 2 pieces..... 84 (b) Cross section of the crack..... 84
5.12	Critical stress intensity factor of neat epoxy and epoxy composite coatings..... 84
5.13	Effects of cure temperature, cure time, and sand filler on the critical stress intensity factor of epoxy composites..... 86
5.14	Contour of the critical stress intensity factor of epoxy composites between the amount of sand and the cure time at a constant cure temperature of 31°C..... 87
5.15	Fracture energy of neat epoxy and epoxy composites..... 87
5.16	Effects of cure temperature, cure time, and sand filler on fracture energy of the epoxy composites..... 88
5.17	Contour of fracture energy of epoxy composite between the amount of sand and the cure time at a constant cure temperature of 31°C..... 89
5.18	Concrete coated specimen from compression test.....90

LIST OF FIGURES (CONTINUED)

FIGURE	PAGE
(a) Side view of epoxy-composite-coated concrete cracked under compression test.....	90
(b) Top view of epoxy-composite coated on concrete cracked by compression.....	90
5.19 Compressive strength of uncoated and coated concrete.....	90
5.20 Effects of cure temperature, cure time, and sand filler on compressive strength of concrete coated with the epoxy composites.....	92
5.21 Contour of the compressive strength of concrete coated with epoxy composite at a constant cure temperature of 25 °C.....	93
5.22 Fracture of mortar coated with epoxy composite by the impact test.....	94
(a) Fracture surface of mortar coated with epoxy composite.....	94
(b) Mortar coated with epoxy composite broke into 2 halves upon impact.....	94
5.23 Principle of the impact by pendulum.....	95
5.24 Impact strength of various coated mortar.....	96
5.25 Effects of cure temperature, cure time, and sand filler on impact strength of mortar coated with the epoxy composites.....	97
5.26 Contour of the impact strength of mortar coated with epoxy resin between the amount of sand and the cure time at a constant cure temperature 31°C.....	98
5.27 Impact strength of the epoxy composite cured with 20% and 27% sand, both were cured at 65°C.....	99
5.28 Impact fracture surface of epoxy composite cured at 65 °C 36 h 27% sand.....	105
5.29 Impact fracture surface in the epoxy layer of the epoxy composite cured at 65 °C for 36 h. The amount of sand added was 27%.....	105

LIST OF FIGURES (CONTINUED)

FIGURE	PAGE
5.30	The sand layer in the epoxy composite cured at 65 °C for 36 h. The amount of sand added was 27%..... 106
5.31	The sand layer in the epoxy composite cured at 65 °C for 36 h. The amount of sand added was 15.23%..... 106
5.32	Adhesion between sand filler and the epoxy resin in the epoxy composite..... 106
5.33	Fracture surface of the epoxy composite cured at 65°C for 36 h. The amount of sand added was 27%..... 107
5.34	Section of the fracture area of the epoxy composite cured at 65°C for 36 h. The amount of sand added was 38.77%..... 108
5.35	River markings in the epoxy composite cured at 65°C for 36 h..... 109
5.36	The sand layer of the epoxy composite cured at 65°C for 36 h. The amount of sand added was 38.77%..... 109
5.37	Adhesion between the sand filler and the epoxy resin in epoxy composite cured at 65°C for 36 h. The amount of sand added was 38.77%..... 110
5.38	Pulled-out glass fibers in the fracture surface of epoxy composite failed by double torsion..... 110
5.39	Glass fibers and the epoxy resin adhered to them..... 110
5.40	Adhesion between the glass fiber and the epoxy resin..... 111
5.41	Fracture surface of concrete coated with epoxy composite..... 111
5.42	Adhesion between the concrete and the epoxy composite..... 112
5.43	The dynamic mechanical spectrum (storage modulus and loss tangent plotted against the temperature at the frequency of 1 Hz) of neat epoxy cured at 65 °C for 36 h..... 112

CHAPTER I

INTRODUCTION

1.1 GENERAL INTRODUCTION

The polymer invention has led to an introduction of new alternatives for industrial materials. This is primarily due to the several advantages readily offered by polymers, such as lightness and the ease of processing. In addition, its cost is relatively lower than metal while still maintaining the comparable material properties. Many industrial sectors have gained benefits from the applications of polymers. In the last few decades, many industries have expanded much faster than before thanks to the aforementioned advantages polymers contributed to their development.

Corrosion of concrete floor is one significant problem found in the production area of many industries, for example, chemical plants, food factories, pharmaceutical industries, steel industries, nuclear plants and etc. Although concrete is a well-known construction material for its high compressive strength, its chemical resistance property is, unfortunately, an adverse. The concrete material that is vulnerable to chemical corrosion can deteriorate into a poor condition within a short period of time. Severe usage also lessens the lifetime of concrete floor. Examples of concrete floor corrosion have been frequently reported from several types of industries, examples of which are described as follow [1]. In 1970, a food manufacturer of vegetable products, faced a problem with the concrete floor deterioration in the potato and cabbage production area. The bare concrete floor was severely deteriorated from years of forklift traffic, water, and vegetable by-products showing a lot of cracks and exposed aggregate in many areas. In 1985, concrete floor of a steel plant was reported to have corroded badly by high temperatures and humidity. Another example found in Thailand as recent as 1999 was a manufacturer of food products as supplement such as omega-3 extracted from tuna fish. Daily cleaning with chlorine is inevitable to prevent bacteria in the food production area. Chemical corrosion due to the reaction of chlorine with the calcium carbonate in the

concrete leads to rapid deterioration of the concrete floor. To take care of this problem, a huge expenditure has been spent on floor maintenance task. Hence, there is an urgent need to minimize this maintenance cost through an improvement in corrosion resistance property of the concrete floor. One potential solution has been directed towards the application of polymer as surface coating material. This is because some polymers are well known for their chemical resistance. Therefore, the polymer-coated concrete floor has been attracting considerable attention in the last three decades [2]. Maintenance of concrete floor in the aforementioned plants was later conducted by the application of polymer composite coating. In the case of vegetable production plant, the polymer coated concrete floor has been reported to be used for last for almost 20 years without any special attention except daily cleaning and is still in reasonably good condition [1]. Coating concrete floors with polymers not only extends the service life, but also provides the ease of cleaning and maintenance.

Although industries use epoxy-coated concrete floors increasingly nowadays, some coating applications were found to perform as satisfactorily as the vegetable plant reported. Many still suffer from the problem of delamination, cracks lack of chemical resistance leading to short service life or severe hygiene problems in the plant. The greater expansion of industrial floor coating application, the more need is there for thorough investigation and research in this area. There is still lack of understanding and information on how fiber-reinforced epoxy composite would perform on effect substrates such as concrete or mortar. Earlier studies concentrated on either material by investigating them separately [2-4, 6-21]. Hence, the influences of curing factors on the mechanical properties of glass fiber-reinforced epoxy composite for surface or floor coating on concrete and mortar is still opened for further research. Such study is envisaged to induce better understanding and development on polymer coating.

1.2 OBJECTIVES OF THE PRESENT STUDY

The aims of this investigation are twofolds. One is to establish the relationship between curing factors and major mechanical properties of the fiber-reinforced epoxy resin coating on concrete. The mechanical properties of the epoxy systems depend on several factors; three significant of which are *curing temperature*,

curing time, and the ratio of the epoxy resin per curing agent. Most studies use the stoichiometric ratio of epoxy and curing agent to cure the epoxy system [5, 10-12, 14, 15, 17, 19]. Results drawn from previous studies revealed that good mechanical properties are compromised at this ratio [7, 9]. In accordance with these reports, the ratio of the epoxy resin per curing agent in this study is thus kept at stoichiometry. Two other curing factors are studied in the current research. As an endeavor to find the most suitable amount of fillers to be added in the coating system, the ratio of sand per epoxy resin will be considered as well. The three mechanical properties to be investigated are compression strength, impact strength and fracture energy. As a result of numerous variables included in the present work, Central Composite Rotatable (CCR), an experimental design technique will be performed. The obvious benefit of CCR is to minimize the number of experimental runs while the results yielded remain statistically reliable. Experimental results are analyzed by the technique of Response Surface Methodology (RSM) in order to verify the relationship between the proposed curing factors and the mechanical properties of the filled epoxy-glass fiber coating system.

The other aim of this study is an attempt to gain better understanding on the mechanical properties of the glass fiber-reinforced epoxy composite coating and the concrete substrate in industrial floor coatings.

1.3 SCOPE OF THE PRESENT STUDY

The scope of the current research begins with selecting a polymeric resin to function as matrix for the composite coat. Several thermoset polymers can be applied as floor coating material such as unsaturated polyester, epoxy resin and polyurethane. In addition to high chemical resistance, the coating material must exhibit good adhesion property to the concrete floor. Epoxy resin is selected as floor coating material for the present study. It is an excellent bonding material. It also possesses excellent mechanical properties as well as high electrical insulation. Moreover, epoxy resin can be reinforced with glass fiber in order to increase its tensile strength and stiffness. Therefore, in this research, the coating material is a composite polymer in which epoxy resin and glass fiber are matrix and reinforcement respectively. However, the addition of glass fiber alone may lead to a significant increase in floor coating cost. In order to address this problem, the use of fillers is

considered as one potential solution. Among several possible fillers, sand and quartz are commercially used in the coating task since they are believed to be effective reinforcing fillers. Sand will be used as filler in the present research.

In order to achieve the objectives of the study, two groups of samples are prepared. The first one is a neat epoxy system. The curing conditions for each sample in the first group are designed following the CCR technique. After the mechanical properties namely the compression strength, impact strength, and fracture energy have been evaluated, empirical models in the form of response surface equations will be conducted.

The second group of samples is prepared by coating the glass fiber-reinforced epoxy composite on the concrete substrate. A comparison of the major mechanical properties of the uncoated and coated concrete will be conducted systematically. Though the samples in the present study have been designed to focus on imitating real concrete floors, the epoxy-glass fiber composite coated concrete samples prepared will not be subjected to impact test due to lack of appropriated testing equipment. Instead of concrete as a substrate, mortar, a material composed with cement and sand, is used in the study on impact behavior of the coated floor. The difference between the impact strength of uncoated mortar and the epoxy-glass fiber coated ones will be compared.

Macroscopic observation of each coating material will be conducted by using Scanning Electron Microscope (SEM) in order to view each component in the structure microscopically.

1.4 THESIS ORGANIZATION

This thesis is organized into five chapters. Relevant results and detailed analysis are documented in the appendices.

Chapter 1 introduces this research with the general background, the problem statement, research objectives and the scope of study.

Chapter 2 combines primary theories relative to the field of coating. This chapter prepares requisite knowledge in order to construct the research plan and implementation.

Chapter 3 provides a summary of literature relevant to the present study, which is an important background to this field.

Chapter 4 illustrates experiment results and discusses the influences of the proposed curing factors on the mechanical properties of glass fiber-reinforced epoxy composite for coating concrete and mortar.

Chapter 5 finalizes the research with conclusion of validated results. In addition, recommendations for further studies are proposed.



สถาบันวิทยบริการ
จุฬาลงกรณ์มหาวิทยาลัย

CHAPTER II

THEORY

2.1 COATING

Coating is a process of applying a material to form a dry film on a substrate. It is performed for two main purposes, i.e. for decoration and for protection [22, 23]. Generally, the coatings may be distinguished as organic and inorganic. Nevertheless, there is an overlap. The current study is focused on organic coating.

2.1.1 COMPOSITION OF COATINGS

Organic coatings are complex mixtures of the following chemical substances [22]:

2.1.1.1 Binders or Primers

Binders are materials that form continuous film, which adheres to a substrate, the surface of which being coated, on one side and binds together substances in the coating to form a film on the other side.

2.1.1.2 Volatile Components

Volatile components were called *solvents* in the past. After many coatings have been developed, the binder components are no longer fully soluble in solvents. Therefore, volatile components are a better term to define liquids that make the coating material fluid enough for application. Volatile components evaporate during and after application. For coating with thermosets, film can be formed without adding solvents. Instead of the usual solvent evaporation, cross-linking reaction between thermoset resin and curing agent can form the thermoset coating film.

2.1.1.3 Pigments

Pigments provide color and opacity to the coating film. There are two types namely *organic* and *inorganic* pigments. Both are used in surface coating applications, but the latter ones are used more extensively.

2.1.1.4 Additives

Additives are included within the coating mixture in small quantities in order to modify some physical properties of the coating film. For example, antioxidants are used to protect against atmospheric oxidation. Heat stabilizers can be applied to perform a similar function i.e. to prevent degradation at high processing temperatures.

2.1.2 SURFACE PREPARATION

The surface preparation for concrete coating is usually based upon its location, condition and history of the existing concrete. Preparing the surface is a pre-step to ensure the strength and integrity of concrete. Before coating, concrete should be meticulously clean. All grease, dirt, paint, oil, tar, glaze, loose mortar and cement should be removed in order to provide good adhesion. The process of surface preparation involves several steps of removals of impurities. They include getting rid of grease and oils, providing a surface profile or texture, removing dust and contaminants, removing salts, and removing moisture [24].

2.1.3 FILM FORMATION

Coating films can be formed simultaneously in three steps generally known as resin application, fixation and curing. The coating material is firstly applied on the substrate by using a brush or a roller, or by spraying, or by dipping or by other appropriate means. Fixation is the step by which the coating material is fixed or adhered to the substrate. The final step of curing is performed to dry the coating film. Curing can be done by two approaches namely, physical drying and chemical drying. The coating films can be physically dried by evaporation of the solvent. In chemical drying, reactions between the coating material and the curing agent will take place and a dried film of coating is eventually formed. Some coating material may react with oxygen and hence it is dried by oxidation. The physical properties of the coating film are much improved in the curing step. In this research, the chemical drying is adopted. The coating material is cured by the reaction between the epoxy coating resin and the curing agent [22].

2.1.4 INDUSTRIAL FLOOR COATING

Concrete is by far the most widely used industrial floor material; it is frequently left uncovered. However, concrete does not possess high chemical resistance. Fats and oils split on concrete floor are absorbed by concrete. Therefore it is often necessary to cover concrete with a topping in order to protect the sub-floor from corrosive materials or to protect the sub-floor from severe mechanical wear. The coating of concrete may also seal the concrete surface from moisture and/or hence reduce dust. Often a higher standard of cleaning can be attained. Non-slip surface can also be achieved depending on the coating surface texture [24].

2.2 COMPOSTIES

The uses of polymeric materials have been expanded continuously in the last few decades owing to the development of materials in the form of polymeric composites. A composite generally consists of two or more materials combined physically in a macroscopic structural unit. The materials combined to make up the composites can be distinguished as two different phases. The main phase, known as matrix, is usually a continuous and often uniform phase. The other phase, generally acts as a reinforcement, is a discontinuous phase surrounded by the matrix. It can be found in various forms such as particles, platelets and rod as shown in Figure 2.1 [25].

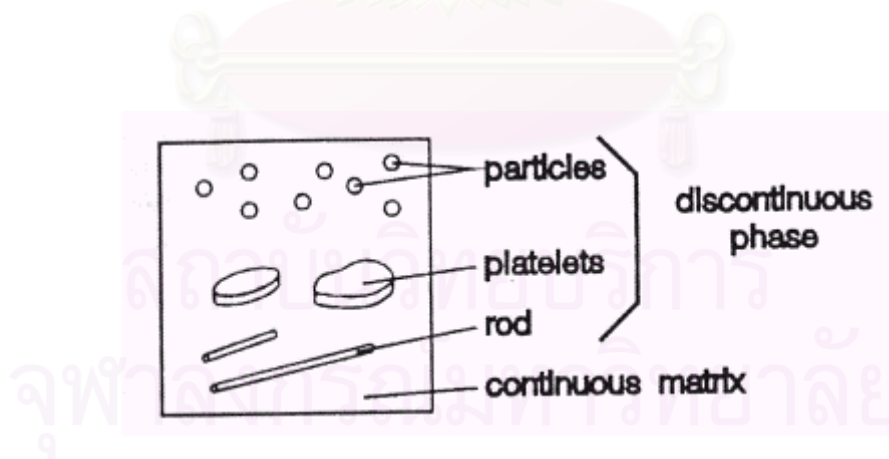


Figure 2.1 : Continuous and discontinuous phase in a composite material.

Polymeric composites comprise at least one type of polymeric material and other materials, which can be either another polymer or any other material. Polymer blends are usually not classified as composites since the structural unit is

formed at a microscopic level rather than a macroscopic one. However, this may soon change with the development of molecular composites, which consist of the oriented rodlike polymer molecules in a polymeric binding matrix.

Composites generally possess some properties better than those of the constituent on its own. Reinforcement like fibers allows maximum tensile strength and stiffness of a material to be obtained. Fibers alone cannot support longitudinal compressive loads and their transverse mechanical properties are generally not so good as the corresponding longitudinal properties. Hence, they are useless without the matrix, which not only holds the fibers together in a structural unit, but also serves to protect them from external damage and environmental attack. The matrix functions by transferring the applied load from the surface of the composite to the reinforcing fiber and distributing the applied loads among the fibers within the composite. As a result, the capability of the composite in receiving loads is enhanced significantly [25-27].

2.3 EPOXY RESIN

Epoxy resin is characterized by an epoxide group, which is a three-membered ring consisting of an oxygen atom attached to two carbon atoms. The structure of epoxide group is shown in Figure 2.2. They have also been known by other names such as, epoxides, ethoxylines, oxiranes, glycidyl polyethers and diepoxide polymers.

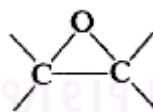


Figure 2.2 : The structure of epoxide group.

Having the most appropriate properties for industrial floor coating application, which are high chemical resistance, good mechanical properties, and good adhesion to concrete, epoxy resin was chosen among other thermosets in this study. Epoxy resin acts as the matrix in the composite floor coating system.

2.3.1 TYPES OF EPOXY RESINS

Epoxy resins have been classified by the raw material from which they were derived. Three major types of commercial epoxy resins are cycloaliphatic epoxy resins, epoxidized oils and glycidated resins. Their structures are illustrated in Figure 2.3 [24, 28].

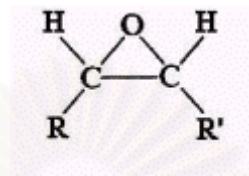


Figure 2.3 : General structure of an epoxy resin. Three major types of epoxy resins are

- (a) Cycloaliphatic epoxy resins (R and R' are part of a six-membered ring)
- (b) Epoxidized oils (R and R' are fragments of an unsaturated fatty acid)
- (c) Glycidated resins (R is hydrogen and R' can be a polyhydroxyphenol, polybasic acid, or polyamine)

2.3.1.1 Cycloaliphatic epoxy resins

Cycloaliphatic epoxides are made by epoxidizing appropriate cycloolefin with peracetic acid. Since no chlorine-containing raw materials are used, these resins are free of hydrolyzable chlorine. They are low in ash content and ionic content. As a result of their high UV resistance, high arc-track resistance and good weathering, cycloaliphatic epoxides have been widely used in electrical applications.

2.3.1.2 Epoxidized oils

The epoxidized oils (triglycerides) and other epoxidized esters naturally occur from fatty acids. They are also made by peroxidation of the corresponding unsaturated material. These liquids are effective plasticizers and stabilizers for polyvinyl chloride and copolymers when cured. Epoxidized soybean oil is the most widely used epoxidized oils [28].

2.3.1.3 Glycidated epoxy resins

Glycidated epoxy resins are the types used in most commercial applications. Conveniently three generalized glycidated polyhydroxy phenols have been postulated namely bisphenol A, bisphenol F and novolac epoxy resins.

Most epoxy resins are made from bisphenol A, its chemical structure is shown in Figure 2.4. They can, unless diluted or altered, typically handle 70% sulphuric acid and a temperature range of 65-95 °C.

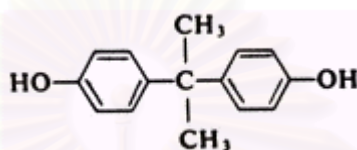


Figure 2.4 : The chemical structure of bisphenol A.

Novolac resins, as shown in Figure 2.5, combine the reactivity of the epoxide group and the thermal resistance of the phenolic backbone in the cured polymer. They can handle 98% sulphuric acid and withstand temperatures as high as 200-260 °C.

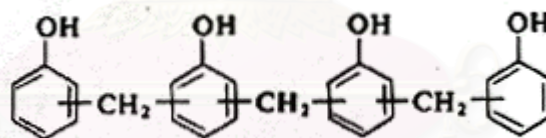


Figure 2.5 : The chemical structure of novolac resins.

The properties of bisphenol F resins fall between bisphenol A and novolac resins. Figure 2.6 shows the chemical structure of bisphenol F.

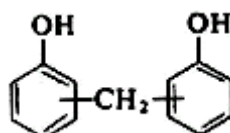


Figure 2.6 : The chemical structure of bisphenol F.

In industrial floor coating application, epoxy resins derived from bisphenol A are extensively used. This is due to their desirable properties in conjunction with the fact that they are easy to both process and control. Therefore, bisphenol A epoxy resin is also the material of choice in the present study.

2.3.2 PREPARATION OF EPOXY RESIN

Epichlorohydrin (ECH) and bisphenol A (BPA) are the two most significant raw materials used in the production of epoxy resin [28, 29].

ECH is obtained as a by product from the production of glycerine from petroleum feedstock. Chlorination of propylene under high temperature and pressure yields allyl chloride by product, when allyl chloride is treated with hypochlorous acid, glycerol dichlorohydrin will be produced. Finally, dehydrochlorination takes place and produces ECH, as shown in Figure 2.7 .

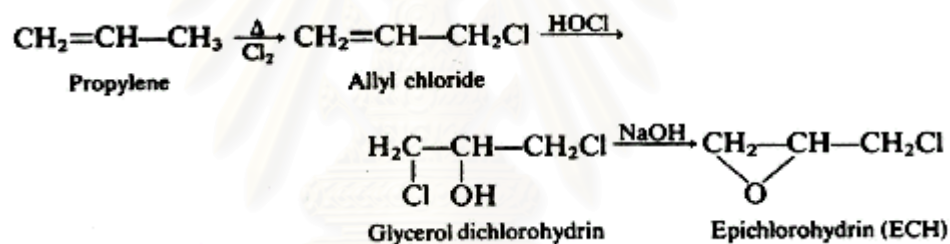


Figure 2.7 : Formation of epichlorohydrin.

BPA or 2,2'-bis (*p*-hydroxyphenyl) propane is synthesized by reacting acetone with phenol in the presence of acidic catalyst. The reaction is shown in Figure 2.8 .

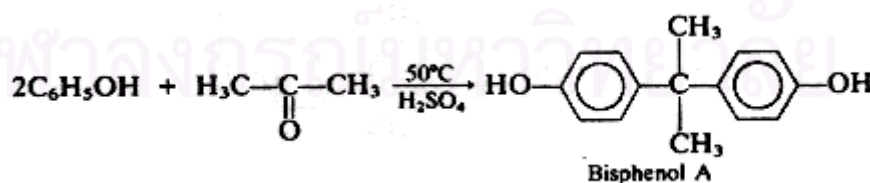


Figure 2.8 : Formation of bisphenol A.

The reaction to form epoxy resin from ECH and BPA are as those shown in Figure 2.9 . Epoxy resin derived from ECH and BPA is called diglycidyl ether of bisphenol A (DEGDA).

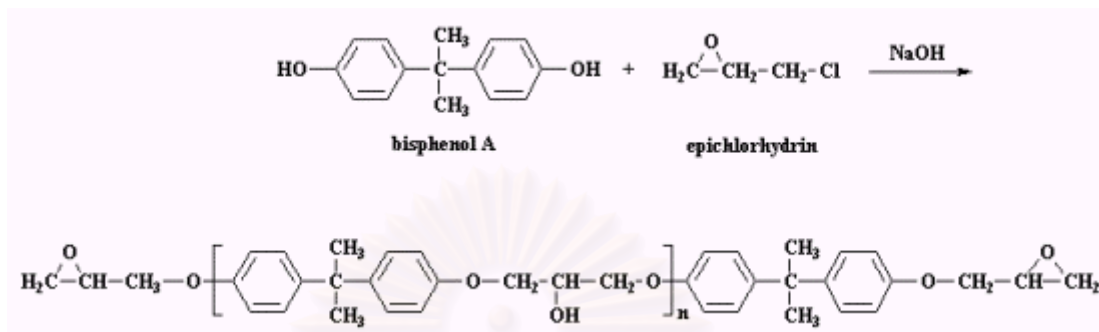
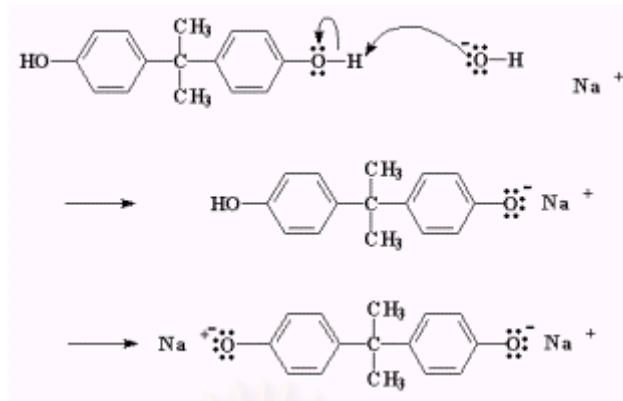
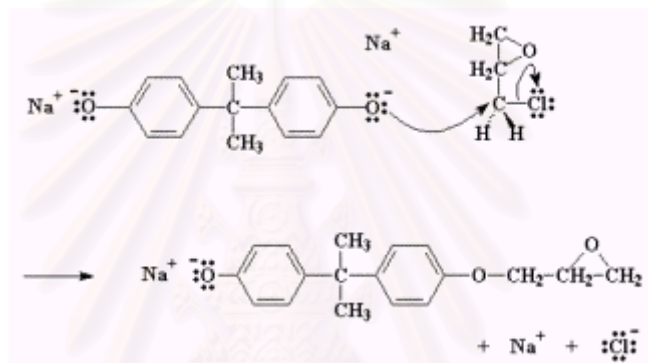


Figure 2.9 : The formation of diglycidyl ether of bisphenol A (DEGDA).

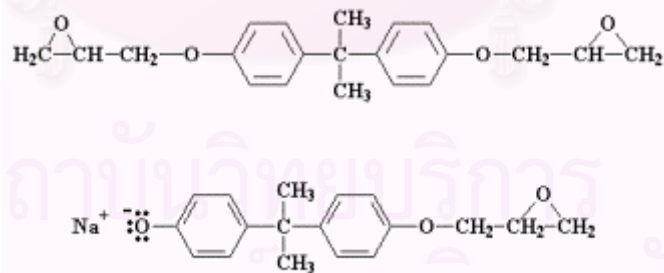
The mechanism of the reactions above is shown in Figure 2.9 (a) to (e) [29]. First, sodium hydroxide swap with bisphenol A thus giving bisphenol a sodium salt as shown in Fig 2.10 (a). The oxygen atom in the salt is postulated to possess three pairs of electrons, so it shared its excess electron to a carbon atom, which is next to chlorine on a nearby ECH. In order to get rid of the excess electrons pairs, such carbon atom stops sharing pairs of electron with the chlorine atom. Then, epoxide group is formed as illustrated on the right of the reacted molecule in Figure 2.10 (b). Such reaction also occurs at the other side of the molecule. Consequently, the epoxy resin is formed as shown in Figure 2.10 (c). The aforementioned reactions stop when no bisphenol A salt is left to react. Two molecules of ECH are added to react with one BPA molecule. However, if there are less than two molecules of ECH for every BPA, not all of the BPA salt groups can react with ECH. In this case, the unreacted part will react with the epoxide group as shown in Figure 2.10 (d). Sodium salt is obtained from this reaction. The negative charge on the oxygen atom of the sodium salt will reaction with the hydrogen atom from water as shown in Figure 2.10 (e). The greater the amount of ECH relative to that of BPA salt, the higher will be weight of the oligomer attained. In practice, the reactions are carried out in the presence of a large excess of ECH, so as to obtain essentially epoxide-terminated resin molecules.



(a) Substitution of sodium atom in bisphenol A

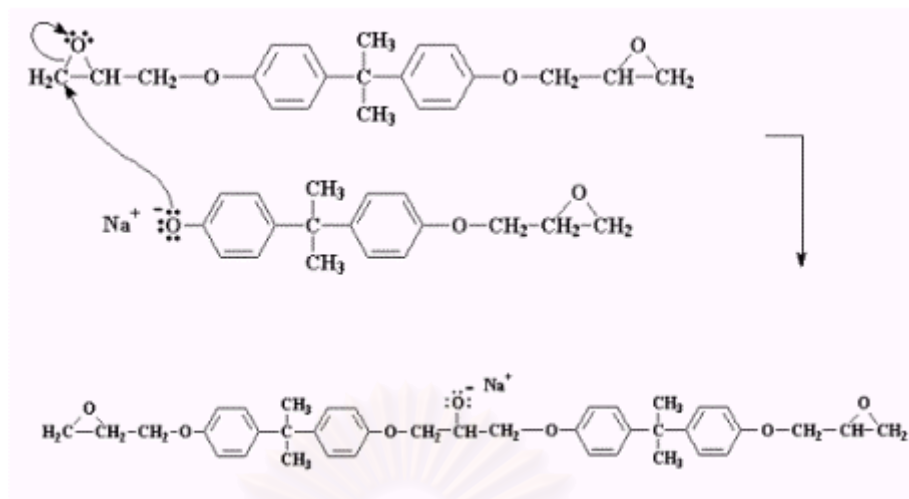


(b) The reaction between bisphenol A salt and epichlorohydrin.

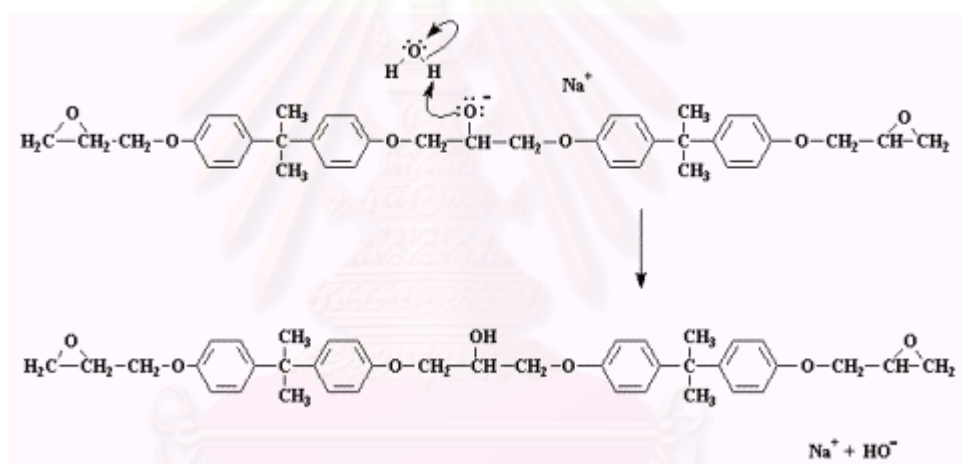


(c) Reaction to form diglycidyl ether of bisphenol A.

Figure 2.10 : Mechanism of the reaction to form DGEBA



(d) Reaction between three epichlorohydrin and two bisphenol A.



(e) Reaction between sodium salt and water.

Figure 2.10 : Mechanism of the reaction to from DGEBA (continued)

สงวนลิขสิทธิ์
จุฬาลงกรณ์มหาวิทยาลัย

2.3.3 BASIC CHARACTERISTICS OF EPOXY RESINS

Epoxy resins possess a number of unusually valuable properties listed as follow [30-32].

2.3.3.1 Versatility

Numerous curing agents for epoxy resins are available, and epoxy resins are compatible with a wide variety of modifiers. Therefore, the properties of cured epoxy resin system can be in wide diversity available for the selection of almost any desired application.

2.3.3.2 Good handling characteristics

Many epoxy systems can be worked at room temperature, and those, which cannot require only moderate heat during mixing. Epoxy resins have definite shelf life before the curing agent is incorporated.

2.3.3.3 Toughness

Cured epoxy resins are approximately seven times tougher than cured phenolic resins [32]. The relative toughness has been attributes to the distance between crosslinking points, which is longer in epoxy resins than phenolic resins [32].

2.3.3.4 Adhesion

Epoxy resins have high adhesive strength due to the polarity of aliphatic hydroxy and ether groups present in the initial resin chain and in the cured system. The polarity of these groups serves to create electromagnetic bonding forces between the epoxy molecule and the adjacent surface [32]. The epoxy groups will react to provide chemical bonds with surfaces where active hydrogens may be found. Since the resin changed from liquid state to solid state, the bonds initially established are preserved.

2.3.3.5 Low shrinkage

The epoxy resins differ from many thermosetting compounds because they give no by-products during cure. Curing is by direct addition and shrinkage is approximately less than 2% [32], which indicates that little internal rearrangement of the molecules is necessary. The condensation and crosslinking of phenolic and polyester resins, on the other hand, yield significantly higher shrinkage values.

2.3.3.6 Inertness

Epoxy resins are highly resistant to a wide range of acids, alkalies, solvents, fuels and corrosive materials. Cured epoxy resins are very inert chemically. The ether groups, the benzene rings and aliphatic hydroxyls in the cured epoxy system are virtually invulnerable to caustic attack and are extremely resistant to acids.

2.3.3.7 Low viscosity

Liquid epoxy resin mixed with respective and their curing agent can provide a liquid system with low viscosity liquid. Hence, it is easy for both applying on a surface and impregnating fibers.

2.3.3.8 High mechanical properties

Mechanical properties of cured epoxy resins are usually greater than most of other resins. This is due to their low shrinkage and relatively unstressed structure after curing. For epoxy, these properties are retained even at elevated temperatures.

2.3.3.9 Electrical properties

Epoxy resin systems exhibit good electrical properties over a range of frequencies and temperatures [32]. They are excellent insulating materials.

2.3.3.10 Thermal stability

The cured epoxy resin systems generally exhibit good thermal stability up to over 250 °C [32].

2.3.3.11 Water resistance

Epoxy resins serves as excellent moisture barriers. Water absorption and moisture vapor transmission in epoxy resins are low.

2.3.3.12 Fungi resistance

Epoxy resin systems exhibit resistance to most fungi. Thus they have found use under adverse tropical conditions.

2.3.4 APPLICATIONS OF EPOXY RESINS

The rapid growth of epoxy resins results from its felicitous combinations of properties. Table 2.1 summarizes the major applications of epoxy resins [33].

Table 2.1 : Major applications of epoxy resins.

Solid Epoxy Resins	Liquid Epoxy Resins
Surface Coatings Electrical	Surface Coatings Electrical Tooling Adhesives Laminates Flooring

2.4 CURING AGENTS

One problem with all the thermosets as coating material is the relationship between the coating stability during storage and the time and temperature required to cure the film after application. This problem can be solved by using “two-package coating”. In two-package coating, the first package contains a resin with one of the reactive groups and the second package contains component with the other reactive group. The latter component is called “curing agent” or “hardener”, which can formulate crosslinks with epoxy resins. This separation keeps the reactive groups away from each other and gives a longer storage life. Before curing, epoxy resins are thermoplastic which can be repeatedly softened by heating and hardened by cooling. Curing is an irreversible change and once the resin has been cured it cannot be recovered again in its original form [23].

Curing agents for epoxies can be divided into two categories: those that give cured films at ambient temperature, and those that require elevated temperature to cure. Ambient temperature cure is predominantly carried out using aliphatic polyamines and polyamides while the heat cure systems use aromatic amines and anhydrides as curing agents.

Selection of curing agents depends upon many factors. Major factors to be considered are the properties imparted by the coating material, reaction temperature, pot life, and cure time. Pot life is the workable time before the coating material begins to harden. Cure time is the time that the coating material takes to harden. As far as ease of processing is concerned, a curing agent with a long pot life, short cure time, and ambient temperature cure is preferable in floor coatings. For that reason, aliphatic amine is selected as the curing agent for most industrial floor coating.

As a result of its high reactivity, aliphatic amine is capable of curing at ambient temperature. Diethylene triamine (DETA) is the most widely used primary aliphatic amine. It is also used in the current research. The structure of DETA is shown in Figure 2.11.

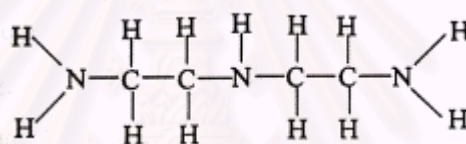


Figure 2.11 : The structure of diethylene triamine (DETA).

The curing reaction between DETA and epoxy resins is exothermic. Properties of DETA-cured resins, such as chemical resistance and electrical resistance, are generally good [31].

2.5 CURING MECHANISM

Epoxy resins coatings obtain their excellent properties through reaction with curing agents. The curing agent reacts with epoxide groups and/or hydroxyl groups of the epoxy resin, to give stable carbon-carbon, carbon-oxygen, or carbon-nitrogen links [29, 32]. It is these stable linkages that confer the epoxy resin film with excellent chemical and solvent resistance.

In curing an epoxy resin with a curing agent, first, the electronegative epoxy oxygen atom sucks electrons away from the carbon atom next to it. The lone pairs of electrons on the amine groups give their electrons to the carbon atom in the end of the molecule. As a consequence, the bond between the carbon atom and the

oxygen atom is broken and a new bond forms between the carbon atom and the amine atom. This produces a negative charge on the oxygen atom, and a positive charge on the nitrogen atom as shown in Figure 2.12 .

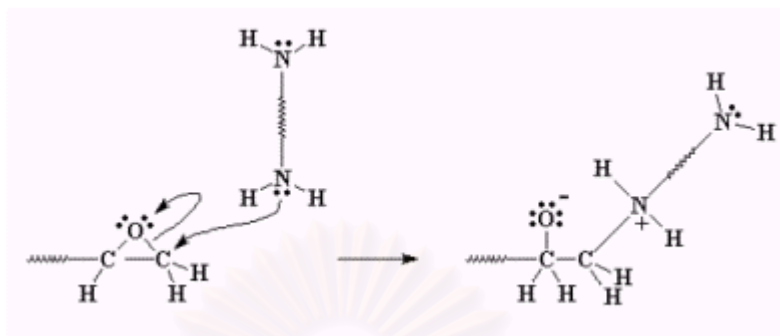


Figure 2.12 : Bonding between carbon atom and nitrogen atom.

Second, in Figure 2.13, excess electrons in oxygen atom are shared with hydrogen atom attached to the positive nitrogen. So, a bond between hydrogen atom and oxygen atom is formed. Separation of hydrogen atom from nitrogen atom makes the positive charge of both nitrogen atom and oxygen atom become neutral. An alcohol group and an amine group are produced now.

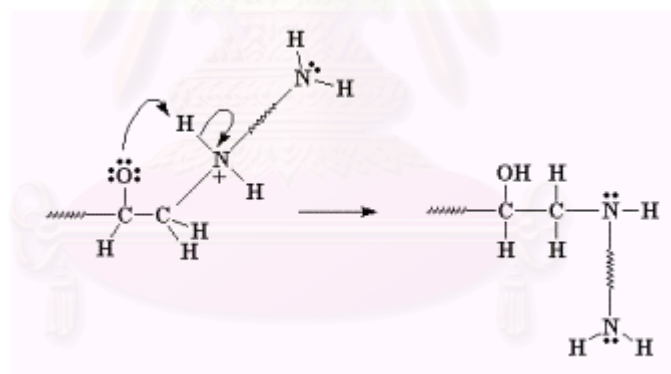


Figure 2.13 : Formation of alcohol group and amine group.

Next, the other hydrogen atom left on amine reacts with another epoxide group in the exact same manner as shown in Figure 2.14 .

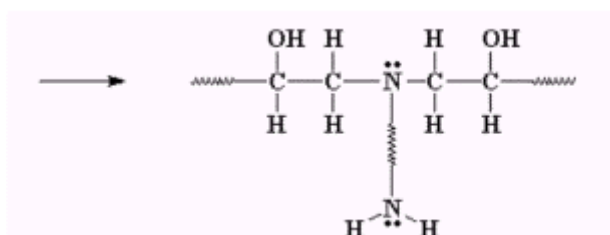


Figure 2.14 : Another epoxide end group is added to the same amine group.

Then, the other amine group reacts with epoxide group as well. In Figure 2.15, four epoxy prepolymers is tied to one diamine molecule.

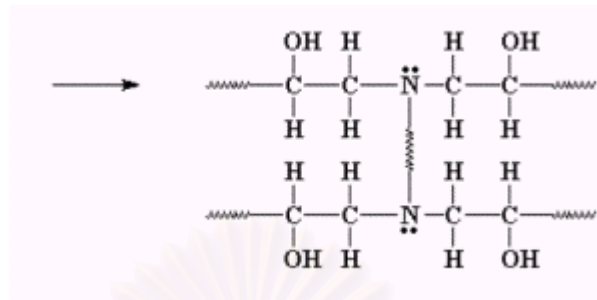


Figure 2.15 : Two more epoxide groups reacts with amine at the other end.

The other ends of the diepoxy prepolymers are attached to other diamine molecules. Finally, all the diamine molecules and all the diepoxy molecules become tied together in one big molecule, a crosslinked network as shown in Figure 2.16 .

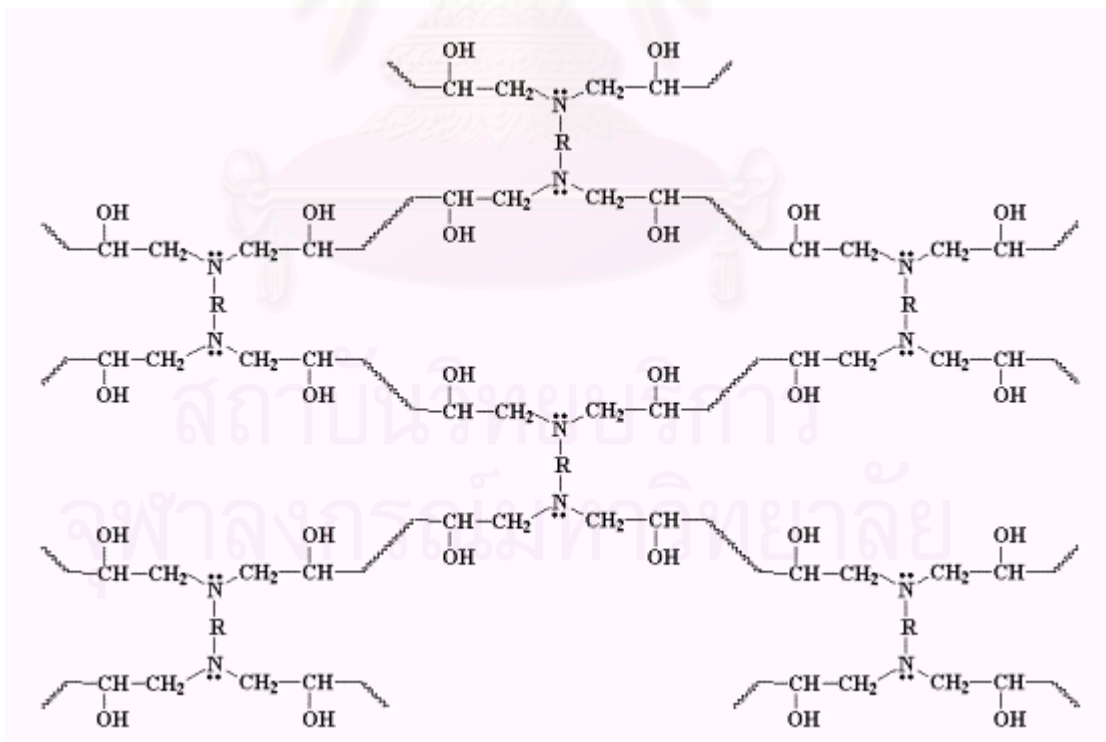


Figure 2.16 : Crosslink network.

2.6 GLASS FIBER

The presence of the reinforcing fibers add strength and stiffness to the final composite which permits applications not normally associated with resinous composites. The combination of high-strength fibers with epoxy resin yields physical properties unsurpassed by other similar materials of construction. Hence, glass fiber is chosen as a reinforcement in the current study. Glass fiber consists primarily of silica (silicon dioxide) and metallic-oxide-modifying elements produced by mechanical drawing of molten glass through a small orifice in general [27, 32].

2.6.1 TYPES OF GLASS FIBER

While several types of glass fibers are used as a reinforcement for composites, only two of them are commonly used. The first one, E-glass, is the most industrially important reinforcement for composites. And the second is S-glass that has roughly thirty percent greater tensile strength and twenty percent greater modulus of elasticity than E-glass. Although S-glass illustrates better properties than E-glass, it is not widely used because of its higher cost. Other glass fiber such as R-glass, C-glass, ECR glass, and AR glass are used in special purposes. Where higher mechanical performance is required, R-glass can be used. For acid and alkali resistance ECR and AR glasses can be used respectively. C-glass is also available for chemical resistant.

2.6.2 GLASS FIBER REINFORCEMENT COMPOSITE

Particular application of each composite has led to various types of fibers so as to fit the individual requisition. The placement of fibers in different directions gives dissimilar properties. Continuous fiber composite shown in Figure 2.17 (a) is used extensively but still encounter delamination or separation of laminae. Figure 2.17 (b) shows a woven fiber composite, which do not have distinct laminae and are not susceptible to delamination, yet strength and stiffness are sacrificed. Chopped fiber composite composes with short fibers dispersed randomly in matrix as shown is Figure 2.17 (c). This type of composite is broadly used owing to low manufacturing cost even though their mechanical properties are inferior to continuous

fiber composites. Figure 2.17 (d) shows a hybrid composite that consists of mixed chopped and continuous fibers [25].

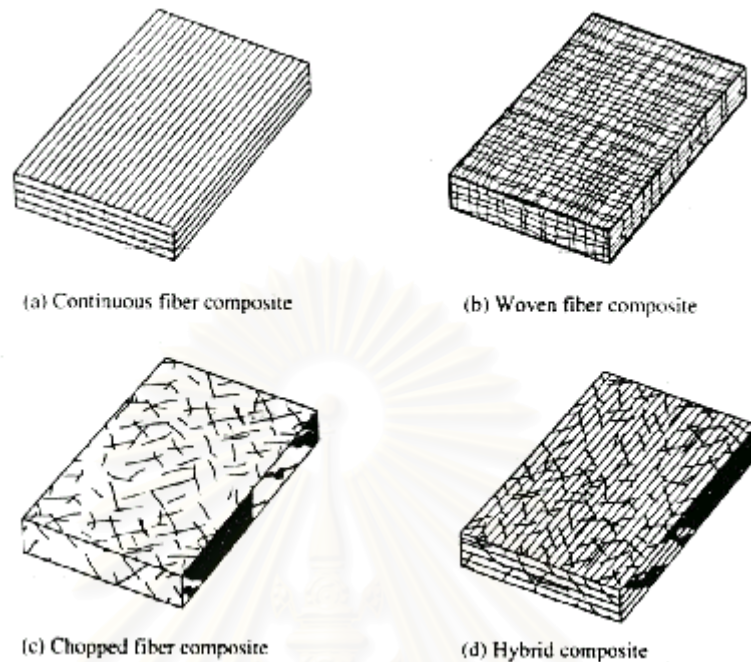


Figure 2.17 : Types of fiber-reinforced composites.

In industrial floor coating, woven fiber is used as a reinforcement as well as in this study.

2.7 SAND

A wide variety of fillers can be used with epoxy systems to reduce cost, shrinkage, exotherm, and coefficient of thermal expansion. Sand can be used as a filler to improve several properties such as mechanical properties and abrasion resistance [34]. Furthermore, sand is very easy to mix with epoxy resins. However, they alter other properties. Hence, the combination of sand used in epoxy systems must be carefully selected to obtain the desired properties.

The performance of an epoxy-sand system is good abrasion resistance, low shrinkage, low thermal coefficient of expansion, high thermal conductivity, and good electrical insulator.

Sand used in the current research is purified by caustic wash to get rid of all chlorides and sulfur residues because chlorides absorb moisture specifically in high humidity countries, which can lead to failure of floor coatings. Furthermore, the

chloride residues in contact with the epoxy resin can lead to reaction causing small bubbles and loose performance of the floor such as cracks.

2.8 FRACTURE OF POLYMERS

The presence of preexisting crack-like flaws such as, impurities or cavities in the material or even defects in the surface, start fractures. For that reason, the prediction of the strength of composites with through-thickness cracks and notches is necessary for a satisfactory material design.

A crack in a solid can be formed in more than one way. The three basic modes of crack deformation are shown as Figure 2.18 . Cracks that are in an opening or tensile mode are referred to as Mode I. Shear within the plane of the material gives the Mode II, in-plane shear or sliding mode. The out-of-plane shear give Mode III , antiplane shear or tearing mode [27, 35]. Of the three, the most fracture mode that occurs is Mode I. This mode is caused by normal loading.

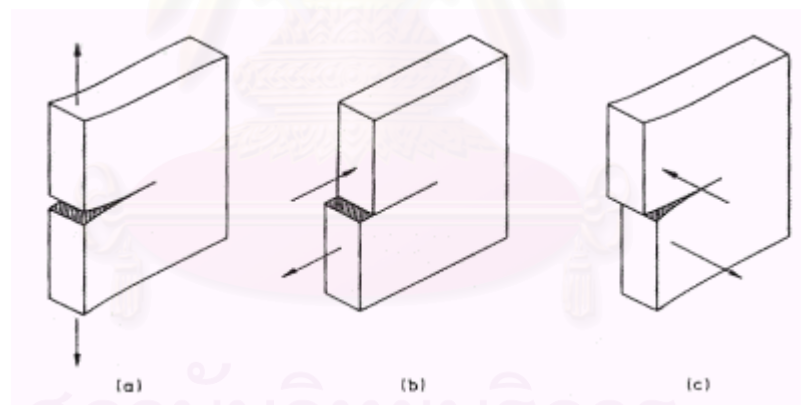


Figure 2.18 : The three modes of crack extension.

2.8.1 Stress intensity factor

When load is applied to a material with a through-thickness flaw, stress is generated in around the flaw as shown in Figure 2.19 .

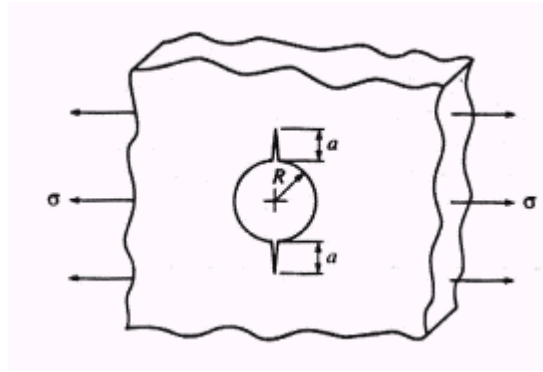


Figure 2.19 : Uniaxially stressed plate with a cracked hole (fracture in Mode I).

Stress intensity factor for Mode I, K_I , is defined by equation 2.1

$$K_I = \sigma \sqrt{\pi a} f\left(\frac{a}{R}\right) \quad 2.1$$

where σ = applied stress

a = length of the crack

R = radius of the crack

$f\left(\frac{a}{R}\right)$ = geometrical function of the crack

When the stress reaches the critical fracture stress, σ_c , the stress intensity factor now is at a critical value corresponding to the critical stress as shown in Equation 2.2 .

$$K_{IC} = \sigma_c \sqrt{\pi a} f\left(\frac{a}{R}\right) \quad 2.2$$

K_{IC} is the critical stress intensity factor. It is a material property that indicates the maximum stress intensity of the material before the crack propagates, in other words, fracture occurs when the stress intensity factor exceeds a critical value, K_{IC} . The critical stress intensity factor obviously depends upon the amount of plastic work that occurs in the growth of the crack, which will depend on the state of stress in the region.

2.8.2 Fracture energy

The loading of an arbitrarily elastic body leads to the definition of strain-energy release rate. Strain-energy release rate for Mode I is G_I . It is synonymous with the stress intensity factor. G_I and K_I are interrelated through the strain-rate dependent Young's modulus, E , as shown in equation 2.3

$$G_I = \frac{K_I^2}{E} \quad 2.3$$

The critical strain-energy release rate, G_{IC} , is related to the critical stress intensity factor, K_{IC} , in the same manner. Equation 2.4 shows this relation.

$$G_{IC} = \frac{K_{IC}^2}{E} \quad 2.4$$

G_{IC} is also called by the term fracture energy or fracture toughness. Fracture energy is the amount of energy required to make the crack propagates. Both K_{IC} and G_{IC} can be used to define toughness of the material.

2.9 STATISTICAL APPROACHES FOR EXPERIMENTAL ANALYSIS

2.9.1 Response Surface Methodology

Response Surface Methodology (RSM) can be used to model or optimize any response that is affected by levels of one or more quantitative factors. Response surface is a plot of the mean response as a function of the treatment combination as in Figure 2.20 .

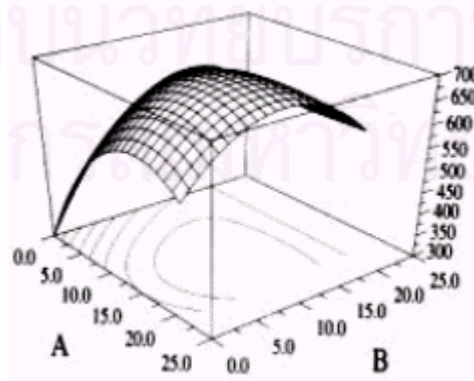


Figure 2.20 : Example of response surface.

RSM not only locate a feasible treatment combination for maximizing or minimizing the mean response but also estimate the response surface in the vicinity of a location in order to understand the local effects of the factors on the mean response [36-39].

The general response surface model is of the form in Equation 2.5

$$y = \eta + e \quad 2.5$$

where y is the response, η is the response surface and e is a random error component. The relationship between the response surface and the independent variables (x_1, x_2, \dots, x_k) is represented as Equation 2.6 .

$$\eta = f(x_1, x_2, \dots, x_k) \quad 2.6$$

When still far from the peak, a first-order model is often adequate. The standard first-order model is a first-order polynomial regression model as shown in Equation 2.7 .

$$y = B_0 + B_1x_1 + B_2x_2 + \dots + B_kx_k + e \quad 2.7$$

As the local response comes close to the peak, the surface generally exhibits greater curvature. A first-order regression model becomes inadequate, exhibiting lack of fit. A higher-order model is fitted instead. The standard second-order model is shown in Equation 2.8 .

$$y = B_0 + \sum_{i=1}^k B_i x_i + \sum_{i=1}^k B_{ii} x_i^2 + \sum_{i=1}^k \sum_{j=1}^k B_{ij} x_i x_j + e \quad 2.8$$

If there is significant lack of fit of the second-order model, a higher-order model could be used.

2.9.2 Central Composite Design

Central Composite Design (CCD) is nowadays the most popular experimental design for fitting a second order design. The size of experiment in this design is reduced for from elder experimental design like 2^k factorial design. CCD consist of a standard first order design with n_f orthogonal factorial (or cube) points, n_o center points and augmented by n_a axial (or star) points. The position of factorial points, center points and axial points are placed ± 1 , 0, and $\pm\alpha$ from the origin

respectively. The number of points depends on the independent variables (k). In rotatable central composite design, the value of α is $2^{k/4}$. Rotatable central composite design for $k = 2$ and $k = 3$ are shown in Figure 2.21 .

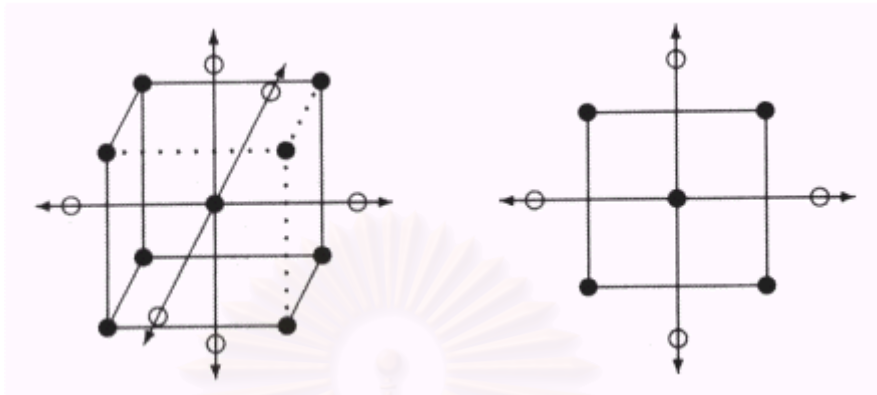


Figure 2.21 : Rotatable central composite designs for $k = 2$ and $k = 3$

From Table 2.2, it is obvious that at a same level of variables rotatable central composite design can reduce the number of experiment from factorial design.

Table 2.2 : Comparison between the number of experiments designed by factorial design and rotatable central composite design at 5 levels of variables.

Number of Independent variables (k)	Number of experiments with 5 levels of variables				
	Factorial (2^k)	Rotatable Central Composite			
		Cube Point	Star Point	Center Point	Total
2	$5^2 = 25$	4	4	5	13
3	$5^3 = 125$	8	6	6	30
4	$5^4 = 625$	16	8	7	31
5	$5^5 = 3,125$	16	10	6	32
6	$5^6 = 15,625$	32	12	9	53

Dealing with numbers of variables, it is more convenient to convert them from actual numerical measures of the variables (X) to standardized (or coded) variables (x) by using Equation 2.9 [39]

$$x = \frac{X - X_0}{t}$$

where X_0 is the center of the region and t is the current region of interest for X .
Examples of rotatable central composite design is shown in Table 2.3 and Table 2.4 .

Table 2.3 : Rotatable central composite design for $k = 2$.

Run	Coded variables of independent variables		Response (y)
	x_1	x_2	
1	-1	-1	y_1
2	1	-1	y_2
3	-1	1	y_3
4	1	1	y_4
5	-1.414	0	y_5
6	1.414	0	y_6
7	0	-1.414	y_7
8	0	1.414	y_8
9	0	0	y_9
10	0	0	y_{10}
11	0	0	y_{11}
12	0	0	y_{12}
13	0	0	y_{13}

Table 2.4 Rotatable central composite design for k = 3.

Run	Coded variables of independent variables			Responses (y)
	x ₁	x ₂	x ₃	
1	-1	-1	-1	y ₁
2	1	-1	-1	y ₂
3	-1	1	-1	y ₃
4	1	1	-1	y ₄
5	-1	-1	1	y ₅
6	1	-1	1	y ₆
7	-1	1	1	y ₇
8	1	1	1	y ₈
9	-1.682	0	0	y ₉
10	1.682	0	0	y ₁₀
11	0	-1.682	0	y ₁₁
12	0	1.682	0	y ₁₂
13	0	0	-1.682	y ₁₃
14	0	0	1.682	y ₁₄
15	0	0	0	y ₁₅
16	0	0	0	y ₁₆
17	0	0	0	y ₁₇
18	0	0	0	y ₁₈
19	0	0	0	y ₁₉
20	0	0	0	y ₂₀

2.9.3 Regression Analysis

Regression analysis is a statistical approach to find the relationship between independent variables and dependent (or response) variables. This relationship is further plotted as a response curve [38].

2.9.3.1 Linear Regression Model

The relationship between the k independent variables x_1, x_2, \dots, x_k and response variable y in first-order linear regression is modeled by Equation 2.10 .

$$y = B_0 + B_1x_1 + B_2x_2 + \dots + B_kx_k + e \quad 2.10$$

Regression coefficients (B) are unknown parameters and e is a random error term. Second-order linear regression can be written as Equation 2.11 .

$$y = B_0 + \sum_{i=1}^k B_i x_i + \sum_{i=1}^k B_{ii} x_i^2 + \sum_{i=1}^k \sum_{j=1}^k B_{ij} x_i x_j + e, (i < j) \quad 2.11$$

The desired equation cannot be received until the regression coefficients are found. In order to obtain these values, least square estimation is proceeded.

2.9.3.2 Least Square Estimation

The relationship between the response variable and independent variables from a set of experiment in Table 2.5 can be written as Equation 2.12

Table 2.5 : Data for multiple linear regression.

Independent Variables				Response Variables
X ₁	X ₂	...	X _k	y
X ₁₁	X ₂₁	...	X _{k1}	y ₁
X ₁₂	X ₂₂	...	X _{k2}	y ₂
⋮	⋮		⋮	⋮
X _{1u}	X _{2u}	...	X _{ku}	y _u
⋮	⋮		⋮	⋮
X _{1n}	X _{2n}	...	X _{kn}	y _n

$$y = B_0 + B_1 x_{1u} + B_2 x_{2u} + \dots + B_k x_{ku} + e_u \quad 2.12$$

y value in equation 2.12 can be estimated with a new equation shown in Equation 2.13

$$\hat{y}_u = b_0 x_{0u} + b_1 x_{1u} + b_2 x_{2u} + \dots + b_k x_{ku} \quad 2.13$$

when $x_{0u} = 1$, $b_0 = B_0$, $b_1 = B_1, \dots$, $b_k = B_k$ and the error of the observed value of y_u from the \hat{y}_u is shown in Equation 2.14 .

$$e_u = y_u - \hat{y}_u \quad 2.14$$

Now, the problem is to estimate $b_0, b_1, b_2, \dots, b_k$ from the sample for the unknown parameters $B_0, B_1, B_2, \dots, B_k$. This can be done by the method of “Least square”. This method minimizes the sum of square, SS_E , of the differences between

the predicted values and the experimental values for the dependent variable. The sum of square can be obtained by using Equation 2.15 .

$$\begin{aligned} SS_y = L &= \sum_{u=1}^n e_u^2 = \sum_{u=1}^n (y_u - \hat{y}_u)^2 \\ &= \sum_{u=1}^n (y_u - b_0 - b_1 x_{1u} - b_2 x_{2u} - \dots - b_k x_{ku})^2 \end{aligned} \quad 2.15$$

To determine the minimum, partial derivatives of L with respect to $b_0, b_1, b_2, \dots, b_k$ are taken and then they are set to equal zero, as shown in Equation 2.16 to 2.19 .

With respect to b_0 :

$$\begin{aligned} \frac{\partial L}{\partial b_0} &= \frac{\partial}{\partial b_0} \left[\sum_{u=1}^n (y_u - b_0 x_{0u} - b_1 x_{1u} - b_2 x_{2u} - \dots - b_k x_{ku})^2 \right] \\ &= -2 \sum_{u=1}^n (y_u - b_0 x_{0u} - b_1 x_{1u} - b_2 x_{2u} - \dots - b_k x_{ku}) \\ &= 0 \end{aligned}$$

then

$$\begin{aligned} -2 \sum_{u=1}^n y_u + 2nb_0 + 2b_1 \sum_{u=1}^n x_{1u} + 2b_2 \sum_{u=1}^n x_{2u} + \dots + 2b_k \sum_{u=1}^n x_{ku} &= 0 \\ nb_0 + b_1 \sum_{u=1}^n x_{1u} + b_2 \sum_{u=1}^n x_{2u} + \dots + b_k \sum_{u=1}^n x_{ku} &= \sum_{u=1}^n y_u \end{aligned} \quad 2.16$$

where $\sum_{u=1}^n x_{0u} = n$, so $b_0 \sum_{u=1}^n x_{0u} = nb_0$

With respect to b_1 :

$$\begin{aligned} \frac{\partial L}{\partial b_1} &= \frac{\partial}{\partial b_1} \left[\sum_{u=1}^n (y_u - b_0 x_{0u} - b_1 x_{1u} - b_2 x_{2u} - \dots - b_k x_{ku})^2 \right] \\ &= -2x_{1u} \sum_{u=1}^n (y_u - b_0 x_{0u} - b_1 x_{1u} - b_2 x_{2u} - \dots - b_k x_{ku}) \\ &= 0 \end{aligned}$$

then

$$\begin{aligned}
 -2 \sum_{u=1}^n x_{1u} y_u + 2nb_0 \sum_{u=1}^n x_{1u} + 2b_1 \sum_{u=1}^n x_{1u}^2 + 2b_2 \sum_{u=1}^n x_{1u} x_{2u} + \dots + 2b_k \sum_{u=1}^n x_{1u} x_{ku} &= 0 \\
 nb_0 \sum_{u=1}^n x_{1u} + b_1 \sum_{u=1}^n x_{1u}^2 + b_2 \sum_{u=1}^n x_{1u} x_{2u} + \dots + b_k \sum_{u=1}^n x_{1u} x_{ku} &= \sum_{u=1}^n x_{1u} y_u \quad 2.17
 \end{aligned}$$

and with respect to b_k :

$$\begin{aligned}
 \frac{\partial L}{\partial b_k} &= \frac{\partial}{\partial b_k} \left[\sum_{u=1}^n (y_u - b_0 x_{0u} - b_1 x_{1u} - b_2 x_{2u} - \dots - b_k x_{ku})^2 \right] \\
 &= -2 x_{ku} \sum_{u=1}^n (y_u - b_0 x_{0u} - b_1 x_{1u} - b_2 x_{2u} - \dots - b_k x_{ku}) \\
 &= 0
 \end{aligned}$$

then

$$\begin{aligned}
 -2 \sum_{u=1}^n x_{ku} y_u + 2nb_0 \sum_{u=1}^n x_{ku} + 2b_1 \sum_{u=1}^n x_{1u} x_{ku} + 2b_2 \sum_{u=1}^n x_{2u} x_{ku} + \dots + 2b_k \sum_{u=1}^n x_{ku}^2 &= 0 \\
 nb_0 \sum_{u=1}^n x_{ku} + b_1 \sum_{u=1}^n x_{1u} x_{ku} + b_2 \sum_{u=1}^n x_{2u} x_{ku} + \dots + b_k \sum_{u=1}^n x_{ku}^2 &= \sum_{u=1}^n x_{ku} y_u \quad 2.18
 \end{aligned}$$

Equations 2.16, 2.17 and 2.18 are called “Normal equations” as

$$\begin{aligned}
 nb_0 + b_1 \sum_{u=1}^n x_{1u} + b_2 \sum_{u=1}^n x_{2u} + \dots + b_k \sum_{u=1}^n x_{ku} &= \sum_{u=1}^n y_u \\
 nb_0 \sum_{u=1}^n x_{1u} + b_1 \sum_{u=1}^n x_{1u}^2 + b_2 \sum_{u=1}^n x_{1u} x_{2u} + \dots + b_k \sum_{u=1}^n x_{1u} x_{ku} &= \sum_{u=1}^n x_{1u} y_u \\
 &\vdots \\
 nb_0 \sum_{u=1}^n x_{ku} + b_1 \sum_{u=1}^n x_{1u} x_{ku} + b_2 \sum_{u=1}^n x_{2u} x_{ku} + \dots + b_k \sum_{u=1}^n x_{ku}^2 &= \sum_{u=1}^n x_{ku} y_u \quad 2.19
 \end{aligned}$$

It is simpler to solve the normal equations if they are expressed in matrix notation as

$$Y = XB + E \quad 2.20$$

where

$$Y = \begin{bmatrix} y_1 \\ y_2 \\ \vdots \\ y_n \end{bmatrix}_{n \times 1} \quad X = \begin{bmatrix} x_{01} & x_{11} & x_{21} & \dots & x_{k1} \\ x_{02} & x_{12} & x_{22} & \dots & x_{k2} \\ \vdots & \vdots & \vdots & \dots & \vdots \\ x_{0k} & x_{1k} & x_{2k} & \dots & x_{kk} \end{bmatrix}_{n \times (k+1)}$$

$$B = \begin{pmatrix} B_0 \\ B_1 \\ B_2 \\ \vdots \\ B_k \end{pmatrix}_{(k+1) \times 1} \quad E = \begin{pmatrix} e_1 \\ e_2 \\ e_3 \\ \vdots \\ e_n \end{pmatrix}_{n \times 1}$$

In general, Y is an $(n \times 1)$ vector of the responses, X is an $n \times (k+1)$ matrix of the levels of the independent variables, B is a $(k+1) \times 1$ vector of the regression coefficients and E is an $(n \times 1)$ vector of random errors.

The solution to the normal equations will be the least square estimators, b . Equation 2.19 may be written in matrix form as shown in Equation 2.21 .

$$\begin{pmatrix} n & \sum X_{1u} & \sum X_{2u} & \dots & \sum X_{ku} \\ n \sum X_{1u} & \sum X_{1u}^2 & \sum X_{1u} X_{2u} & \dots & \sum X_{1u} X_{ku} \\ n \sum X_{2u} & \sum X_{1u} X_{2u} & \sum X_{2u}^2 & \dots & \sum X_{2u} X_{ku} \\ \vdots & \vdots & \vdots & \ddots & \vdots \\ n \sum X_{ku} & \sum X_{1u} X_{ku} & \sum X_{2u} X_{ku} & \dots & \sum X_{ku}^2 \end{pmatrix} \begin{pmatrix} b_0 \\ b_1 \\ b_2 \\ \vdots \\ b_k \end{pmatrix} = \begin{pmatrix} \sum Y_u \\ \sum X_{1u} Y_u \\ \sum X_{2u} Y_u \\ \vdots \\ \sum X_{ku} Y_u \end{pmatrix} \quad 2.21$$

which simplifies to

$$(X'X)b = X'Y \quad 2.22$$

Equations 2.22 are the least squares normal equations. To solve normal equations, multiply both sides of Equation 2.22 by an inverse of $X'X$. Thus, the least square estimator of b is

$$b = (X'X)^{-1} X'Y \quad 2.23$$

where

$$X'Y = (jy) = \begin{pmatrix} 0y \\ 1y \\ \vdots \\ ky \end{pmatrix} \quad 2.24$$

$$(XX)^{-1} = c_{\bar{y}} = \begin{vmatrix} c_{00} & c_{01} & \dots & c_{0k} \\ c_{10} & c_{11} & \dots & c_{1k} \\ \vdots & \vdots & \dots & \vdots \\ c_{k0} & c_{k1} & \dots & c_{kk} \end{vmatrix} \quad 2.25$$

so Equation 2.23 can be rewritten as

$$b_i = \sum_{j=0}^k C_{\bar{y}}(i_j) \quad 2.26$$

2.9.4 Analysis of Variance

One of the most important tools for analyzing data from designed experiments is the analysis of variance (ANOVA). ANOVA analyzes the variation of response by parting the sum of square of deviations as shown in Table 2.6, the ANOVA table.

Table 2.6 : ANOVA table for multiple regression.

Source of Variation	Sum of Square	Degree of Freedom	Mean Square	F ₀
Regression	SS_R	$k(k+3)/2$	MS_R	MS_R/MS_E
- First order terms	SS_{R1}	k	MS_1	MS_1/MS_E
- Second order terms	SS_{R2}	$k(k+1)/2$	MS_2	MS_2/MS_E
Error	SS_E	$n-1-[k(k+3)/2]$	MS_E	
- Lack of Fit	SS_{LOF}	$n_2-[k(k+3)/2]$	MS_{LOF}	MS_{LOF}/MS_{PE}
- Pure Error	SS_{PE}	n_1-1	MS_{PE}	
Total	SS_T	$n-1$		

From the ANOVA table, the total sum of square (SS_T) can be written as Equation 2.27

$$SS_T = SS_R + SS_E \quad 2.27$$

wher SS_T = Total sum of square is overall variability in the data

SS_R = Regression sum of square is variable of responses y due to effect of independent variables x_1, x_2, \dots, x_3

SS_E = Error sum of square is variable of responses due to the influence of uncontrollable factor

The total sum of square (SS_T) is derived from the following equation

$$\begin{aligned}
 SS_T &= \sum_{i=1}^n (y_i - \bar{y})^2 \\
 &= \sum_{i=1}^n y_i^2 - \frac{(\sum_{i=1}^n y_i)^2}{n} \\
 &= \sum_{i=1}^n y_i^2 - \frac{G^2}{n}
 \end{aligned} \tag{2.28}$$

where \bar{y} = The mean of all response

$\sum_{i=1}^n y_i^2$ = Grand total of square

G = Grand total of responses y

$\frac{G^2}{n}$ = Correction factor (CF)

n = Total observations

Thus, SS_T has $n-1$ degrees of freedom. Regression sum of square SS_R may be obtained as shown in Equation 2.29 .

$$SS_R = b_0(0y) + \sum_{i=1}^k b_i(iy) + \sum_{i=1}^k \sum_{j=1}^k b_{ij}(ijy) - \frac{G^2}{n} \tag{2.29}$$

It can also written in the matrix form as shown in Equation 2.30 .

$$SS_R = b'XY - \frac{G^2}{n} \tag{2.30}$$

Regression sum of square estimated with second order polynomial equation has $k(k+3)/2$ degree of freedom and can be categorized into

First order terms regression sum of square (SS_{R1}) with degree of freedom k derived from Equation 2.31 .

$$SS_{R1} = \sum_{i=1}^k b_i(iy) \tag{2.31}$$

Second order terms regression sum of square (SS_{R2}) with degree of freedom $k(k+1)/2$ derived from Equation 2.32 .

$$SS_{R2} = b_0(\sum y) + \sum_{i=1}^k \sum_{j=1}^k b_{ij}(ijy) - \frac{G^2}{n} \quad 2.32$$

2.9.4.1 Lack of Fit

When using a regression model to show the relationship between the response and the independent variable, it is important to check that the model is adequate for estimating. Lack of fit is a term used in doing this.

The error sum of square consists of two components as shown in Equation 2.33.

$$SS_E = SS_{PE} + SS_{LOF} \quad 2.33$$

where SS_{PE} is the sum of squares attributable to "pure" experimental error, and SS_{LOF} is the sum of squares attributable to the lack of fit of the model.

$$SS_E = \sum_{i=1}^n (y_i - \hat{y}_i)^2 \quad 2.34$$

Equation 2.34 may be written in matrix form as shown in Equation 2.35

$$\begin{aligned} SS_E &= (Y - Xb)'(Y - Xb) \\ &= Y'Y - b'X'Y \end{aligned} \quad 2.35$$

A derivative of Equation 2.27 yields the SS_E as shown in Equation 2.36.

$$SS_E = SS_T - SS_R \quad 2.36$$

The pure error sum of squares, SS_{PE} , is computed from the responses obtained by repeated observations at the same level of x at the center point (0, 0, ..., 0) of the central composite rotatable experimental design. The pure error sum of squares, SS_{PE} , could be obtained by

$$SS_{PE} = \sum_{u=1}^n (y_{1u} - \bar{y}_1)^2 \quad 2.37$$

when y_{lu} is the response of each experiment at the center point. The sum of square for lack of fit is as shown in Equation 2.38.

$$SS_{LOF} = SS_E - SS_{PE} \quad 2.38$$

2.9.4.2 Hypothesis Testing in Multiple Linear Regression

A statistical hypothesis is a statement or claim about some unrealized true state of nature. Testing for significance of regression is a test to determine if there is a linear relationship between the response y and a subset of the independent variables, x_1, x_2, \dots, x_k . If the response depends on the independent variables, at least one regression coefficient is not zero. The actual hypothesis to be tested consist of two complementary statements about the true state of nature, which are

$$H_0 : B_1 = B_2 = \dots = B_k = 0$$

$$H_1 : B_i \neq 0 \text{ for at least one } i \quad 2.39$$

The total sum of squares, SS_T , is partitioned into regression and error sums of squares, SS_E and SS_R are independent. Therefore, the hypothesis is tested by calculating F_0 :

$$F_0 = \frac{\frac{SS_R}{k(k+3)}}{\frac{SS_E}{n-1-\frac{k(k+3)}{2}}} = \frac{MS_R}{MS_E} \quad 2.40$$

where MS_R and MS_E are called mean square of regression and error respectively.

Rejection of H_0 in Equation 2.39 if $F_0 > F_{\alpha, v_1, v_2}$ implies that at least one variable in the model contributes significantly to the fit. On the other hand, in case H_0 is accepted, if $F_0 < F_{\alpha, v_1, v_2}$; H implies that response has no relationship with independent variables x_1, x_2, \dots, x_k .

F_{α, v_1, v_2} could be obtained from table in index D in which α means the level of significance at a degree of confidence $1 - \alpha$. The term v_1 is the degree of freedom of the numerator in Equation 2.39 and v_2 is the degree of freedom of the denominator.

Once the hypothesis is checked and a relationship between the response and the independent variables is accepted. The next step is to find whether to model fits for the relationship or not by checking lack of fit.

Lack of fit can be tested by using F_0 shown in Equation 2.41

$$F_0 = \frac{\frac{SS_{LOF}}{n_2 - \frac{k(k+3)}{2}}}{\frac{SS_{PE}}{n_1 - 1}} = \frac{MS_{LOF}}{MS_{PE}} \quad 2.41$$

From the hypotheses

H_0 : The model adequately fits the data

H_1 : The model does not fit the data 2.42

If $F_0 > F_{\alpha, v_1, v_2}$; rejecting H_0 , this indicates that the model does not fit the data. If $F_0 < F_{\alpha, v_1, v_2}$ accepting H_0 , this indicates that the model fits the data.

There is frequent interest in testing hypotheses on the individual regression coefficients. Such test would be useful in determining the value of each of the independent variables in the regression model.

The hypotheses for testing the significance of any individual regression coefficient, b_i , are

H_0 : $b_i = 0$

H_1 : $b_i \neq 0$ 2.43

If H_0 : $b_i = 0$ is not rejected, then this indicates that x_i can be deleted from the model. The appropriate test statistic for this hypothesis is

$$t_0 = \frac{b_i}{\sqrt{MS_E C_{ii}}} \quad 2.44$$

The hypothesis H_0 : $b_i = 0$ is rejected if $|t_0| > t_{\alpha/2, v_1}$. Where C_{ii} is the diagonal element of $(X'X)^{-1}$ corresponding to b_i and v is the degree of freedom of

error. It should be noted that this is really a partial or marginal test, because the regression coefficient, b_i , depends on all the other regressor variables x_j ($i \neq j$) that are in the model.

2.9.4.3 Cross Validation

When conducting simple linear or multiple linear regression, coefficient of determination (R^2) is used as a measure of strength of the model [37]. R^2 is defined as Equation 2.45

$$R^2 = \frac{SS_R}{SS_T} = 1 - \frac{SS_E}{SS_T} \quad 2.45$$

It measures the proportionate reduction of total variation in Y associated with the use of the set of X variables x_1, x_2, \dots, x_k . Since $0 \leq SS_E \leq SS_T$, it follows that

$$0 \leq R^2 \leq 1 \quad 2.46$$

R^2 assumes the value 0 when all $b_i = 0$ ($i = 0, 1, \dots, k$). R^2 takes on the value 1 when all observations fall directly on the fitted response surface, that is, when $y_u = \hat{y}_u$ for all u .

R^2 is dependent on the model, the sample and the sample size. It is possible to continue to add variables up to $k = n - 1$ to produce an R^2 , which is monotonically increasing up to 1.0. This result in an overfit condition that inaccurately predicts the strength of the model. To compensate for models with large numbers of terms compared to number of observations, the adjusted coefficient of determination (R_a^2) value is used instead.

$$R_a^2 = 1 - \frac{\frac{SS_E}{(n-k-1)}}{\frac{SS_T}{(n-1)}} = 1 + \frac{(n+1)}{(n-k-1)}(R^2 - 1) \quad 2.47$$

CHAPTER III

LITERATURE REVIEW

One of the aims of the current investigation concentrates on finding the suitable condition for curing epoxy-composite coating for industrial floor coating. The following literatures in this chapter review the physical, chemical and mechanical properties of epoxy coating technology.

M. Gaschke, *et al.* [2] studied the performance of epoxy-coatings by using DGEBA epoxy resin and various curing agents including aliphatic polyamines, aromatic polyamines and cycloaliphatic polyamines. The result drawn from their experiment showed that the chemical resistance produced by different curing agents varies, as did the pot-life, viscosity and time to handle with the liquid epoxy-coating before it crosslinked to form a solid coating. Curing agents with higher molecular weight exhibited better chemical resistance due to higher crosslink density. The chemical resistance of both short-chain aliphatic polyamine and oxyalkylated short-chain polyamine for distilled water, inorganic acids, alkalies and dilute alcohol is excellent but for dilute organic acid was poor. Using long-chain polyamine adduct produced a better dilute organic acid resistant but the viscosity increased about twice. Though higher viscosity gave longer pot-life, the epoxy-coating was more difficult to handle. Aromatic polyamine adduct was a perfect curing agent for dilute organic acid resistance but it had even higher viscosity. However, epoxy-coating using these curing agents gave poor chlorinated solvents resistant. Cycloaliphatic polyamine was the only curing agent that could be used for chlorinated hydrocarbons resistant. It also possesses low viscosity, but its resistance for acids were a tradeoff. Cycloaliphatic polyamine had poor acid resistance property. So, the choice of curing agent for the epoxy system depends upon the required performance.

Marianne DiBenedetto [3] studied the chemical resistance of multifunctional epoxy resins namely, epoxy phenol novolac (EPN), epoxy cresol novolac (ECN) and triglycidyl para-aminophenol (TGpAP) by using DGEBA as a control epoxy resin. The curing agents used in this study were cycloaliphatic polyamines. Relative to the control, the system containing the EPN resin exhibited a threefolded improvement in acetic acid and ammonium hydroxide resistance, a

sixfolded improvement in ethanol resistance and thirty fourfolded improvement in methanol resistance. The use of ECN resin was not as effective, but did extend the resistance to include a twofolded improvement to acetone. Resistance to HCl, however, was decrease. This was probably caused by steric hindrance due to the presence of the ortho-methyl groups in this material. The group was believed to prevent the formation of higher degree of crosslink density. As a result, the ECN is not an effective upgrader. On the contrary, the most dramatic results were found in the TGpAP system. Although both inorganic and organic acid resistance was lost, startling improvements were obtained in the resistance to acetone, methyl ethyl ketone, ammonium hydroxide, butyl acetate, methylene chloride, trichloroethylene and ethanol. The loss of acid resistance was explained by the presence of the amino nitrogen in the molecule. This site was quite vulnerable to the attack by acids. Mechanical properties were also investigated. All pot lives were found to be similar to that of the control with the exception of the system based on the ECN resin. The EPN-based system exhibited a faster dust dry time than other systems. Impact resistance and film appearance properties were fairly comparable for all systems. However, there was a major difference in adhesion. DGEBA, the control, exhibited excellent adhesion, while that of the other systems was only considered as fair.

In-Chul Choy, *et al.* [4] analyzed the physical properties of epoxy resins during and after curing. The coating system comprised of DGEBA epoxy resin and DDS (4,4'-diamino diphenyl sulfone) curing agent. During curing of epoxy resin, the volume contraction occurred. This was a result of the exchange of Van der Waals bonds for shorter covalent bonds when the resin was cured. The decrease in the volume continued while the curing temperature was constant. When exothermic started, the specific volume increased and decreased again after the temperature cooled down. The volume change after the exothermic occurred was only a change induced by temperature. The viscosity of liquid epoxy resin increased gradually at first and increased rapidly to above 10^5 poise, the curing resin ceased to behave simply as a viscous liquid. It became markedly viscoelastic for a period of time. After the gelation point, when the covalent bonded molecular network extended throughout the sample, the viscosity became infinite. The liquid resin was crosslinked to solid. In case of incomplete curing, additional postcuring at room temperature by epoxy itself is found. However, incompletely cured samples had lower glass

transition temperature (T_g) and therefore contracted with a larger thermal expansion coefficient to higher densities.

J.C. Graham, *et al.* [5] investigated the effect of temperature and relative humidity on intercoat adhesion failure of aliphatic amine cured by epoxy coating. The epoxy resin and amine crosslinking agent used in this study was DGEBA and polypropylene glycol amine, respectively. The mixed material was applied to concrete blocks. Absorption of moisture into the cured epoxy/amine system often resulted in a decrease in mechanical properties. This absorption depended on the amount of the amine used; with those systems containing more than an equivalent amount of amine absorb more water. In general, the amount of water absorbed ranged between 2 and 5% of the weight of the film. The intercoat adhesion appeared to be dependent on both the temperature and the humidity. At room temperature or above, intercoat adhesion failure occurred only at extremely high humidities, whereas, at lower temperatures approaching 13 °C, intercoat adhesion failure could occur at relative humidities as low as 40%. The reason for the temperature and humidity effect on delamination appeared to be related to the unreacted amine that formed carbamate salts from reaction with CO₂. Carbamate salt at or near the surface result in incomplete crosslinking at the interface might be involved in intercoat adhesion failure.

Won Ho Jo and Kyoung Jin Ko [6] studied the effects of physical aging on the thermal and mechanical properties of an epoxy polymer. The epoxy resin and the curing agent used were DGEBA and ethylene diamine (EDA) respectively. The mixing ratio was varied. As the epoxies were aged, the density and modulus increased. The determining factor of glassy state modulus was packing density, but not the crosslink density. The yield stress of an aged specimen seemed to be related to the packing density like modulus; however, in the quenched state, the yield stress seemed to be more related to the crosslink density. That was, in the lower free volume state, the major factor, which determined the properties of epoxy polymer, was the packing density. However, in the state of sufficient free volume, the major factor that determined the properties of cured epoxies was crosslink density. The effect of composition was described as followed. The highest T_g was observed at a little excess amine system and the T_g of the DGEBA excess side decreases more sharply than that of the EDA excess side. Though the equal stoichiometry of an

epoxy/amine system should give the highest crosslink density theoretically, the curing reaction does not occur completely due to a steric hindrance. In the cured epoxy polymer of a stoichiometric nonequivalent mixing ratio, there existed greater numbers of unreacted functional groups than in the equal stoichiometry. Unreacted functional groups had higher enthalpy difference between the quenched and aged specimens than the crosslink groups. Therefore, the more distance from the stoichiometry, the higher the degree of an enthalpy recovery.

Eliane Urbaczewski-Espuche, *et al.* [7] analyzed the influence of adding diepoxy aliphatic diluent on the fracture behavior of epoxy/amine networks. The network comprised of DGEBA epoxy resin, 4,4' diamino 3,3' dimethyldicyclohexylmethane cycloaliphatic diamine curing agent, and 1,4 butanediol diglycidyl ether (DGEBD) aliphatic epoxy diluent. Results from this study showed that the introduction of DGEBD in the network had two opposing effects: it decreased the average molecular weight between crosslinks while increasing the chain flexibility. The non linear dependence of fracture energy (G_{Ic}) on the amount of DGEBD might be considered with these two aspects. The variation of G_{Ic} reflected both the increase in the toughness of the network and the decrease in Young's modulus and shows a stronger dependence on the DGEBD content than stress intensity factor or fracture toughness (K_{Ic}) did. In addition, crack propagation was related to the ability of the networks to deform plastically. When the amount of DGEBD was added, the ability to deform plastically decreased.

F. Fernandez-Nogrago, *et al.* [8] studied the mechanical properties of amine based epoxy coating as a function of stoichiometry. DGEBA was the selected epoxy resin. Two poly(propylene oxide) (PPO) based polyamines, poly(propylene oxide) diamine and poly(propylene oxide) triamine was used as curing agents. Results from three-point loading showed that both systems exhibited the best mechanical property at epoxy-rich composition around a stoichiometric ratio of 0.8-0.9. Both elastic modulus and strength reached their maximum at the aforementioned ratio. The lower strength presented by the mixtures richer in epoxy was undoubtedly due to the network imperfections such as holes and uncrosslinked chain-ends. On the other hand, at stoichiometric and amine-rich compositions, the yield stress and the strength at break slowed down as amine content increased. Contradictorily, the best composition giving the highest fracture toughness for both mixtures was an amine-

rich composition of 1.0-1.2. The fracture toughness increased when the amount of amine increased and attained the maximum value at a composition a little higher than the stoichiometric ratio. Then, the fracture toughness decreased when the composition was much greater than the stoichiometric one. The result of this investigation showed that a small amount of amine made the epoxy-coating brittle. This can be improved by adding the amine composition, but amine-rich mixtures with too much amine would reduce the strength of the coating material. However, the change in fracture toughness from varying the composition in each curing agent was different. This was because the fracture toughness might be taken as a property related to the strength and the ductility of the material, and thus depended on factors such as crosslink density, chemical structure, intermolecular packing and molecular building network.

L. Barral, *et al.* [9] analyzed the effect of thermal degradation on the impact strength of cured epoxy resin system. The resin used was DGEBA and the curing agent was acycloaliphatic diamine, 1, 3-bisamino-methylcyclohexane (1,3-BAC). The mixture was subjected to two different curing cycles. A long cycle consists of 24 hours at room temperature followed by 8 hours at 60 °C, and a post cure of 2 hours at 120 °C, while a short cycle was not cured at 60 °C. The experimental results showed that the material cured with the long cycle had better impact strength at any aging time. There was a decrease in the value of the Izod impact strength when the thermal aging was increased for the two cycles, and also the material cured with the long cycle presented a higher value of the Izod impact strength than those cured one with the short cycle for the same aging time. Moreover, the variation of the Izod impact strength with aging time was related with the variation of the peak of β transition in $\tan \delta$ curve obtained by dynamic mechanical analysis (DMA). A relation between the decrease in the intensity of the β peak and a decrease of the Izod impact strength as thermal aging was increased was found. Phase morphology of samples was also examined. There is a good correlation between the increase in fragility of the material with aging time and the morphology of fracture surfaces observed by SEM. The fracture surfaces for the specimens of the material cured with the short cycle presented four characteristics zone; a defect initiation zone, a smooth mirror-like zone, a slightly less smooth zone and a rough three-dimension zone. In the last

zone mentioned, trend about the depth of the folds and the separation between two folds with aging time that in the material cured with both cycles was the same.

Anthony E. Mayr, *et al.* [10, 11] investigated the effect of strain rate, composition and temperature on the yielding behavior in epoxy thermosets by selecting DGEBA epoxy resin and two similar pairs of curing agent. The aliphatic butylamine (BA) and its dimeric analogue, diamino-octane (DAO), along with the aromatic aniline (An) and the dimeric analogue, diaminodiphenyl methane (DDM) were selected as curing agents. Result from studying the curing behavior illustrated that despite the chemical similarity in molecular structure between the two aliphatic amines or aromatic amines, a linear chain structure resulted from the copolymerization of DGEBA with monoamine whilst diamine curing produced a three-dimensional network. The T_g values of DGEBA epoxy resin cured with BA, DAO, An and DDM were 56, 104, 86, 166 °C respectively. The T_g increased as the crosslink density was raised for the two series and the aromatic-based amines had a higher T_g than the corresponding aliphatic analogues. Result from studying the yielding behavior by compression test showed that aromatic-amine based networks exhibited a higher yield stress than that of the epoxies cure with aliphatic amines. The network cured with the aromatic amines have a much stiffer and/or bulkier backbone due to the benzene rings inhibiting molecular movement and thus requiring higher stresses for the molecular segments to slide past each other during the yielding process. Additionally, when the curing temperature increased, the yield strain and yield stress in all systems decreased until at the T_g where no yielding was observed. At each temperature for both amine series, the yield stress increased when the crosslink density was raised. At low temperature, the epoxies cured with aromatic amines exhibited a higher yield stress than those with the aliphatic amine systems. However, this trend was not observed at temperature approaching the T_g .

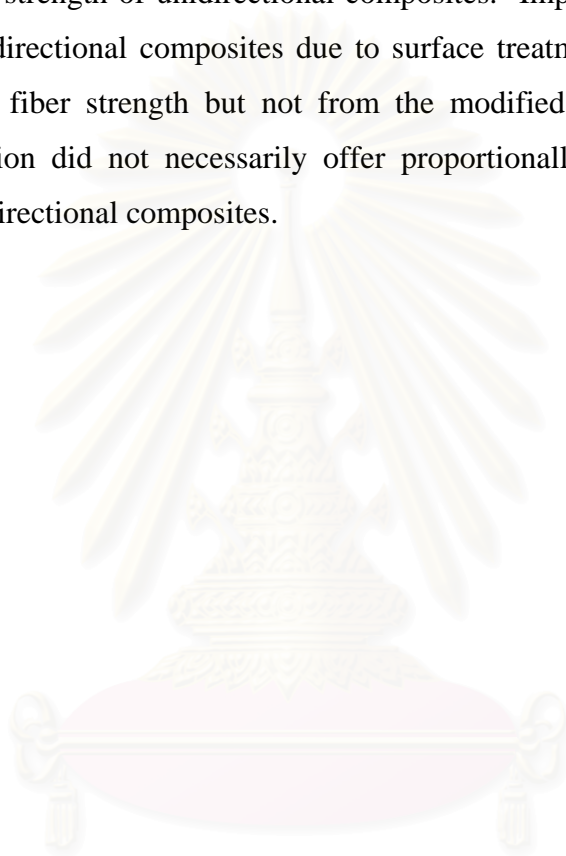
F. Ellyin and C. Rohrbacher [12] studied the effect of aqueous environment and temperature on glass fiber-epoxy resin composites. Results drawn from this research illustrated that the degree of damage strongly depended on the immersion temperature. At temperatures below 35 °C, the rate of moisture absorption reached a saturated state at about 0.8% moisture content, but at 90 °C, no saturation state was observed. The mechanical properties of the composite laminates were not appreciably affected by moisture absorption at temperatures below 35 °C. In contrary,

the strength and ductility are decreased as a result of immersion in 90 °C. The reason for this was because glass fiber reinforced-epoxy resin matrix composites absorbed moisture and swelled when it was immersed in distilled water. This led to plasticization and swelling of the matrix and a release of thermal residual stresses. Moreover, the threshold strain for the matrix crack initiation increased when the laminate were immersed in ambient water in comparison to that of a dry environment. Immersion at high water temperature led to embrittlement of the glass fibers and matrix blistering resulting in a slight decrease in the threshold crack initiation strain.

M. Alagar, *et al.* [13] investigated mechanical properties of E-glass-reinforced siliconized epoxy polymer composites by using DGEBA epoxy resin and three curing agents: aliphatic amine, aromatic amine and polyamidoamine. A silane derivative, γ -aminopropytriethoxysilane, was used for curing hydroxyl terminated polydimethylsiloxane and for the formation of network structure with epoxy resins along with dibutyltindilaurate catalyst. From the data gathered in the mechanical studies, it was inferred that the siloxane introduction imparts flexibility to the epoxy resin system and in turn improved the impact behavior and percentage elongation at breaking level. Impact strength of E-glass reinforced composites made from the siliconized epoxy resin was enhanced to 2-4 times over that measured on the composites made from a pure epoxy resin. Hence, the siliconized epoxy matrix resin system was more suitable than pure epoxy resin system for the fabrication of composites for high impact performance engineering applications. However, siloxane had a flexible molecular structure. For that reason, the introduction of siloxane into the epoxy skeleton decreased the value of tensile strength and flexural strength with an increase in amount of siloxane moiety. Comparison among the curing agents showed that composites cured with aromatic amine imparted better mechanical properties than those cured with aliphatic amine and polyamidoamine. This was due to the orientation of rigid molecular structures in the aromatic amine.

F. M. Zhao and N. Takeda [14] studied the effect of interfacial adhesion and statistical fiber strength on tensile strength of unidirectional glass fiber /epoxy composites. DGEBA epoxy resin and triethylenetetramine (TETA) were used as the matrix system. Many kinds of surface treatments for glass fiber were used. The experimental results showed that the maximum ultimate tensile strength was obtained for the relatively strong interfacial adhesion (glass/ γ -methacryloxypropyl-

trimethoxysilane, MPS/epoxy), but not for the strongest interfacial adhesion (glass/ γ -glycidooxypropyltrimethoxysilane, GPS/epoxy). For the interface of glass/ γ -MPS/epoxy, the micro-damage was the interface debonding along the interface and an associated matrix crack. For the interface of glass/ γ -GPS/epoxy, the micro-damage was matrix-crack-controlled. The result indicated that the micro-damage mode related to interfacial adhesion strongly affected the fracture process, and thus the ultimate tensile strength of unidirectional composites. Improving of ultimate tensile strength of unidirectional composites due to surface treatments mainly results from the increase in fiber strength but not from the modified interface. The stronger interface adhesion did not necessarily offer proportionally higher ultimate tensile strength of unidirectional composites.



สถาบันวิทยบริการ
จุฬาลงกรณ์มหาวิทยาลัย

CHAPTER IV

EXPERIMENTAL WORK

The experimental work for this study was pursued in order to investigate the most appropriate condition for coating and curing epoxy resin for industrial floor coating. This chapter includes selection of raw materials, processing of the selected materials, proposal of experimental design, characterizing and testing conducted to evaluate the mechanical properties of the coating prepared.

4.1 MATERIALS

4.1.1 Epoxy Resins

Many types of epoxy resin can be used in industrial floor coating. The choice of epoxy resins would depend on the particular requirements of the coating material. One of the most widely used epoxy resins in many industries is diglycidyl ether of bisphenol-A (DGEBA), the structure of which is shown in Figure 4.1 .

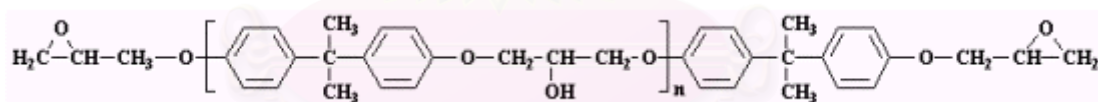


Figure 4.1 : The chemical structure of diglycidyl ether of bisphenol-A (DGEBA).

DGEBA can be cured at room temperature. It gives a coating material with excellent adhesion, chemical resistance and mechanical property, which fits the application of industrial floor coating. In the present work, DGEBA manufactured by Shell Chemical Company Limited under the trade name of EPIKOTE 828 is used. The epoxy content is about 5,260-5,420 millimol/kg. Its molecular weight is 380. It is a colorless liquid with viscosity about 12-14 Pa.s at ambient temperature and a density of 1,160 kg/m³.

4.1.2 Curing Agents

Curing agent was selected based on the chosen epoxy resin. Diethylene triamine (DETA). Its chemical structure is shown in Figure 4.2, is a suitable curing agent for curing at room temperature.

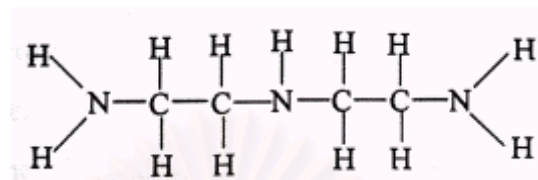


Figure 4.2 : The chemical structure of diethylene triamine (DETA).

DETA allows adequate pot life for processing whilst requires quite a short time for gelation. It also gives a coating with high chemical resistant. In this study, DETA from Shell Chemical Company Limited with 98% amine content is used. Its molecular weight is 103. It is a light, colorless liquid with a density of 952 kg/m³.

4.1.3 Glass Fiber

In order to enhance the mechanical properties of the coating material, woven E-glass fiber is used as a reinforcement. Its structure is 1x1 woven cloth with density of 1.111 kg/m³. The glass fiber was produced by Thai Vetrotech Company Limited and woven by Asia Kung Num Company Limited. The glass fiber has been coated with silane coupling agent to promote adhesion at the interface between epoxy resin and glass fiber.

4.1.4 Sand

Sand is used as a filler in the coating material in order to improve some mechanical properties as well as to reduce cost. In this research, purified sand with a particle size up to 0.8 mm is used. It was obtained from Thai-German Industries Company Limited. Sand was caustic washed to eliminate all chlorides and sulfur residues as chlorides can absorb moisture, especially in highly humid countries like Thailand.

4.1.5 Concrete

Concrete is a composite material that consists essentially of binding mediums. These mediums are embedded particles or fragments of relatively inert mineral filler. Mixture of concrete is a carefully proportioned of cement, water, fine aggregate, and coarse aggregate. After appropriate reaction with water, cement develops adhesive and cohesive properties necessary to bond the inert aggregates into a solid mass of adequate strength and durability. Any material that can pass No. 4 sieve or smaller than 3/16" in diameter is classified as fine aggregate, while materials coarser than those aforementioned are classified as coarse aggregate [40-44]. Figure 4.3 shows macroscopically the fine and coarse aggregates in concrete [45].

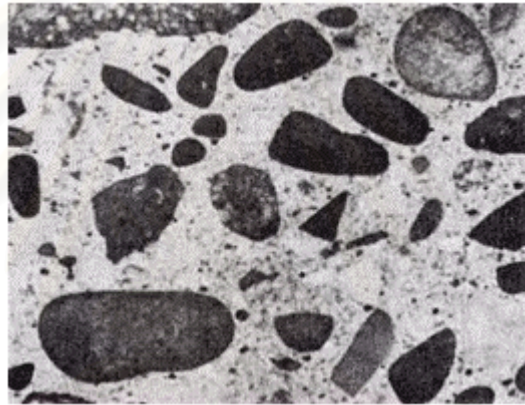


Figure 4.3 : Section through concrete showing aggregate.

This research models a concrete floor by using a cube concrete of 150 mm x 150 mm x 150 mm. They are then coated on one side with the proposed glass fiber-reinforced epoxy composite coating material. Portland cement for making structural concrete is used in this study. Construction sand and rock of 1 inch in diameter are used as fine and coarse aggregates respectively.

4.1.6 Mortar

Mortar is used instead of concrete as a substrate for the impact test in the present study. This is because the dimensions of the specimen for the impact are too small to be formed from concrete, of which rock is an important constituent. Mortar is simply described by concrete without the mixture of rock. The cement and

sand used for the preparation of mortar in this study are identical materials used in the preparation of concrete.

4.2 EXPERIMENTAL DESIGN

Three independent variables of which are cure temperature, cure time and amount of sand are examined in this research. Designing the condition for curing epoxy composite systems to cover these variables requires numerous experimental samples and runs, which are costly and time-consuming. In order to minimize the number of experiments in the present study, an experimental design had been applied so that the results, obtained from a minimal number of experiments, would still be statistically conclusive. The experimental design in this study was conducted following the technique of Central Composite Rotatable (CCR) design for 3 independent variables, which consist of 20 experimental runs. Table 4.1 showed the curing conditions for each run, which were derived from the center points (0), cube points (± 1), and star points (± 1.682) described in chapter 2.

In this study, certain constrains are considered in the experimental design upon selecting the abovementioned points. Firstly, the highest cure temperature (in run 10 from Table 4.1) must not be too high because this may cause an over cure condition. Secondly, the shortest cure time (in run 11 from Table 4.1) must be long enough to give a fully cured specimen. A preliminary test was performed in order to find the curing range following these constrains, which showed that epoxy composites might not be cured at temperatures higher than 110 °C and not less than 15 h. The suitable curing condition from the preliminary test is tabulated in Table 4.2 .

สถาบันวิทยบริการ
จุฬาลงกรณ์มหาวิทยาลัย

Table 4.1 : Central Composite Rotatable design for three dependent variables.

Experimental	Coded variables of independent variables			Responses (y)
	Cure temperature (°C)	Cure time (h)	Amount of sand (%)	
1	-1	-1	-1	y ₁
2	1	-1	-1	y ₂
3	-1	1	-1	y ₃
4	1	1	-1	y ₄
5	-1	-1	1	y ₅
6	1	-1	1	y ₆
7	-1	1	1	y ₇
8	1	1	1	y ₈
9	-1.682	0	0	y ₉
10	1.682	0	0	y ₁₀
11	0	-1.682	0	y ₁₁
12	0	1.682	0	y ₁₂
13	0	0	-1.682	y ₁₃
14	0	0	1.682	y ₁₄
15	0	0	0	y ₁₅
16	0	0	0	y ₁₆
17	0	0	0	y ₁₇
18	0	0	0	y ₁₈
19	0	0	0	y ₁₉
20	0	0	0	y ₂₀

Table 4.2 : Appropriate curing condition at center point, cube point and star point.

Independent Variables	Star Point (-1.682)	Cube Point (-1)	Center Point (0)	Cube Point (1)	Star Point (1.682)
Cure temperature (°C)	31	45	65	85	99
Cure time (h)	15.8	24	36	48	56.2
Amount of sand (% by volume)	15.23	20	27	34	38.77

From Table 4.1 and Table 4.2, the most appropriate range of cure conditions in each experimental run can be summarized as illustrated in Table 4.3 .

Table 4.3 : Most appropriate test condition from the experimental design.

Run	Coded variables of independent variables			Responses (y)
	Cure Temperature (°C)	Cure time (h)	Sand (%)	
1	45	24	20	y ₁
2	85	24	20	y ₂
3	45	48	20	y ₃
4	85	48	20	y ₄
5	45	24	34	y ₅
6	85	24	34	y ₆
7	45	48	34	y ₇
8	85	48	34	y ₈
9	31	36	27	y ₉
10	99	36	27	y ₁₀
11	65	15.8	27	y ₁₁
12	65	56.2	27	y ₁₂
13	65	36	15.23	y ₁₃
14	65	36	38.77	y ₁₄
15	65	36	27	y ₁₅
16	65	36	27	y ₁₆
17	65	36	27	y ₁₇
18	65	36	27	y ₁₈
19	65	36	27	y ₁₉
20	65	36	27	y ₂₀

4.3 MATERIAL PROCESSING

4.3.1 Preparation of Epoxy Composites

4.3.1.1 Cure of Epoxy with the Curing Agent

DGEBA epoxy resins was mixed with the DETA curing agent. The amount used was at stoichiometry. Since two atoms of carbon in DGEBA are capable of reacting with five atoms of nitrogen in DETA, hence 100 g of DGEBA will react with 10.84 g of DETA. These two ingredients were mixed by stirring slowly for 15 minutes. The mixture was then ready to be transferred to the mold.

Epoxy composite in this study was prepared by Hand Lay Up technique with the use of a metal mold. Hand-lay up is the simplest method for laminating. The laminate may be any number of layers of the same material or

combinations of different materials. Hand-lay up can be done in two ways, i.e. *dry* and *wet*. The *dry* method refers to applying a glass fiber cloth over a dry surface while the *wet* method refers to applying the cloth to an epoxy-coated surface before the coat reaches its initial cure. In the latter method, the cloth is often applied after the wet-out coat becomes tacky, which helps it cling to vertical or overhead surfaces [26, 46]. Therefore, wet-lay up was chosen in this research. The mold was coated with a silicone mold releasing agent before transferring the first layer to the mold. Figure 4.4 shows the layers of epoxy composite in this study.

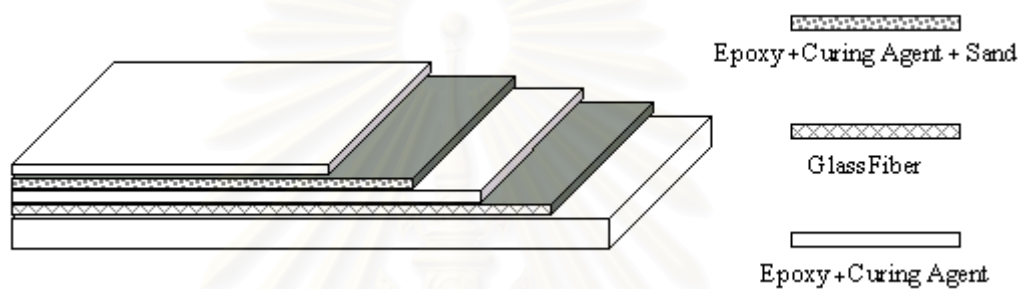


Figure 4.4 : Laminea of the epoxy composite.

The first layer, which is the mixture of epoxy resin and curing agent, was poured to the metal mold with the approximate thickness of 2 mm. One hour later, before this liquid mixture will completely turn into solid by crosslinking mechanism, glass fiber cloth was rolled over neatly with a roller. Some epoxy and curing agent mixture tend to penetrate through the gaps between the glass fibers within the woven structure onto the surface of the cloth. Rolling helped eliminating any air trapped between glass fibers and the epoxy resin. One hour later, the filler layer was applied. This layer is composed of sand and the mixture of epoxy resin and curing agent. Five different quantity of sand, as shown in Table 4.4 is used. Sand was mixed with the mixture of epoxy resin and curing agent. The filled mixture was then poured to the mold. Leveling of sand was conducted by using a spatula. Finally, the top layer of epoxy resin and curing agent was applied. The final thickness of each epoxy composite sample is 6 mm.

Table 4.4 : Amount of sand filler in the epoxy composite coat.

Sample	Sand (%by volume)
run 1 to run 4	20
run 5 to run 8	34
run 9 to run 12 and run 15 to run 20	27
run 13	15.23
run 14	38.77

After the final coating layer was applied to the top of the composite in mold, the composite was left to cure at ambient temperature for 1 hour. Then, each sample was cured by using the conditions shown in the Table 4.5 .

Table 4.5 : Cure condition of epoxy composite.

Sample	Cure temperature (°C)	Cure time (h)
run 1 and run 5	45	24
run 2 and run 6	85	24
run 3 and run 7	45	48
run 4 and run 8	85	48
run 9	31	36
run 10	99	36
run 11	65	15.8
run 12	65	56.2
run 13 to run 20	65	36

4.3.2 Preparation of Concrete Specimens

4.3.2.1 Mixing of Concrete

The various mixing components are proportioned so that the resulting concrete has adequate strength and proper workability. The proportion of cement : sand : rock is 1 : 2 : 3 by volume and water : cement is 0.55 liter : 1 kg in this research. Concrete is mixed by hand by firstly leveling off the pile of fine aggregate, spread cement evenly over the top and mix. Coarse aggregates were then added and mixed. Water was later applied while simultaneously still mixing until a homogeneous mixture is attained.

4.3.2.2 Molding Concrete

Concrete specimens prepared for the compression test were molded with a 150 mm x 150 mm x 150 mm metal mold to give the dimension as required in BS 1881: Part 3 Testing Concrete. Method of making and curing test specimens. Fill each mould of concrete in three layers, tamping each layer 35 times with steel tamping rod before adding the next layer. When the mold is completely filled, smooth off the tops evenly. Concrete specimens can be released from the molds after 24 hours.

4.3.2.3 Curing Concrete

The last step, which is an exceedingly important one in the manufacture of concrete, is the curing. As water was brought into contact with the cement particles, hydration process immediately began. The ultimate strength-giving structure of the hardened cement paste owes its properties primarily to the hydrated calcium silicates. When hydration of cement takes place only in the presence of moisture and at favorable temperature, these conditions must be maintained for a suitable time interval called the curing period. Curing period for compression test of most concrete is 28 days at room temperature. During this period, continuous sprinkling of water is conducted to keep the surface of concrete wet.

4.3.3 Preparation of Mortar Specimens

4.3.3.1 Mixing of Mortar

In this study, the proportion of cement : sand is 1 : 2.75 by volume and water : cement is 0.485 liter : 1 kg. Mortar was also mixed up by hand by the same method as mixing the concrete. Mortar specimens were released from the molds after 24 hours.

4.3.3.2 Molding of Mortar

The combination of cement and sand was filled in a metal mold of a 25 mm x 25 mm x 290 mm in dimension. It was then tamped with tamping steel rod and finally smoothed the top off evenly.

4.3.3.3 Curing Mortar

Like concrete, mortar is cured for 28 days at room temperature with continuous sprinkling of water to achieve high compressive strength from the cure of calcium silicate.

4.3.4 Preparation of Concrete and Mortar Coated Specimens

Moisture is one possible reason for failure of the epoxy composite coating. Therefore, after curing, the concrete and mortar were in a dry place kept at room temperature to let the moisture evaporate gradually. Once the concrete and mortar were completely dried, they are ready for surface coating.

Cleaning is the primary step for surface coating. The surface of concrete and mortar must be free from dust and any other contaminant. Figure 4.5 illustrates the metal frame for molding the epoxy composite coat on concrete. The metal frame around the top of concrete or mortar was tightened before the epoxy composite. Coat was applied on the concrete or mortar by hand-lay up as described in Section 4.3.1.1 .



Figure 4.5 : Concrete tighten with a metal frame.

4.4 MECHANICAL TESTS

4.4.1 Epoxy Composite Specimens

One difficulty in preparing the epoxy composite for each test is to keep the thickness of 6 mm for the epoxy composite coat to be as precisely as possible. If the thickness of the composite materials changes, consequently the volume fraction of glass fiber will also change. As a result, a change in the mechanical properties of the composite could be induced. The thickness of the coating material in industrial floor coating varies in a range of 1 to 6 mm depending on the application in each area [24]. In very heavy loaded areas, coatings can sometimes be thicker than the range cited. Epoxy coating with the thickness of 6 mm can be used widely in many areas and was chosen in this study.

4.4.1.1 Compression Test

Since compression strength is one of the most significant properties of an industrial floor coating material, compression test is one major test in this study. Most compression tests for polymers were conducted following the instruction described in ASTM D695. The test was conducted by compressing or applying load parallel to the thickness or in other words, applying load in the same axis as the length of the specimen, as shown in Figure 4.6 (a).

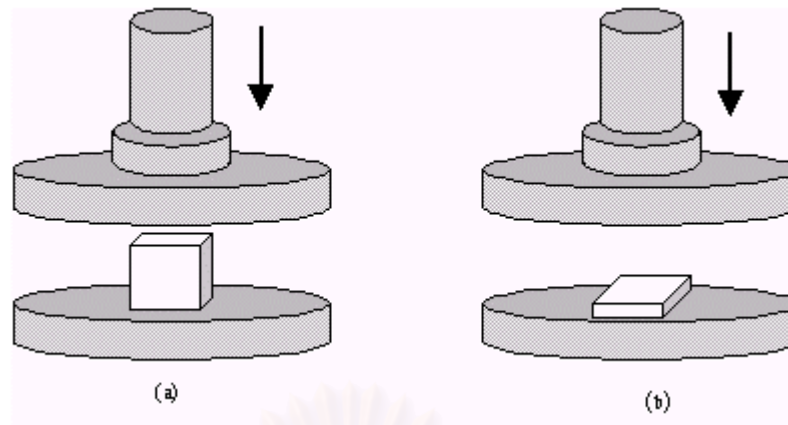


Figure 4.6 : Direction of applying load in compression test.

However, in this study, the direction of load is applied to the specimen as shown in Figure 4.6 (b), which is the same direction as weight applied to the floor. The test specimen is in a square shape of 15 mm x 15 mm with a thickness of 6 mm as shown in Figure 4.7 .

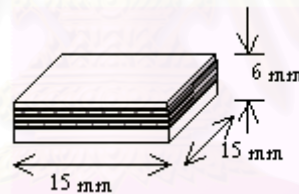


Figure 4.7 : Dimension of the compression test specimen.

Other test conditions were performed as described in taken as ASTM D-695. The crosshead speed was set constant at 1.3 mm/min. The test was conducted at a standard temperature of $23\text{ }^{\circ}\text{C} \pm 2\text{ }^{\circ}\text{C}$. The compression test was performed by using a universal testing machine (Shimadzu). Teflon is used as a lubricant to protect the load cell from abrasion caused by the sand detaching from the specimen upon pressing the sand layer. Five specimens were tested for each run. Average values are further used for calculations in the statistical analysis.

4.4.1.2 Impact Test

In order to evaluate the energy required to break the epoxy composite coat under a sudden load, the impact test was conducted. Because the application of the specimen is a floor coating material, the direction of the load applied to the specimen is most realistic in the direction perpendicular to coating surface. Therefore, a test similar to Izod impact test in ASTM D-256 is applied without notching the specimen. The difference between this test from Izod impact test is the thickness of the specimen. Izod impact test requires a thickness of 12.7 mm, but the thickness of the epoxy composite coat in this test is 6 mm. However, the impact test specimen dimension, as shown in Figure 4.8, is 12.7 in width and 62 mm in length. The ITR-2000 Instrumented Impact test is used in this test, the specimen arrangement is as shown in Figure 4.8 .

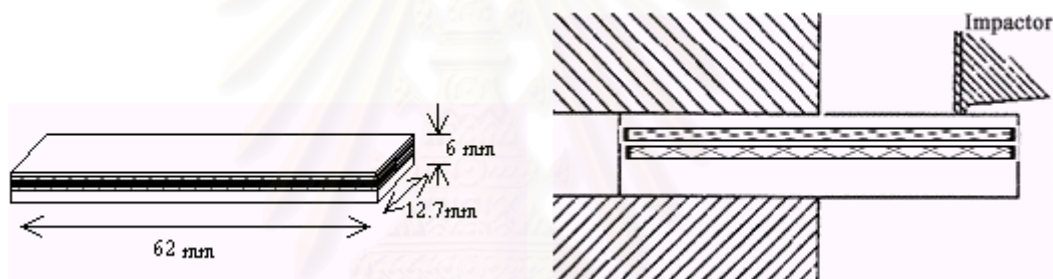


Figure 4.8 : Specimen dimension and specimen arrangement for impact test.

The test was carried out at a standard testing condition of 23 ± 2 °C and 50 ± 5 % relative humidity. Five specimens were tested for each run. Average values are further used for calculations in the statistical analysis.

4.4.1.3 Double Torsion Test

Double torsion test was conducted to find fracture energy i.e. the energy required to break the specimen under Mode I. Figure 4.9 shows the shape and dimension of the double torsion specimen. It was 52 mm in width, 110 mm in length and 6 mm in thickness. It is cut on the resin side to give a U-shape groove with 1.6 mm in width and 2 mm in depth along the specimen length. A sharp crack was introduced along the groove by driving a blade through the groove at temperature

below the T_g of the epoxy. The specimen was placed on a stainless steel double torsion fixture as shown in Figure 4.10 [21].

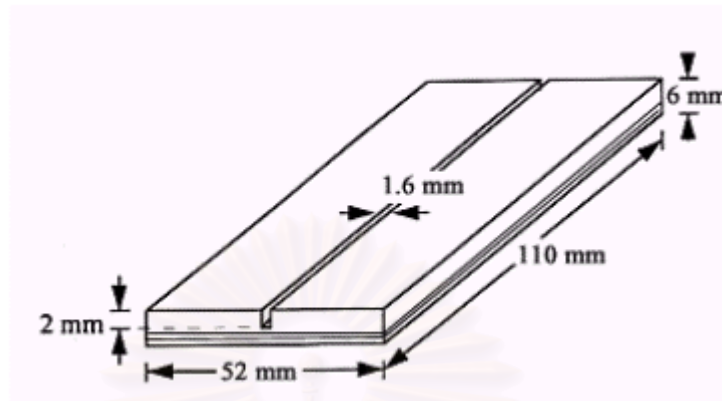


Figure 4.9 : The shape and dimension of the double torsion specimen.

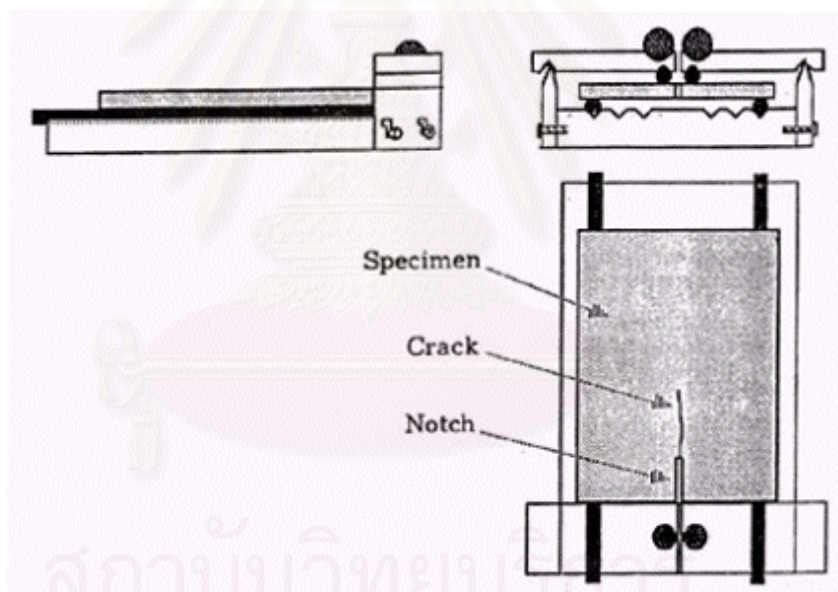


Figure 4.10 : Arrangement of specimen in the double torsion fixture [21].

The above set was located on Instron 4502 universal testing machine. Compression mode is used in operating the machine with a crosshead speed of 0.05mm/min. The test was conducted at a standard testing condition of 23 ± 2 °C and 50 ± 5 % relative humidity for not less than 40 hours prior to the double torsion test. Three specimens were tested for each run. Average values are further used for calculations in the statistical analysis.

4.4.2 Coated Concrete

Concrete coated specimens were prepared for compression test according to the procedure described in BS 1881: Part 4 Testing Concrete. Method of testing concrete for strength. The dimension of the concrete specimen is 150 mm x 150 mm x 150 mm. It is coated on one side with 6 mm epoxy composite coating. Compression load was applied to the coated surface of the concrete. The test was performed on the Amsler testing machine using a crosshead speed of 1.4 kg/cm²/s. Figure 4.11 shows the arrangement and the dimension of the compression test on epoxy composite coated concrete.

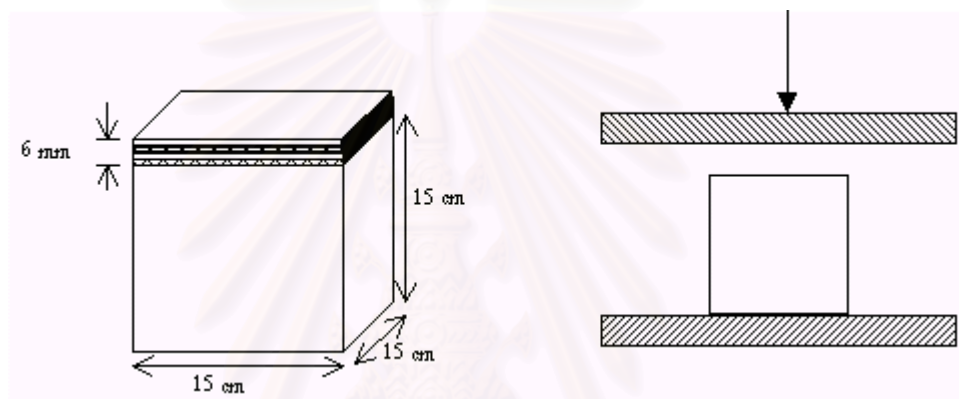


Figure 4.11 : The arrangement and the dimensions of epoxy composite coated concrete specimen.

4.4.3 Coated Mortar

There is no such standard test for finding the impact strength of concrete or mortar since the impact strength is not as useful in the design calculations as other properties such as the compression strength. Therefore, the method to determine the impact strength of epoxy composite coated floor in this study is adapted from that of the wood impact strength. The concrete coated floor was modeled by using coated mortar specimens. The test was performed using Amsler impact testing machine. The dimensions of the mortar beam are 25 mm x 25 mm x 290 mm. It is coated on one side with 6 mm epoxy composite coat and placed on the Amsler impact tester as shown in Figure 4.12 .

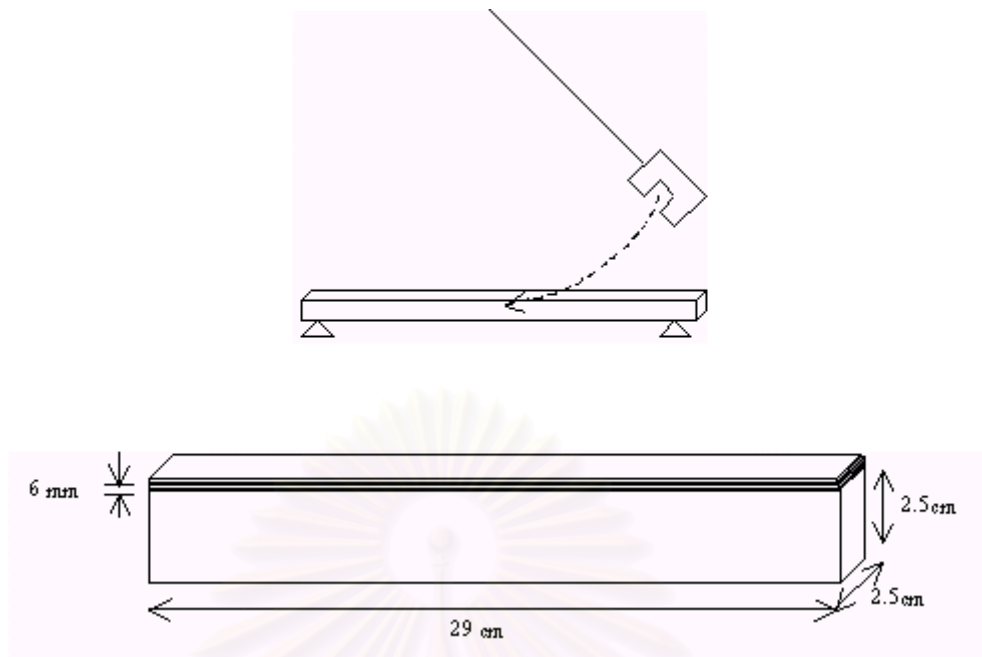


Figure 4.12 : The arrangement and dimension of mortar coated specimen.

4.5 MICROSCOPIC OBSERVATION

In the current research, scanning electron microscope (SEM) is used in observing the morphological clues of the fractured composite. Fractographic studies from SEM illustrated fracture morphology and enable investigators to analyze local crack initiation and propagation. In SEM, electron can be reflected from the surface of an object. The incident electrons from the electron source functioned as a beam, which is then scanned over the entire area of fracture surfaces. Scanning electron microscope JOEL, JSM 840A is used in this study with fracture surfaces sputtered with 300 Å in thickness of gold. The accelerating voltage for SEM was 10 kV.

4.6 SAMPLE CHARACTERIZATION

Many synthetic polymers consist of long and flexible chains that are randomly coiled and intertwined with no molecular order. This physical state is termed as *amorphous*. Cured epoxy resins are amorphous polymers. Below a certain temperature called glass transition temperature (T_g), long-range cooperative motions of individual chains cannot occur. However, short-range motions involving several

contiguous groups along the chain backbone are possible. Such motions are called secondary relaxation process.

The technique of Dynamic Mechanical Analysis (DMA) was used to determine the glass transition temperature (T_g) and the viscoelastic properties of epoxy resins. In this method, sinusoidal stress was applied to the sample cyclically in a function of sine wave while the temperature of the sample is elevated. The results indicated the sinusoidal stress-strain relationship. There are many modes of vibration namely tension, torsion, compression, shear and bending. Bending is the most widely used mode and was chosen in this study. The experimental test was performed by using Perkin Elmer DMA 7e and operated in the single cantilever bending mode. The dimensions of the specimen were 2 mm in thickness, 4 mm in width and 16.5 mm in length. The test was conducted at the frequency of 1 Hz over a temperature ranging from 30 °C to 220 °C. The heating rate was 5 °C/min.



สถาบันวิทยบริการ
จุฬาลงกรณ์มหาวิทยาลัย

CHAPTER V

RESULTS AND DISCUSSIONS

Experimental results from various tests of epoxy composites and concrete/mortar coated with epoxy composites are shown and analyzed in this chapter. The numerical results of these tests are presented in Appendix A.

5.1 REGRESSION ANALYSIS

The mechanical properties obtained from tests in Chapter 4 can be represented in set equations showing respective relationship of the curing factors by regression analysis. The following calculation shows how the response surface equations and the response surface curves displayed in Section 5.3 were derived.

Variable codes from the central composite rotatable design are used to represent the quantity of the curing factors. An example of experimental result obtained following this design is shown in Table 5.1 .

Second-order linear regression, as written in Equation 5.1, is used in fitting the empirical model.

$$y = B_0 + \sum_{i=1}^k B_i x_i + \sum_{i=1}^k B_{ii} x_i^2 + \sum_{i=1}^k \sum_{j=1}^k B_{ij} x_i x_j + \varepsilon, \quad (i < j) \quad 5.1$$

where k is the number of independent variables x_1, x_2, \dots, x_k and B are the regression coefficients. Related calculations in regression analysis are exemplified in Appendix B.

The regression coefficients can be obtained by least square method giving the following equation,

$$y = 7.801 - 0.985x_1 - 0.067x_2 - 0.054x_3 - 0.059x_1x_2 - 0.001x_1x_3 - 0.002x_2x_3 + 0.229x_1^2 + 0.093x_2^2 - 0.295x_3^2 \quad 5.2$$

where $x_1, x_2, and x_3$ are the abovementioned variable codes representing the quantity of cure temperature, cure time, and the amount of sand filler respectively. This

relationship is further plotted as a response curve. Table 5.2 demonstrates the error from using the empirical model. It is evident that the response surface equation from the regression analysis is suitable for estimating the impact strength of the epoxy composite coating material, which exhibits a maximum error of 5.14%.

The regression coefficients derived from the regression analysis of the mechanical properties investigated in the current study is tabulated in Table 5.3 .

Table 5.1 : Impact strength of epoxy composite.

Run	Coded independent variables			Response y
	x ₁	x ₂	x ₃	
1	-1	-1	-1	8.77
2	1	-1	-1	6.98
3	-1	1	-1	8.75
4	1	1	-1	7.14
5	-1	-1	1	8.48
6	1	-1	1	7.11
7	-1	1	1	8.87
8	1	1	1	6.84
9	-1.682	0	0	10.43
10	1.682	0	0	6.46
11	0	-1.682	0	8.40
12	0	1.682	0	7.71
13	0	0	-1.682	7.18
14	0	0	1.682	6.94
15	0	0	0	7.81
16	0	0	0	8.01
17	0	0	0	7.88
18	0	0	0	7.80
19	0	0	0	7.86
20	0	0	0	7.45

Table 5.2 : Experimental and calculated error for impact strength of epoxy composite.

Run	Impact strength (KJ/m ²)		Error $e_i = (y_i - \hat{y}_i)$	%Error
	Experimental y_i	Calculation \hat{y}_i		
1	8.771	8.909	-0.138	-1.574
2	6.984	7.062	-0.078	-1.117
3	8.747	8.897	-0.150	-1.710
4	7.142	6.805	0.337	4.715
5	8.483	8.802	-0.319	-3.757
6	7.112	6.953	0.159	2.233
7	8.869	8.790	0.079	0.893
8	6.843	6.696	0.148	2.157
9	10.425	10.107	0.318	3.052
10	6.461	6.793	-0.332	-5.139
11	8.405	8.177	0.228	2.707
12	7.709	7.950	-0.241	-3.125
13	7.181	7.159	0.022	0.305
14	6.943	6.978	-0.035	-0.505
15	7.810	7.801	0.009	0.115
16	8.012	7.801	0.211	2.629
17	7.876	7.801	0.075	0.956
18	7.800	7.801	-0.001	-0.013
19	7.862	7.801	0.061	0.772
20	7.449	7.801	-0.352	-4.723

Equation	:	$y = b_0 + b_1x_1 + b_2x_2 + b_3x_3 + b_{12}x_1x_2 + b_{13}x_1x_3 + b_{23}x_2x_3 + b_{11}x_1^2 + b_{22}x_2^2 + b_{33}x_3^2$									
Where	:	y = Mechanical Property			x ₁ = Cure Temperature (°C)						
		b = Regression Coefficients			x ₂ = Cure Time (h)						
					x ₃ = Amount of sand filler (% b volume)						
y		b ₀	b ₁	b ₂	b ₃	b ₁₂	b ₁₃	b ₂₃	b ₁₁	b ₂₂	b ₃₃
Epoxy Composite Coating Material											
Compressive Strength (MPa)		98.8209	2.2742	-3.5268	-4.1599	0.6089	0.2262	2.5212	0.2961	-0.1007	-1.2391
Impact Strength (KJ/m ²)		7.8010	-0.9853	-0.0674	-0.0540	-0.0592	-0.0007	-0.0022	0.2294	0.0929	-0.2590
Fracture Toughness (MN/(m ^{3/2}))		3.9724	-0.4129	-0.2080	0.1754	0.0652	-0.0728	-0.0100	0.1965	-0.0519	0.0477
Fracture Energy (J/m ²)		14,909	-2,843	-907	1,761	335	-1,114	-828	1,107	850	223
Concrete Coated with Epoxy Composite											
Compressive Strength (MPa)		51.2307	1.4552	1.5898	-1.5352	-4.0925	1.1725	0.2050	-5.4221	-1.2890	-3.7462
Mortar Coated with Epoxy Composite											
Impact Strength (KJ/m ²)		4.4898	-0.5597	0.0284	-0.0552	0.1047	0.0774	0.0657	-0.1532	-0.1808	-0.1688

Table 5.3 Coefficients deriving from the second-order linear regression analysis for the properties of Epoxy Composites.

5.2 ANALYSIS OF VARIANCE (ANOVA)

ANOVA is one of the most important tools for analyzing data obtained from designed experiments. ANOVA is used in testing the aptness of the response surface equations from experimental design. An example of the variance analysis for the compressive strength of epoxy composite is shown in Tables 5.4 and 5.5 while details are depicted in Appendix B.

Table 5.4 : ANOVA table for the multiple regression analysis of the interactions of cure temperature, cure time, and amount of sand on the impact strength of epoxy composite.

Source of Variation	Sum of Square	DF	Mean Square	F ₀
Regression	21.077	9	2.342	28.67
First order terms	13.360	3	4.453	54.55
Secondary order terms	7.717	6	1.286	15.76
Error	0.817	10	0.082	
Lack of fit	0.639	5	0.128	3.6
Pure error	0.178	5	0.036	
Total	16.251	19	R² =	0.949

Table 5.5 : Statistic-t₀ test of coefficients testing for interactions of cure temperature, cure time, and amount of sand on the impact strength of epoxy composite.

Regression Coefficients		t ₀	Hypothesis test (t _{0.025/2,10} = 2.228)
b ₀	7.801	66.95	Significance
b ₁	-0.985	-12.74	Significance
b ₂	-0.067	-0.97	Not significance
b ₃	-0.054	-0.70	Not significance
b ₁₂	-0.059	-0.58	Not significance
b ₁₃	-0.001	-0.01	Not significance
b ₂₃	-0.002	-0.02	Not significance
b ₁₁	0.229	3.05	Significance
b ₂₂	0.093	1.23	Not significance
b ₃₃	-0.259	-3.44	Significance

The degree of confidence in this study was set at 97.5%, in other words, the level of significance is at 0.025. Hence, the critical values of F-distribution and t-distribution are at the level of significance at 0.025.

The influence of curing factors on the mechanical properties is verified by the rejection of the hypothesis $H_0: B_1 = B_2 = \dots = B_k = 0$. The critical F-distribution at the level of significance at 0.025, $F_{0.025, 9, 10}$, is 3.78. F_0 from the ANOVA table displayed in Table 5.4 is 2.867. In this study, F_0 is evidently greater than $F_{0.025, 9, 10}$. As a result, the hypothesis of $H_0: B_1 = B_2 = \dots = B_k = 0$ is rejected.

Checking F_0 of error proved adequacy of the empirical model. If F_0 of error is less than the critical F-distribution at the level of significance 0.025, then the model can be used satisfactorily. In this experiment, F_0 is 3.6 while $F_{0.025, 5, 5}$ is 7.15. It is obvious that F_0 is less than $F_{0.025, 5, 5}$. Therefore, the hypothesis of H_0 : the model adequately fits the data is acceptable. The regression coefficients obtained from regression analysis are proper for estimating the impact strength of the epoxy composite.

Another statistical value that is useful for indicating the suitability of the empirical model is the coefficient of determination, R^2 . The closer the value of R^2 approaches 1, the more functional the model is. From the ANOVA table, R^2 equals to 0.949, which is approaching 1. This means that 94.9% of the observations fall directly on the fitted response surface.

The above statistical analysis proved that Equation 5.2 is appropriate for estimating the impact strength of the epoxy composite. This equation can be abbreviated by reducing the insignificance terms. If the statistical t_0 of any regression coefficient is less than $t_{0.025/2, 10}$, the critical t-distribution at the level of significance at 0.025, that particular regression coefficient is not significant to the response surface equation. The value of $t_{0.025/2, 10}$ is 2.228, any regression coefficient from Table 5.5 that is less than 2.228 can be eliminated from the response surface equation. Consequently, equation 5.2 can be rewritten as follow: -

$$y = 7.801 - 0.985x_1 + 0.229x_1^2 - 0.295x_2^2 \quad 5.3$$

Equation	:	$y = b_0 + b_1x_1 + b_2x_2 + b_3x_3 + b_{12}x_1x_2 + b_{13}x_1x_3 + b_{23}x_2x_3 + b_{11}x_1^2 + b_{22}x_2^2 + b_{33}x_3^2$									
Where	:	y = Mechanical Property			x ₁ = Cure Temperature (°C)						
		b = Regression Coefficients			x ₂ = Cure Time (h)						
					x ₃ = Amount of sand filler (% by volume)						
	y	b ₀	b ₁	b ₂	b ₃	b ₁₂	b ₁₃	b ₂₃	b ₁₁	b ₂₂	b ₃₃
Epoxy Composite Coating Material											
	Compressive Strength (MPa)	98.8209	2.2742	-3.5268	-4.1599			2.5212			
	Impact Strength (KJ/m ²)	7.8010	-0.9853						0.2294		-0.2590
	Fracture Toughness (MN/(m ^{3/2}))	3.9724	-0.4129	-0.2080	0.1754				0.1965		
	Fracture Energy (J/m ²)	14,909	-2,843	-907	1,761		-1,114		1,107	850	
Concrete Coated with Epoxy Composite											
	Compressive Strength (MPa)	51.2307				-4.0925			-5.4221		-3.7462
Mortar Coated with Epoxy Composite											
	Impact Strength (KJ/m ²)	4.4898	-0.5597							-0.1808	-0.1688

Table 5.6 Significant coefficients deriving from the second-order linear regression analysis for the properties of epoxy composites.

The ANOVA table and the statistical t_0 test for the significance of the regression coefficients in fitting the model of other properties are tabulated in Appendix C. Table 5.6 shows the significant regression coefficients from the statistical t_0 test. These are the coefficients used to demonstrate the relationship between the curing factors and the mechanical properties in the final response surface equations.

5.3 MECHANICAL PROPERTIES OF EPOXY COMPOSITES

The relationships between curing factors and the mechanical properties of epoxy composite, and concrete/mortar coated with epoxy composite were investigated by using Response Surface Methodology (RSM). Three pairs of response surfaces and contour curves were demonstrated in each investigation. Contour curves comprise with plot of cure temperature-cure time, plot of cure time-sand, and plot of cure temperature-sand. These curves are plotted against the mechanical properties giving response surfaces. The aforementioned graphs were plotted with respect to the center point. That is, graphs in Figure 5.4, 5.8, 5.13, 5.16, 5.20, and 5.25, which shows the relationship between the cure temperature-cure time and the mechanical properties were plotted at constant amount of sand 27%, graphs between cure time-sand and mechanical properties were plotted at constant temperature 65°C, and graphs between cure temperature-sand and mechanical properties were plotted at constant time 36 h.

5.3.1 Epoxy Composite Specimens

5.3.1.1 Compression Test

Compression test can provide many useful properties, namely modulus of elasticity, yield stress, and yield strain. Test specimen and the compressed one are shown in Figure 5.1.

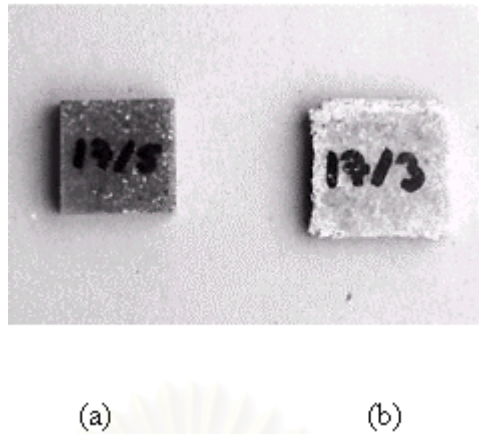


Figure 5.1 : Epoxy composite test specimen from compression test perpendicular to the compression load. (a) before compression and (b) after compression

Figure 5.1 (a) and (b) shows the specimen before and after compression test respectively. Stress-strain curve from compression test in this study is demonstrated in Figure 5.2 . Comparison of compressive strength among epoxy composites, glass fiber-reinforced epoxy composite and glass fiber-reinforced epoxy composite filled with 27% sand cured at 65°C 36 h is shown in Figure 5.3 .

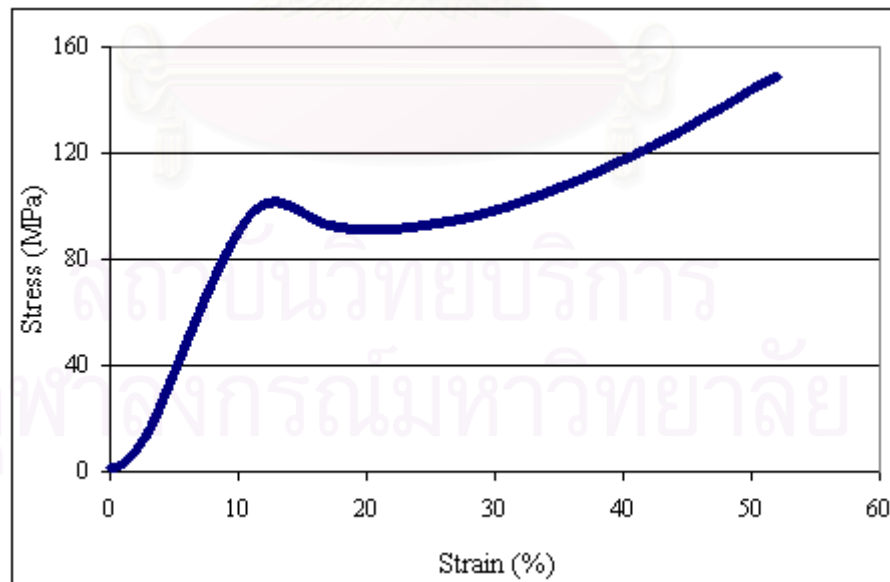


Figure 5.2 : Stress-strain curve from compression test of epoxy composite cured at 65°C, 36 h and 27% sand.

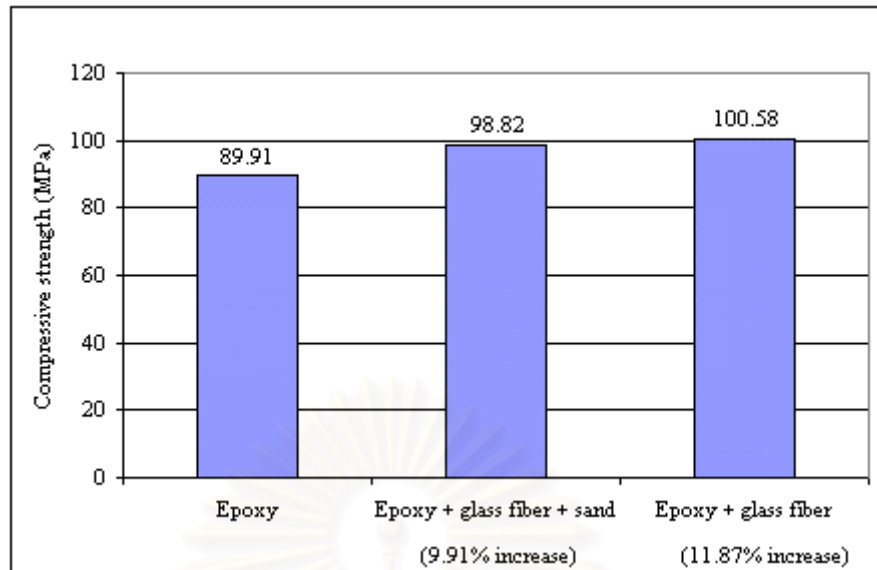
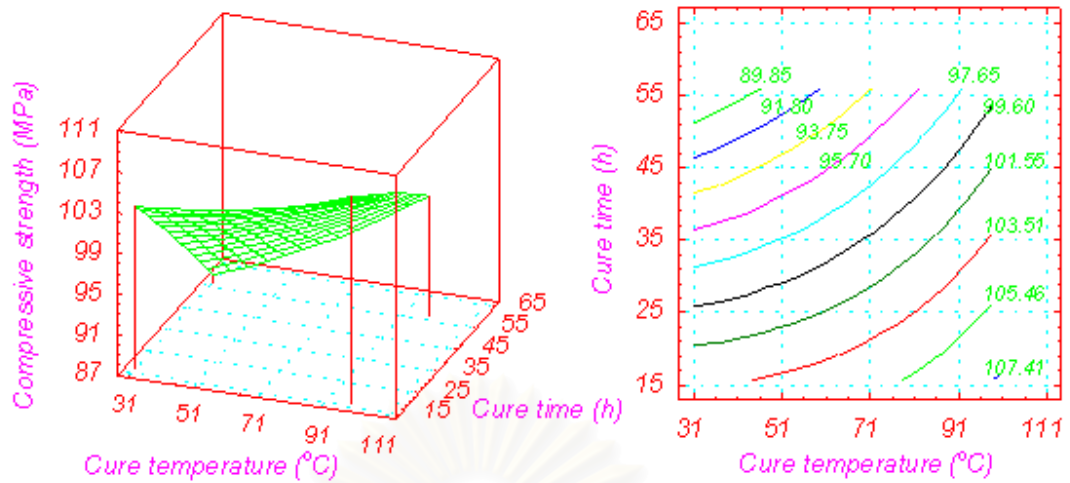


Figure 5.3 : Compressive strength of various epoxy coating composites.

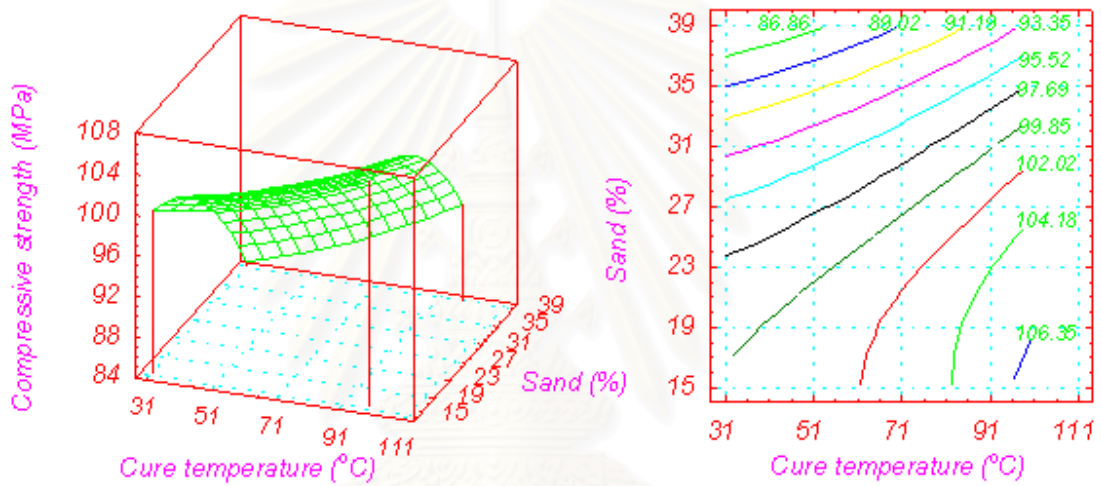
Comparing with pure epoxy, glass fiber-reinforced epoxy composite gives better compressive strength. Although sand-filled glass fiber-reinforced epoxy composite gives less compressive strength than glass fiber reinforced epoxy without adding sand, the compressive strength obtained is only 1.8% slighter. Accordingly, sand can be used as a filler in epoxy coating composite. Adding sand as a filler not only reduces material cost but also extends the pot life. Nonetheless, it might be remarked that adding sand does not enhance compressive strength of the coating material as most researchers might have expected initially. A possible explanation for this may be due to the poor adhesion of sand to other components within the epoxy composite. Better adhesion is achieved at the interface between the glass fiber and the epoxy matrix because the glass fiber had been surface treated with silane coupling agent. The purpose of which was to promote the interfacial adhesion. In contradiction, no treatment was conducted to sand except the caustic wash to remove salt and impurities. As a consequence, some parts of embedded sand in the epoxy composite were detached as compression load was applied and resulted in inferior compression property. Air pockets or air holes that are likely to have developed within aggregates of sand and at the interface between sand and the epoxy matrix in the sand layer may also led to reduction in the compression strength.

The response surface and contour curve for the compressive behavior of the epoxy composite is shown in Figure 5.4 . From the plot of cure temperature-cure time versus compressive strength at a constant amount of sand filler of 27% in Figure 5.4 (a) and (b), the compressive strength is raised as the cure temperature elevates. In contrary, the compressive strength decreases as the cure time increases as shown in Figure 5.4 (a) and (c). The maximum compressive strength from Figure 5.4 (a) is 107.41 MPa at the highest cure temperature of 99 °C and shortest cure time of 15.8 h. However, another interesting cure condition that also offers high compressive strength is that cure at the lowest temperature of 31 °C and over the shortest cure time. The compressive strength achieved at the latter curing condition is 103.51 MPa, which is only 3.6% lower than the maximum but this latter curing condition is much more practical. Therefore, the recommended curing condition for maximum compressive strength is best conducted at the cure temperature of 31°C for 15.8 h.

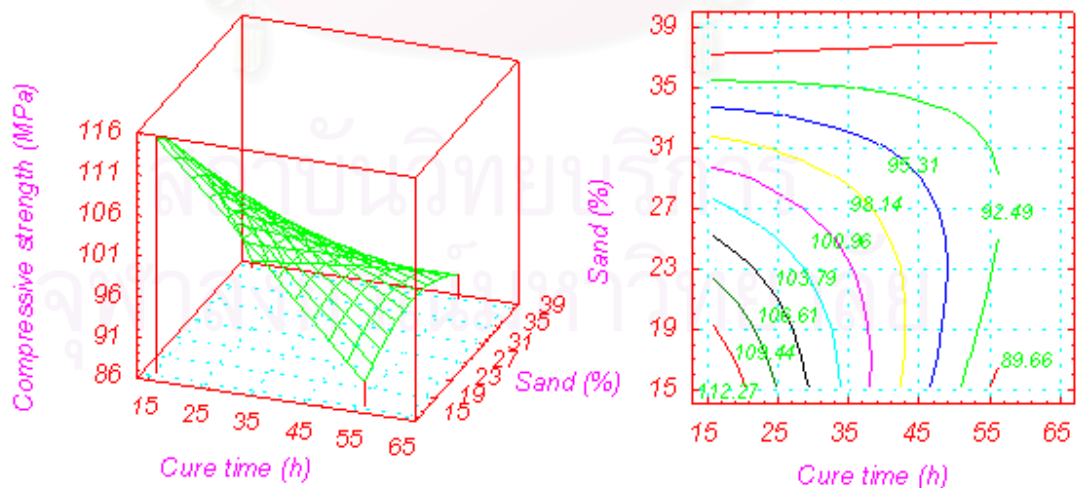
Figure 5.5 shows the contour curve of the compressive strength between the cure temperature and the amount of sand filler at a constant cure time of 15.8 h. The compressive strength of epoxy composite at this optimal cure condition can be even greater if the percentage of sand filler is varied. From Figure 5.5, the highest compressive strength of 114.15 MPa observed from this figure was at the lowest amount of sand, i.e. at 15.2%. If the ease of processing is not a vital factor, the greatest compressive strength can be achieved is 117.42 MPa, which is merely 2.9% higher than the suggested curing condition. The cure condition for which is at a cure temperature of 99 °C for 15.8 h in conjunction with adding sand as a filler by 15.23%. Hence, it can be concluded that the most appropriate condition for curing epoxy composite as far as compressive strength is concerned is at a cure temperature of 31°C for 15.8 h with 15.23% sand added to the epoxy composite formulation.



(a) Effects of cure temperature and cure time at a constant amount of sand 27%.

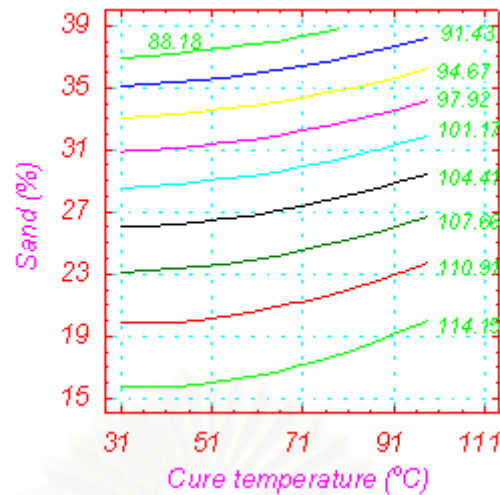


(b) Effects of cure temperature and amount of sand at a constant cure time 36 h.



(c) Effect of cure time and amount of sand at constant cure temperature of 65°C.

Figure 5.4 : Effect of cure temperature, cure time, and sand filler on epoxy composite



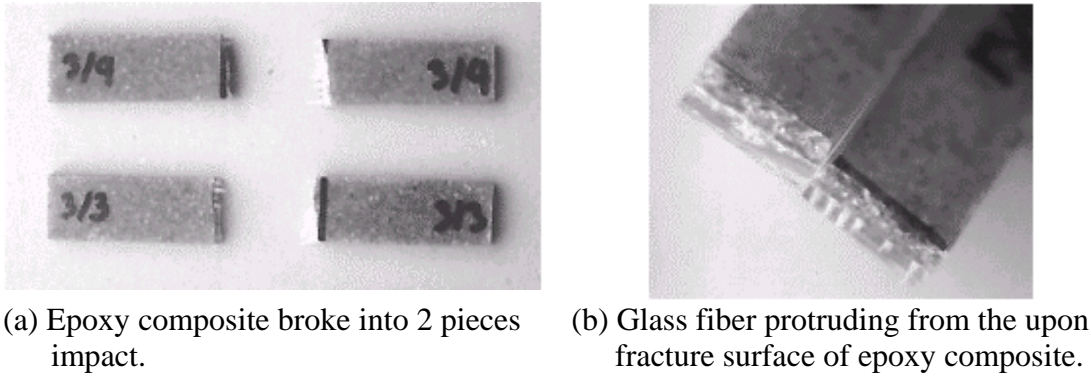


Figure 5.6 : Epoxy composite test specimen from impact test.

A comparison of the impact strength of neat epoxy composites, glass fiber-reinforced epoxy composite and glass fiber-reinforced epoxy composite filled with 27% sand and cured at 65°C for 36 h is shown in Figure 5.7 .

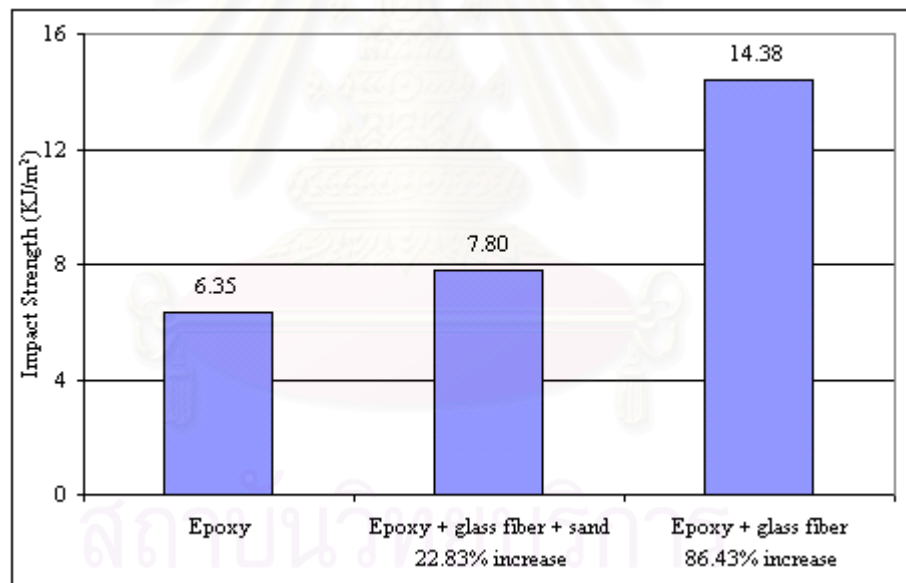
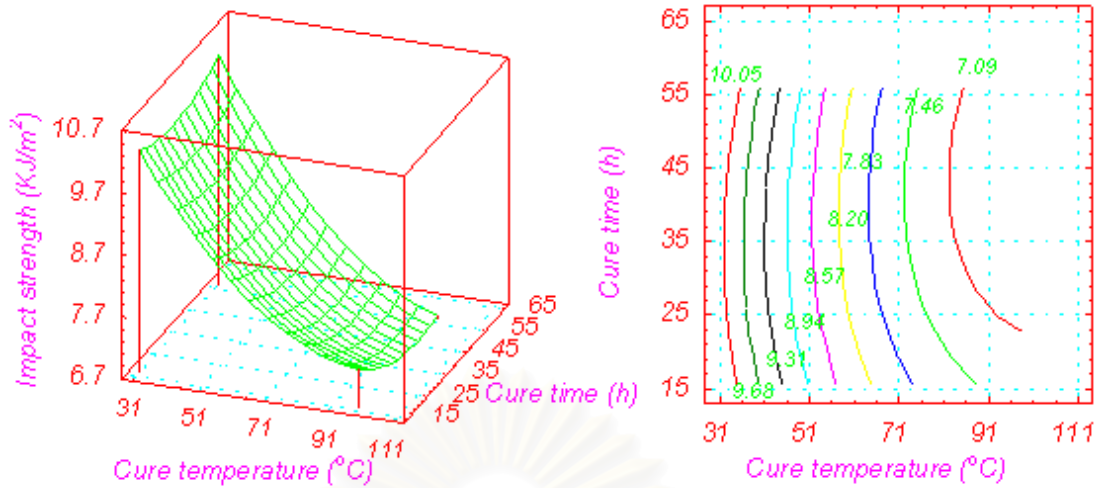


Figure 5.7 : The impact strength of neat epoxy, epoxy composite and sand- filled epoxy composite, all systems were cured at 65 °C for 36 h.

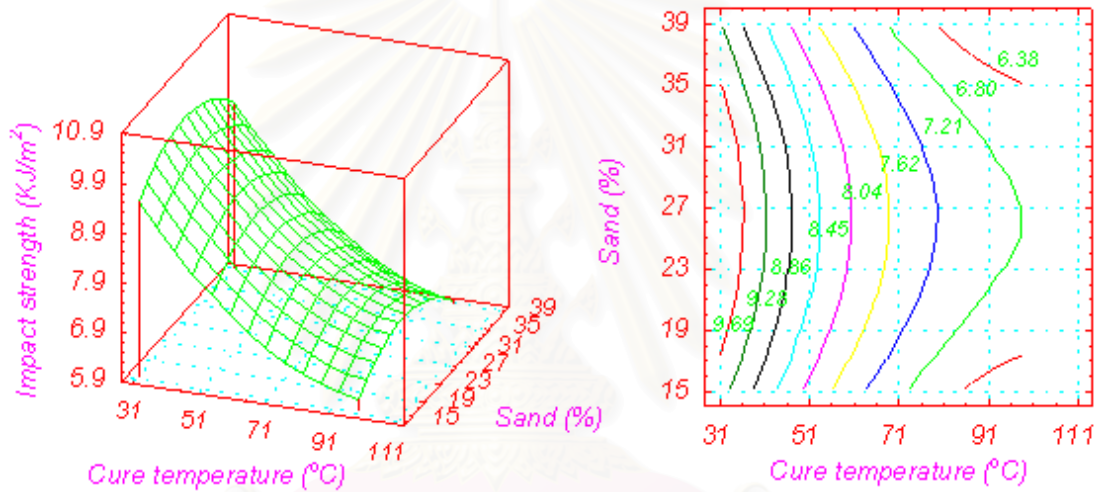
From Figure 5.7, it is apparent that the reinforcing glass fiber is capable of enhancing the impact strength of epoxy. The increase of the impact strength is owing to the energy required to break the reinforced glass fiber. It must be noted that the increase in the impact energy of the sand-filled epoxy composite as

compared with that of the neat epoxy arisen primarily from the glass fiber reinforcement, not from the added sand. A comparison between the fiber-reinforced epoxy composite with and without the sand filler illustrated that the filling sand had detrimental effect by decreasing the impact strength. Though sand was found to deteriorate the impact property, the impact test of sand-filled epoxy composites was still conducted at least to find the most suitable amount of sand filler.

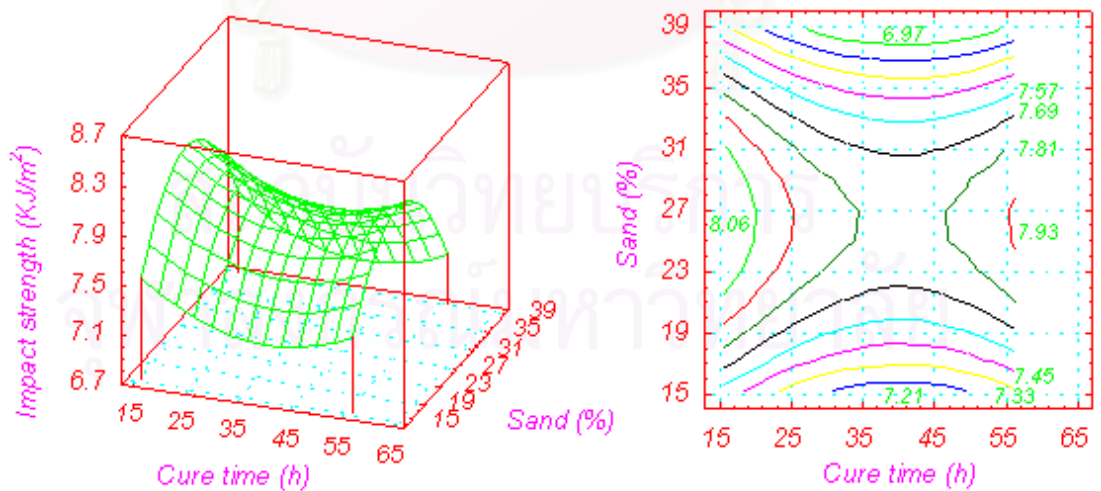
The response surface and contour curves from each impact test of the epoxy composite are shown in Figure 5.8 . From Figure 5.8 (a) and (b), it is evident that the highest impact strength can be obtained at the lowest temperature of 31°C with a moderate amount of sand, i.e. at 27%. From the statistical t_0 test, no regression coefficients that relate the impact strength to the cure time showed any significance. However, in Figure 5.8 (a) and (c), cure time seems to have a slight effect on the impact strength. This is because the response surfaces shown in Figure 5.8 were plotted from the initial response surface equation, which has not eliminated the insignificant terms yet. In order to gain confidence in ignoring the influence of cure time, a brief calculation was conducted as follow. From the contour curve of impact strength between the cure time and the amount of sand at a constant cure temperature of 31°C in Figure 5.9, at 27% sand filler, the impact strength of epoxy composite cured for 21 and 46 h was equally obtained at 10.23 KJ/m². The impact at different cure time varies in the range from 10.23 to 10.46 KJ/m². The difference between the lowest and the highest value is only 2.2%. Therefore, the recommended curing condition is at a cure temperature of 31°C with an addition of sand filler of 27%. Such cure condition gives the maximum impact strength of around 10.46 KJ/m².



(a) Effects of cure temperature and cure time at a constant amount of sand 27%.



(b) Effects of cure temperature and amount of sand at a constant cure time 36 h.



(c) Effect of cure time and amount of sand at constant cure temperature of 65 $^{\circ}\text{C}$.

Figure 5.8 : Effect of cure temperature, cure time, and sand filler on epoxy composite

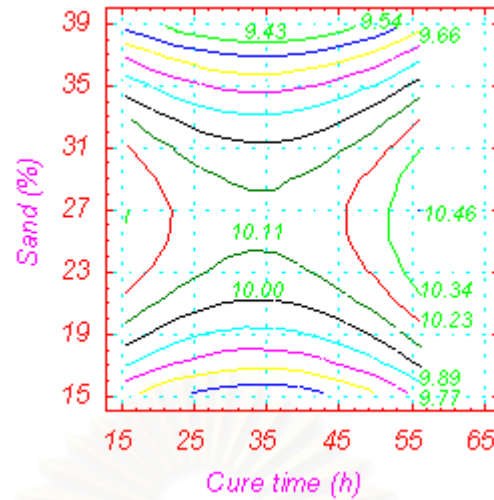


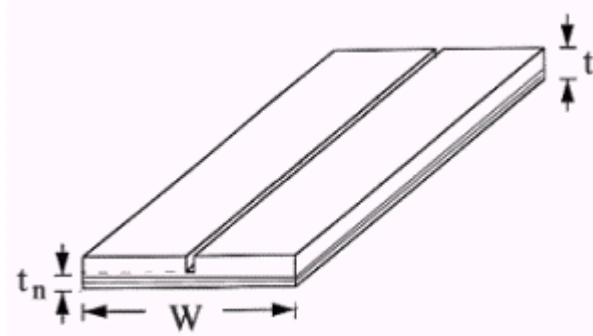
Figure 5.9 : Contour of the impact strength for the epoxy composites between the amount of sand and the cure time at a constant cure temperature of 31°C.

5.3.1.3 Double Torsion Test

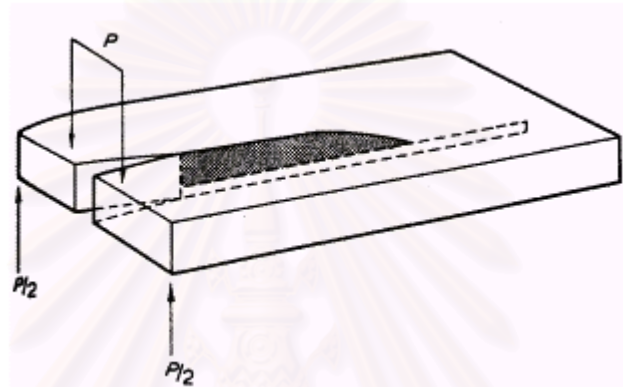
The double torsion test is used in evaluating the energy required to break a material. This energy is known as fracture energy. Pre-existing defects such as cracks in the specimen can initiate fracture. Hence, the critical fracture stress, which indicates the maximum stress intensity of the material before the crack propagates, must be predicted. This value is defined as the critical stress intensity factor, K_{Ic} . The double torsion specimen is shown schematically in Figure 5.10 (a). Load at the break point from the experimental test was substituted in Equation 5.4 giving the stress intensity factor, which is independent of crack length [15, 19-21, 47].

$$K_{Ic} = PW_m \left[\frac{3(1+\nu)}{Wt^3t_n} \right]^{\frac{1}{2}} \quad 5.4$$

where P is load at the break point, W_m is the moment arm, ν is poisson's ratio (0.35 for epoxy resin), W is the width of the test specimen, t is the thickness of the test specimen, and t_n is the plate thickness in the plane of the crack. In Figure 5.10 (b), the shaded showed the fracture surface from double torsion test.



(a) The shape of the double torsion specimen

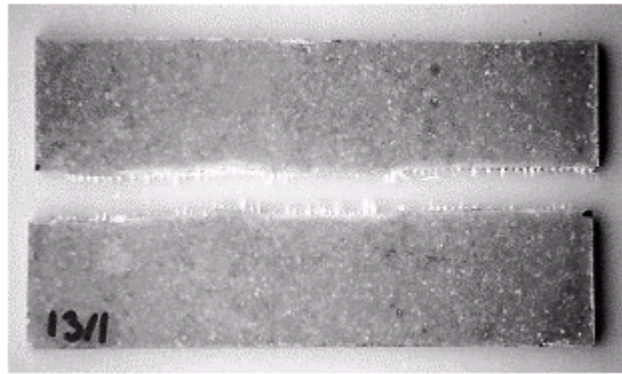


(b) Fracture surface from double torsion test [47]

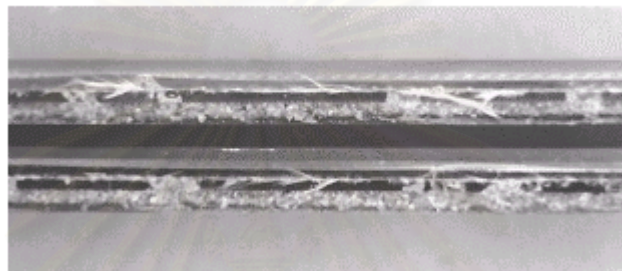
Figure 5.10 : Schematic representation of the double torsion test.

Specimen fractured by the double torsion technique is shown in Figure 5.11 . Upon completion of the test, epoxy composite was fractured along the groove, creating two broken halves as shown in Figure 5.11 (a). The two fracture surfaces with epoxy and glass fiber are shown in Figure 5.11 (b).

A comparison of the stress intensity factor of the neat epoxy, the glass fiber-reinforced epoxy composite and glass fiber-reinforced epoxy composite filled with 27% sand and cured at 65°C for 36 h is shown in Figure 5.12 .



(a) Epoxy composite broke into 2 pieces.



(b) Cross section of the crack.

Figure 5.11 : Epoxy composite specimen from double torsion test.

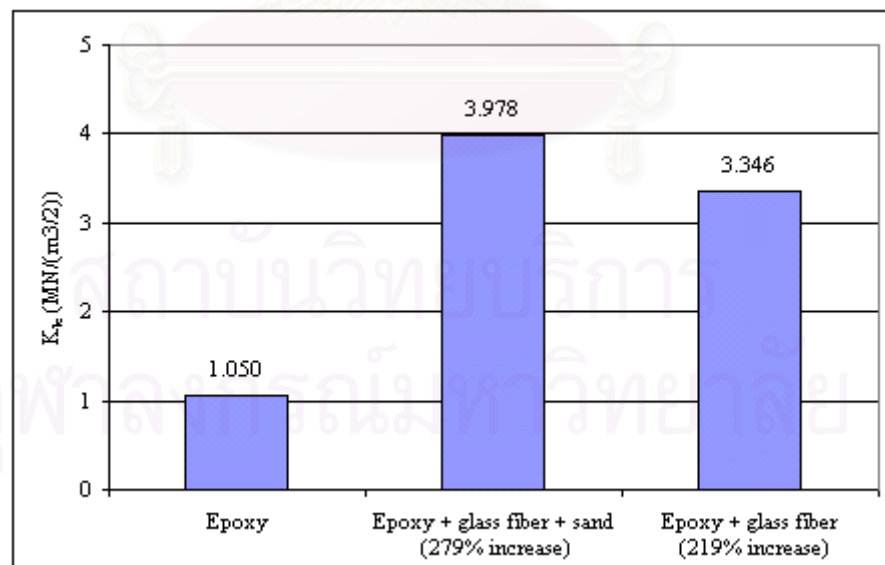


Figure 5.12 : Critical stress intensity factor of neat epoxy and epoxy composites.

From Figure 5.12, the critical stress intensity factor of the glass fiber-reinforced epoxy composite is prominently greater than that of the neat epoxy. This is because more energy is required to break the specimen. Complete fracture of the glass fiber-reinforced epoxy composite required the energy to break the epoxy matrix, the energy to pull-out the embedded glass fiber from the epoxy matrix and the energy to break the woven glass fiber while the neat epoxy only required the energy to break the epoxy matrix. K_{Ic} becomes even greater by adding sand as shown in Figure 5.12. Sand-filled epoxy composite is tougher and requires greater K_{Ic} to break comparing with that of the unfilled one, which is opposite to the effect of sand on the compressive strength and the impact strength.

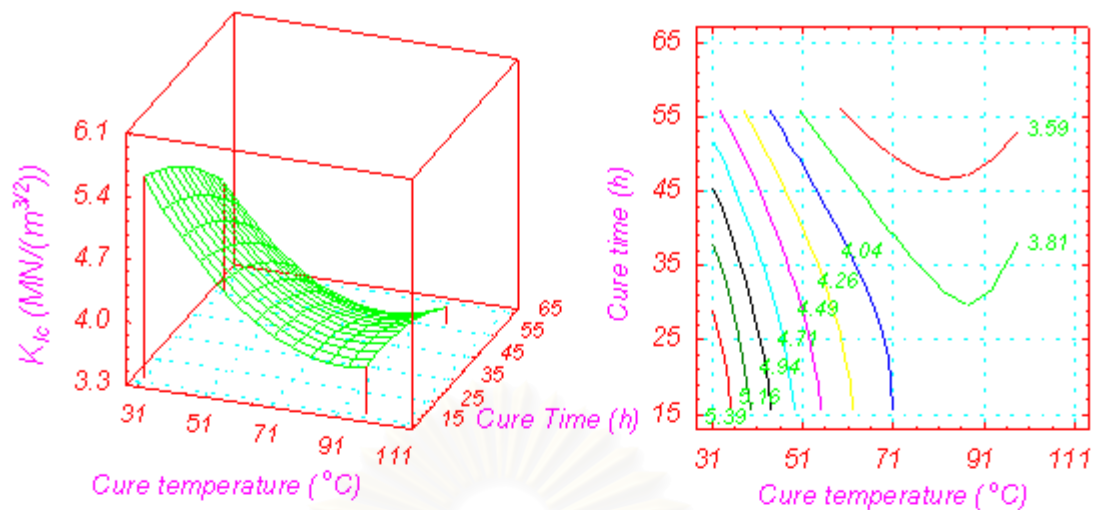
The response surface and contour curves exhibiting the relationship between K_{Ic} and the curing factors from the double torsion test of epoxy composites are shown in Figure 5.13 . Form Figure 5.13 (a), it can be deduced that the critical stress intensity factor can be raised easily by reducing cure temperature and cure time. Therefore, curing the epoxy coating composites for 15.8 h at 31°C was chosen as the most suitable cure condition. Figure 5.13 (b) and (c) demonstrated that increasing the percentage of sand could also promote the critical stress intensity factor. Figure 5.14 displayed the contour curves of the critical stress intensity factor at a constant cure temperature of 31 °C. The highest critical stress intensity factor obtained when the system was cured for 15.8 h is 6.09 MN/m^{3/2} at the amount of 33.87% of sand filler in the epoxy composite formulation.

The fracture energy, G_{Ic} , can be related to the critical stress intensity factor, K_{Ic} , by Equation 5.5

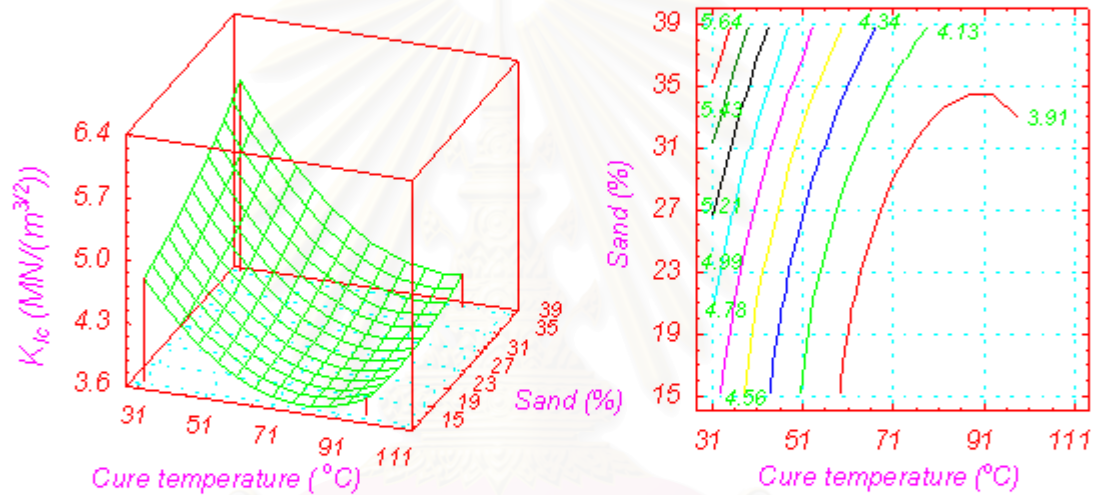
$$G_{Ic} = \frac{K_{Ic}^2}{E} \quad (\text{in plane stress}) \quad 5.5$$

$$G_{Ic} = \frac{K_{Ic}^2 (1-\nu^2)}{E} \quad (\text{in plane strain}) \quad 5.5$$

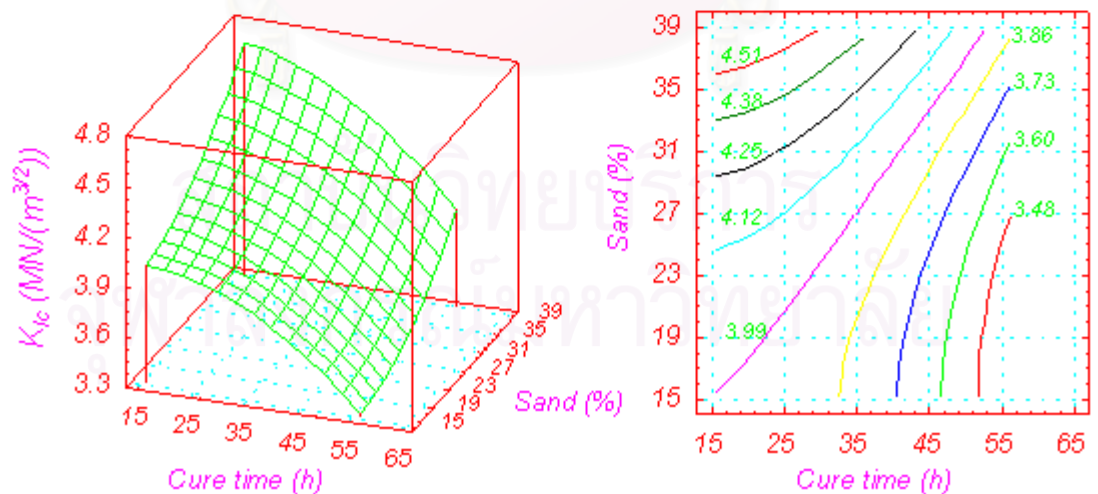
The specimen configuration under the double torsion test in the present study is in plane stress condition. A comparison of the fracture energy of the neat epoxy, glass fiber-reinforced epoxy composite and the glass fiber-reinforced epoxy composite filled with 27% sand and cured at 65°C for 36 h is shown in Figure 5.15 .



(a) Effects of cure temperature and cure time at a constant amount of sand 27%.



(b) Effects of cure temperature and amount of sand at a constant cure time 36 h.



(c) Effect of cure time and amount of sand at constant cure temperature of 65°C.

Figure 5.13 : Effect of cure temperature, cure time, and sand filler on epoxy composite

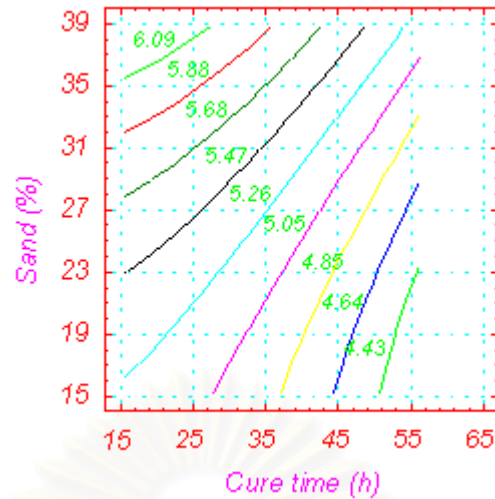


Figure 5.14 : Contour of the critical stress intensity factor of epoxy composites between the amount of sand and the cure time at a constant cure temperature of 31°C.

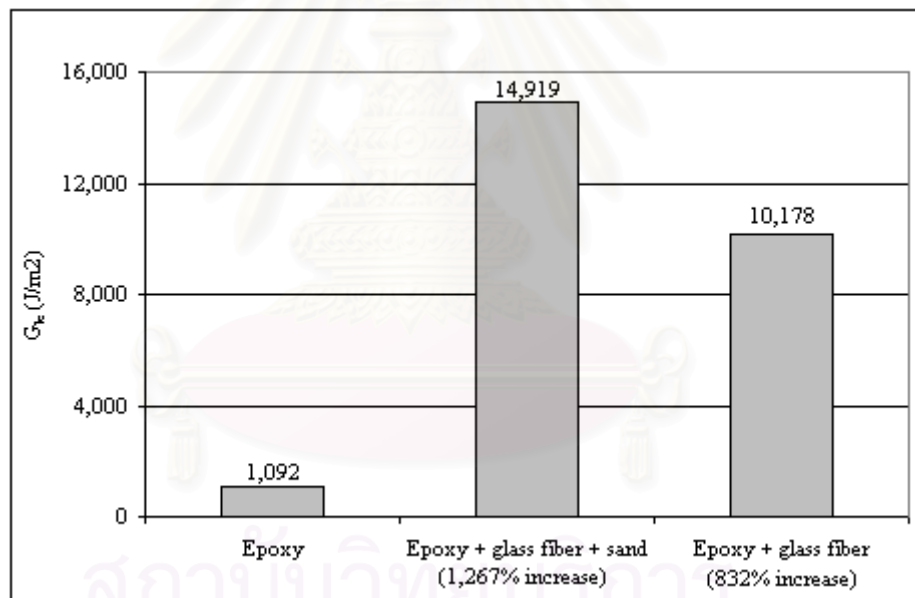


Figure 5.15 : Fracture energy of neat epoxy and epoxy composites.

Fracture energy is improved and still maintains the same sequence as that observed in the stress intensity factor. Reinforcing the epoxy specimen by glass fiber already enhanced fracture energy of the specimen. Fracture energy can be enhanced further by adding sand. In Figure 5.15, it is evidently seen that sand filler makes the filled epoxy composite much tougher than both the unfilled-epoxy composite and the neat epoxy.

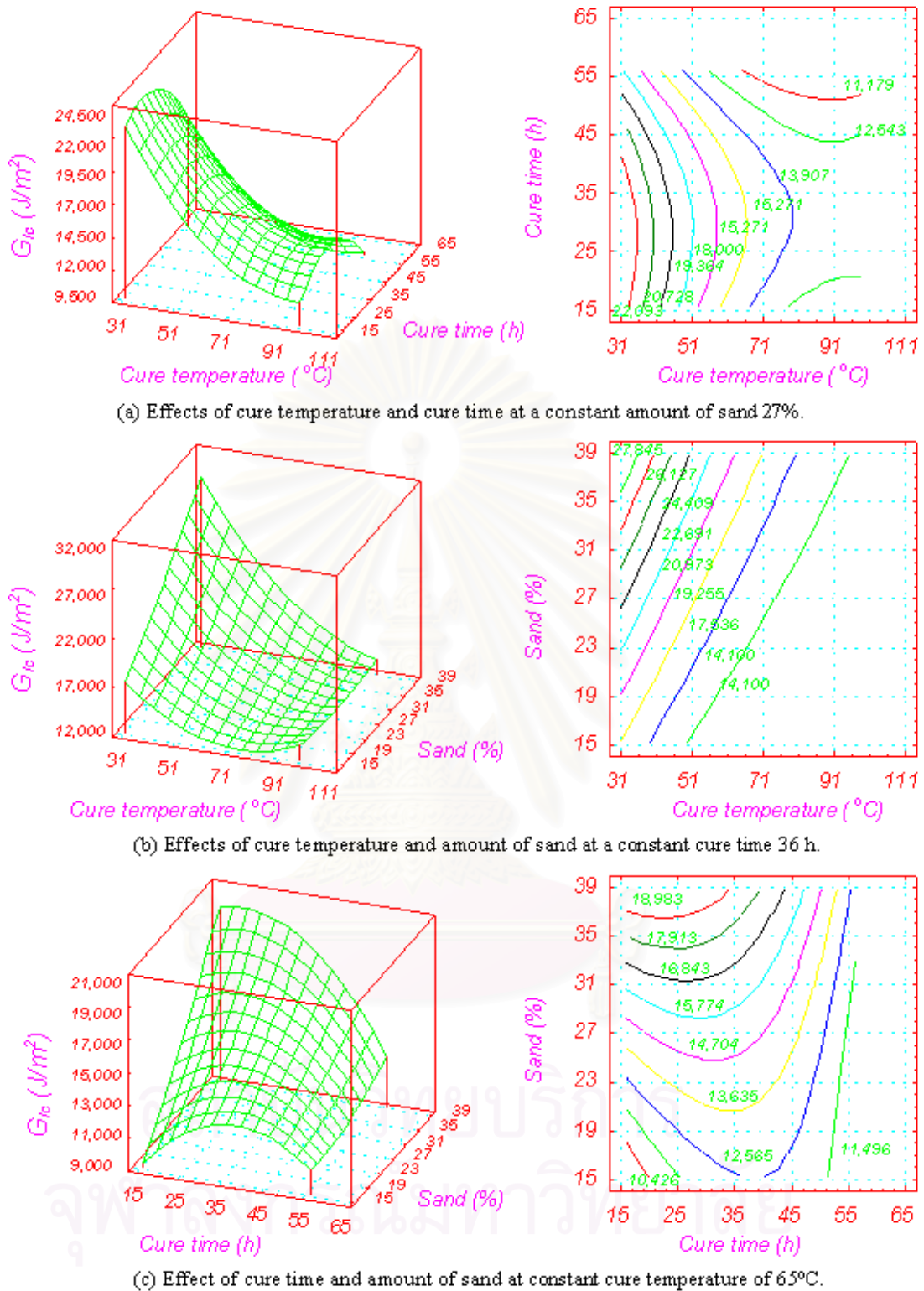


Figure 5.16 : Effect of cure temperature, cure time, and sand filler on epoxy composite

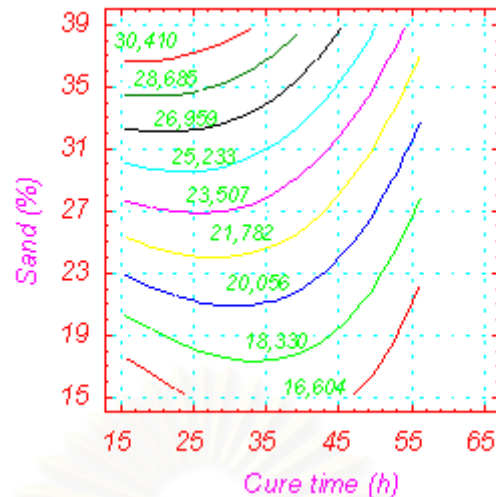


Figure 5.17 : Contour of the fracture energy for the epoxy composite between the amount of sand and the cure time at a constant cure temperature of 31°C.

The response surface and contour curves displaying the relationship between the G_{Ic} and the curing factors in Figure 5.17 are similar to Figure 5.14. The greatest fracture energy obtained at the same condition as that for the greatest critical stress intensity factor when sand was added by 38.77% and the cure was conducted at 31 °C for 15.8 h is at 30,410 J/m² as shown in Figure 5.17.

5.3.2 Concrete Coated Specimens

Compression test of the concrete coated with neat epoxy and epoxy composite was conducted to cross-check whether the most appropriate curing condition derived from the compressive test of epoxy composite remains at the recommended condition when the coating composite was applied to the concrete substrate, which is the modeling concrete floor structure. Despite the fact that curing at high temperatures is probably not so practical for most industrial floor coating, the range of cure temperature for concrete coated specimens in this experiment still covered high temperatures, which is at a maximum of 99 °C. If the results show that the curing at high temperature truly and significantly improves the compressive strength of the coating material, then an attempt to cure the floor coating material at high temperature will be worth, and a methodology for highest temperature curing have to be developed.

Figure 5.18 shows the epoxy composite-coated concrete cracked from compression test. The concrete was the first part to be cracked by shear failure, the crack then propagated further up from concrete to the coating layer.

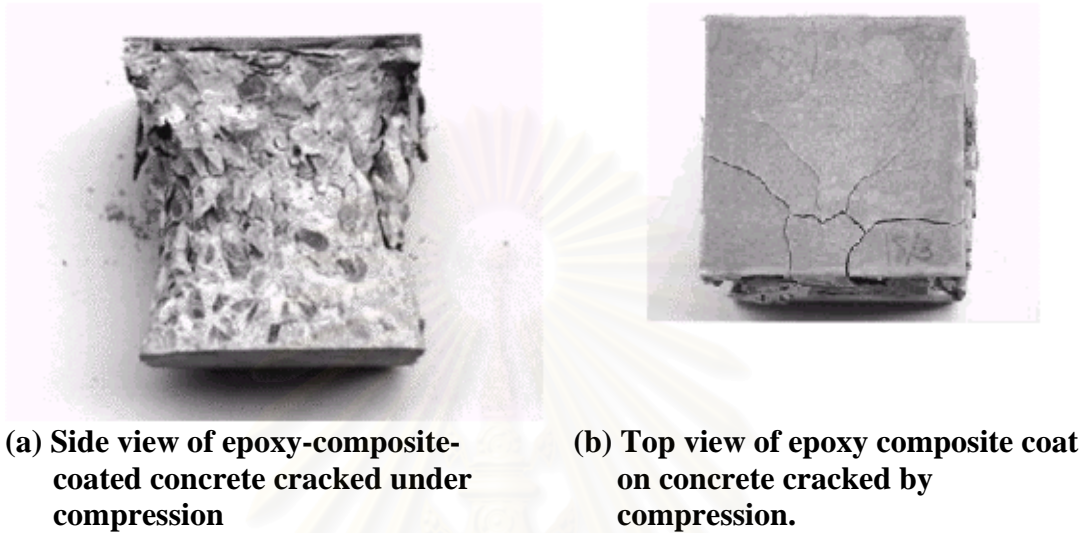


Figure 5.18 : Concrete coated specimen from compression test.

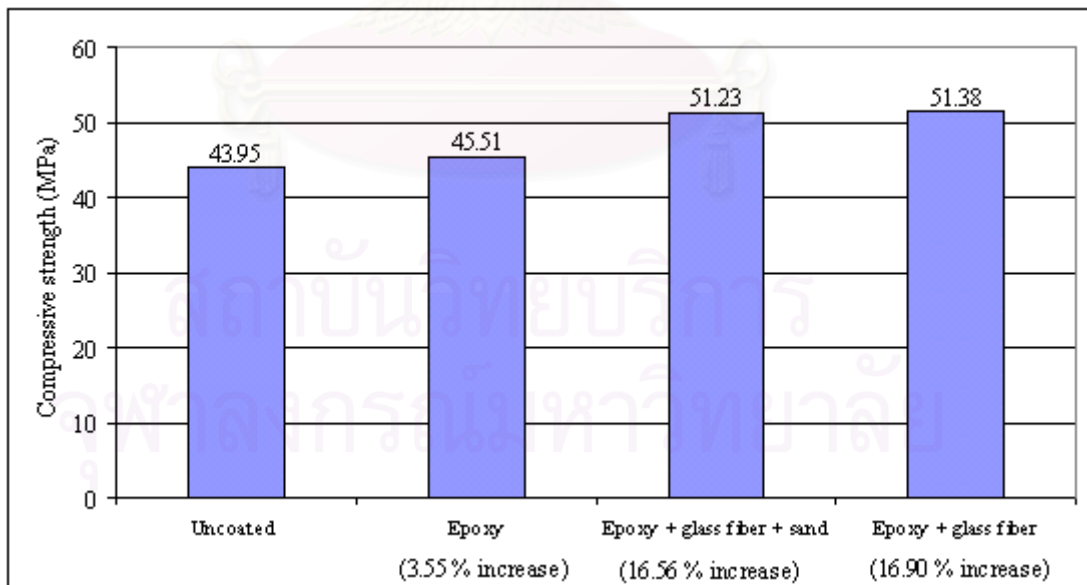


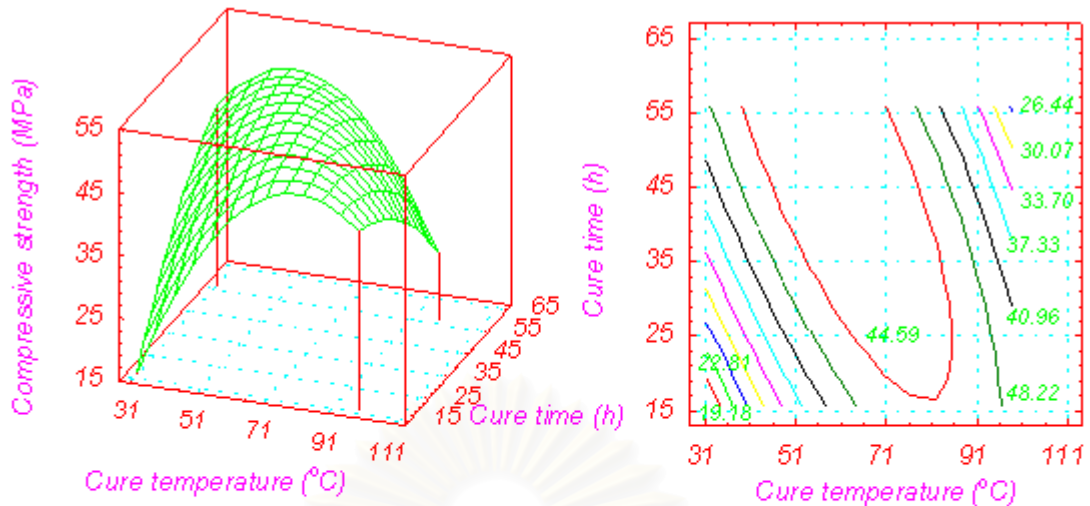
Figure 5.19 : Compressive strength of uncoated concrete and coated concrete.

Figure 5.19 compared the compressive strength of uncoated, epoxy coated, glass fiber-reinforced epoxy composite coated and glass fiber-reinforced

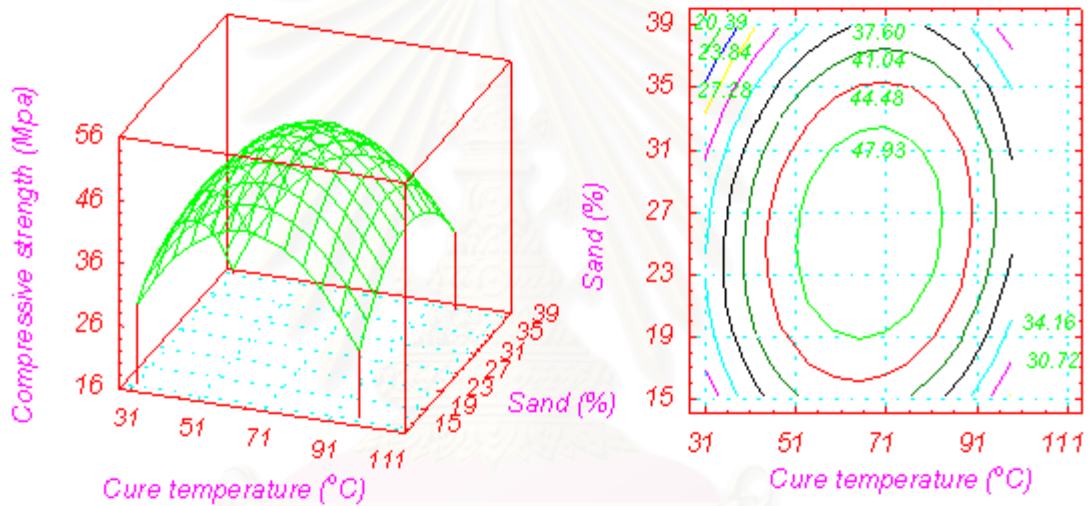
epoxy composite filled with sand 27% coated concrete. All coating was cured at 65 °C for 36 h. Unfilled and filled epoxy composite-coated concretes exhibit slight enhancement in the compressive strength. The sequence of improvement in the coated concrete from the lowest to the highest compressive strength is same as those observed in the epoxy composite coating material alone.

The response surface and contour curves of the compressive strength of epoxy composite coated concrete are shown in Figure 5.20 . Figure 5.20 (a), (b) and (c) illustrated that there are optimum values of all curing factors, which are cure temperature, cure time and amount of sand filler, can be obtained. From Figure 5.20 (c), the amount of added sand that gives the greatest compressive strength is at 25% sand. At this quantity of sand, high compressive strength can be obtained from a wide range of cure temperature and cure time. The greatest compressive strength of 52 MPa can be obtained when cure is conducted at 67 °C for 49 h with an addition of 25% of sand, as shown in Figure 5.21.

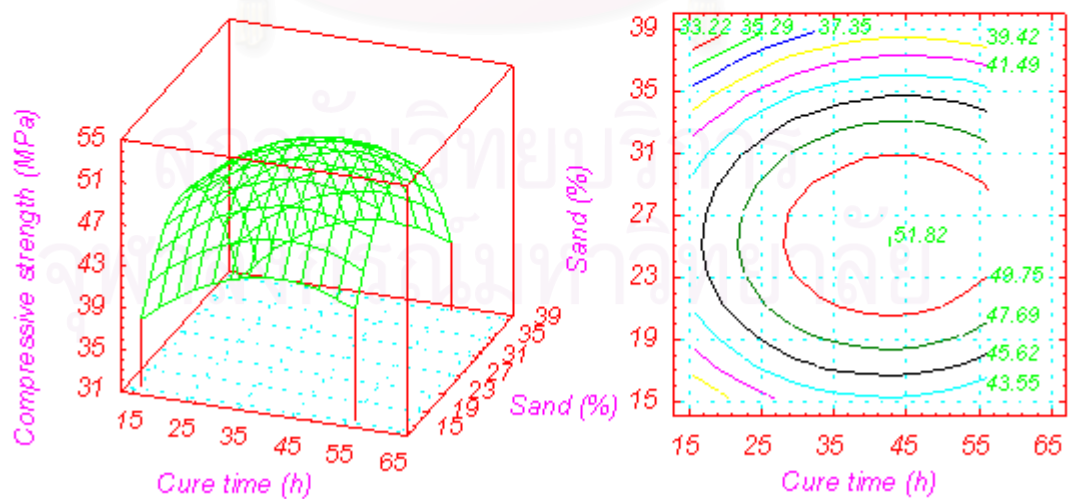
Since the cure temperature that offers this maximum strength may not be practical for large surface area coating as industrial floor, a lower temperature may be used instead. In order to obtain high compressive strength at lower cure temperatures, cure time must be extended. From Figure 5.19, the longest cure time of 56.2 h imparts the highest compressive strength compared with other cure duration. This is the reason why many industrial flooring manufacturers let the coating material cure for about 3-4 days at room temperature. In this study, curing at the lowest cure temperature 31 °C and the longest cure time of 56.2 h gives the compressive strength at 44.87 MPa, which is expected to be higher if the cure period is extended longer.



(a) Effects of cure temperature and cure time at a constant amount of sand 27%.



(b) Effects of cure temperature and amount of sand at a constant cure time 36 h.



(c) Effect of cure time and amount of sand at constant cure temperature of 65°C.

Figure 5.20 : Effect of cure temperature, cure time, and sand filler on epoxy composite

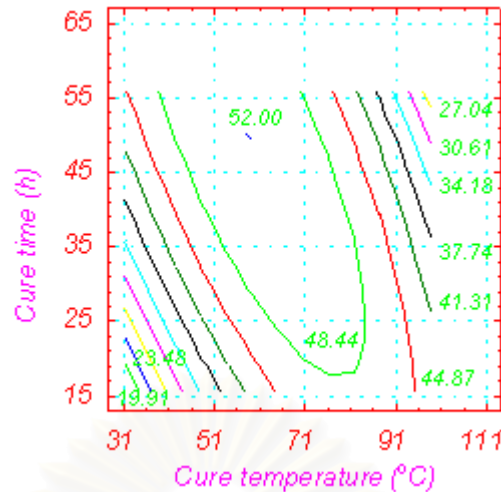


Figure 5.21 : Contour of the compressive strength of concrete coated with epoxy composite between the cure temperature and cure time at a constant amount of sand of 25%.

From the above investigation, the most suitable curing condition that provides the highest compressive strength in this experimental test differs from that obtained for the epoxy composite coating without any substrate. In concrete coated with epoxy composite, sand can be added to the epoxy composite at a higher amount, i.e. 25% compared with 15.23% of sand. This is because more amount of sand was detached from the epoxy composite without the concrete substrate than the coated concrete as the compression load was applied. Detached sand no longer received the compressive load transferred from the epoxy matrix, resulting in a reduction in the compressive strength.

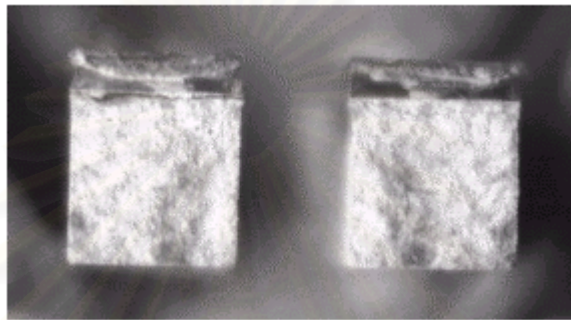
Though speculations can be deduced from the present sets of results, verification would require more tests conducted on filled-epoxy composite coated on concretes cured at extended period and with various amount of sand to induce better compression property.

5.3.3 Mortar Coated Specimens

Impact test of mortar coated with epoxy composite was performed to confirm whether the most suitable cure condition found in the impact test of epoxy composite remains at the recommended condition when the epoxy composite was applied to the mortar substrate, the modeling floor structure. As with the epoxy

composite-coated concrete, the range of cure temperature for concrete coated specimens in this experiment still covered high temperatures with the maximum at 99°C, although high temperature curing may not be practical for industrial floor coating.

Figure 5.22 shows the cracked specimen from impact test. The fracture surface of mortar coated with epoxy composite is shown in Figure 5.22 (a). The broken halves of the specimen from the impact test are shown in Figure 5.22 (b).



(a) Fracture surface of mortar coated with epoxy composite.



(b) Mortar coated with epoxy composite broke into 2 halves upon impact.

Figure 5.22 : Fracture of mortar coated with epoxy composite by the impact test.

The pendulum of the impact testing machine was set so that the striking edge of the free-hanging pendulum hammer would just touch the specimen as shown schematically in Figure 5.23.

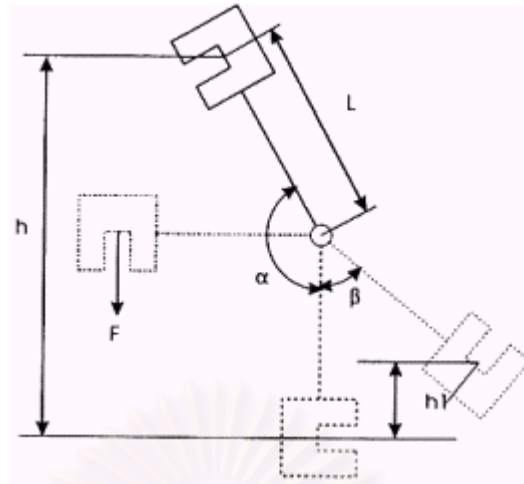


Figure 5.23 : Principle of the impact by pendulum.

The potential energy (A_p) is calculate from the force (F) multiplied by the height of the fall as shown in Equation 5.7 .

$$A_p = F * h = F * L(1 - \cos \alpha) \quad [J] \quad 5.7$$

where L is the distance in metre between the pendulum axis and the point of impact of the striking edge in the center of the specimen. Upon the release of the pendulum hammer, the potential energy is converted into kinetic energy by acceleration owing to gravity. When the pendulum hammer was released and stroke on the specimen, both the mortar and its epoxy composite coat broke upon impact. The pendulum lost part of its velocity and hence part of its impact energy. The excess energy, A_e , is calculated as shown in Equation 5.8 .

$$A_e = F * h_1 = F * L(1 - \cos \beta) \quad [J] \quad 5.8$$

The absorbed impact energy, A_v , is the difference between the potential energy and the excess energy A_e , as shown in Equation 5.9

$$A_v = A_p - A_e \quad [J] \quad 5.9$$

The absorbed impact energy is the energy required to break the mortar coated specimen or the impact strength of the specimen. Though falling weight impact tests generally yields energy in Joules, this experimental work will

report the impact energy in *energy per cross-sectional area of the fracture specimen* (KJ/m^2) so that it can be compared with the impact strength of epoxy composite coat.

Figure 5.24 compared the impact strength of the uncoated mortar, mortar coated with neat epoxy, glass fiber-reinforced epoxy composite and glass fiber-reinforced epoxy composite filled with 27% sand and cured at 65°C for 36 h . It is evident that coating improves the impact strength of the mortar. The sequence of the coated mortar with the lowest to the highest impact strength is the same as those of the epoxy composites.

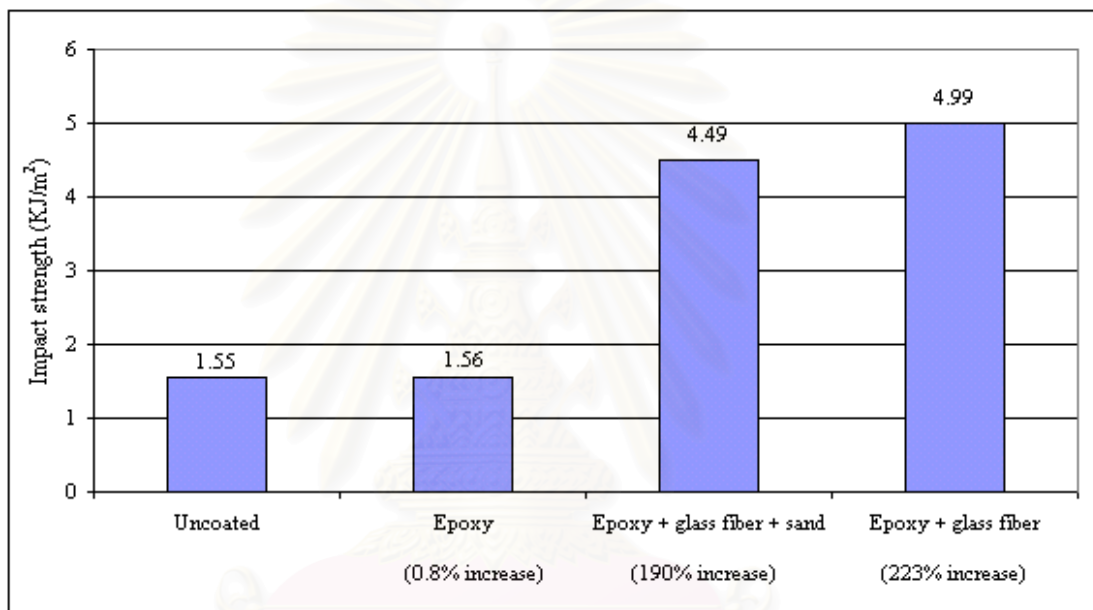
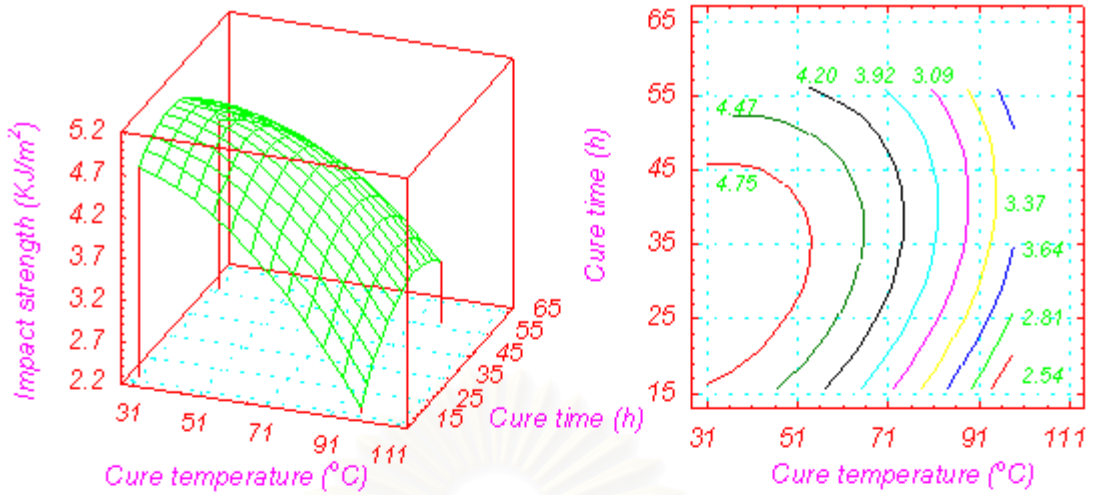
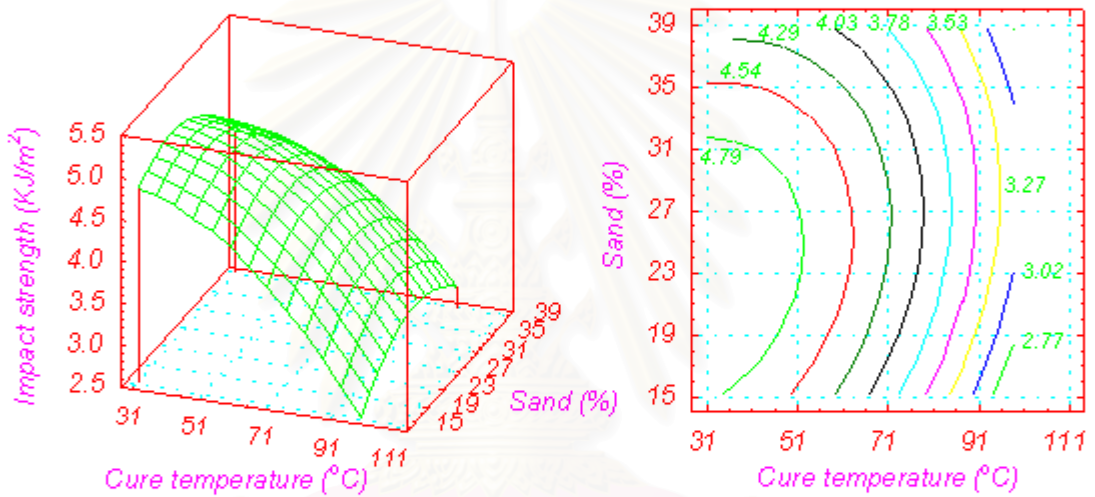


Figure 5.24 : Impact strength of uncoated mortar and coated mortar.

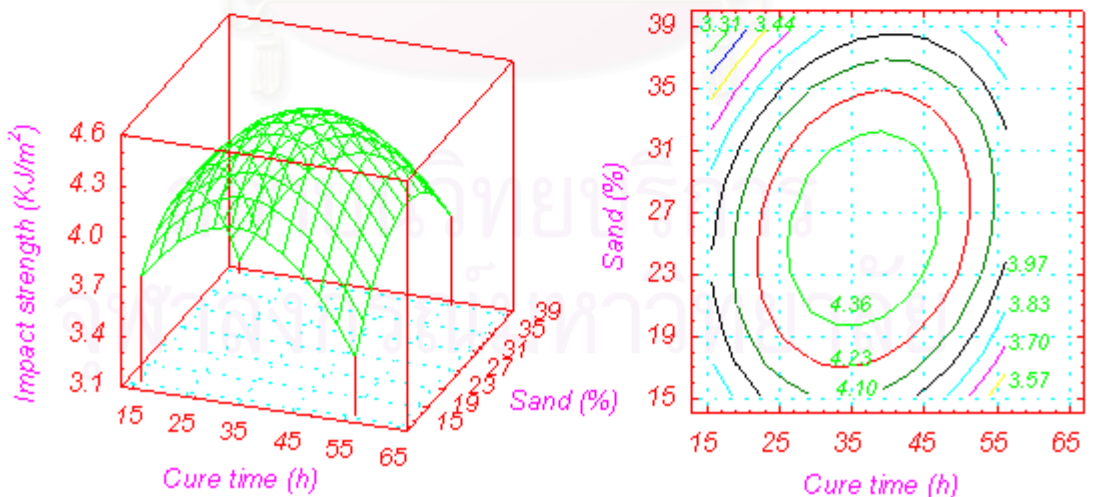
From the response surface and contour curves for the impact strength of coated mortar shown in Figure 5.25 (a) and (b), it is apparent that curing at low temperature imparts better impact properties. Both cure time and amount of sand showed an optimum point as shown in Figure 5.25 (c). At 31°C , the lowest temperature in this study, the optimum cure time and the amount of added sand is 29 h and 23% respectively. Curing at this condition gives the greatest impact strength at 5.10 KJ/m^2 as shown in Figure 5.26.



(a) Effects of cure temperature and cure time at a constant amount of sand 27%.



(b) Effects of cure temperature and amount of sand at a constant cure time 36 h.



(c) Effect of cure time and amount of sand at constant cure temperature of 65°C.

Figure 5.25 : Effect of cure temperature, cure time, and sand filler on epoxy composite

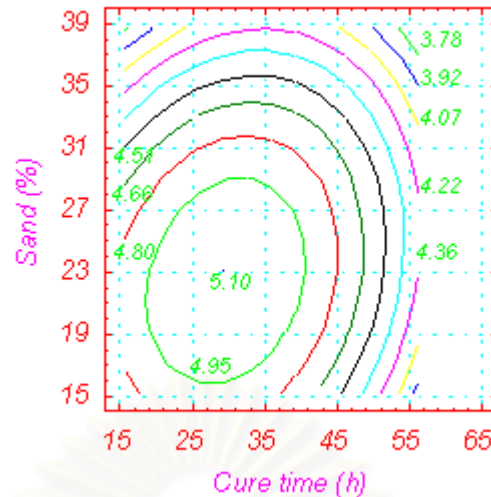


Figure 5.26 : Contour of the impact strength of epoxy composite coated mortar between the cure time and the amount of sand at a constant cure temperature of 31°C.

Comparing with the epoxy coating composite without any substrate, the influences of cure temperature and the amount of sand filler on the mortar coated with epoxy composite are the same. Curing both the epoxy composites and the mortar coated with epoxy composite at low temperature induces better impact properties. The optimum amount for adding sand in each system differs a little, i.e. 27% and 23 % of sand filler for epoxy composite and for mortar coated specimens respectively. The effect of the cure time on mortar coated specimens is obviously shown by a peak in Figure 5.25 (c). On contrary, the effect of the cure time on the epoxy composite is rarely noticed. Therefore, an additional test was conducted to verify the significance of cure time on the impact property for different formulation by curing the epoxy composite at a shorter period of cure time. Figure 5.27 showed the result of this additional test, which verified that an impact strength peak is obtained for the cure time of 9 h and 12 h when the amount of sand added is 20% and 27% respectively. This maximum impact strength in each case implied that there is an optimum condition for cure and cure time does have an effect on the impact property of the epoxy composite. The plot in Figure 5.27 also depicts a diminution in the impact strength beyond the optimal cure time. Hence, both the epoxy composites and the mortar coated with epoxy composite have an optimum value of cure time. The epoxy composite tends to reach its zenith over a longer period of cure time than

that required for curing the same epoxy composite coat on the mortar. This behavior is comparable with that of the discrepancy seen in the influences of the cure time on the concrete coated with epoxy composite and the epoxy composite without any substrate. The discrepancy arise in both cases is attributed to the possible difference in actual temperature profile of each coating system during the process of curing. Curing itself is an exothermic reaction. Although both the epoxy composite and the mortar coated with epoxy composite are cured at temperatures within the same range, the actual temperature within each system during curing may differ due to the non-uniform form exothermic reaction. In the mortar coated with epoxy composite system, temperature may have developed and partially lost to the mortar. Hence, more time is required to build up the temperature profile, leading to a discrepancy in exhibiting the influences of cure time.

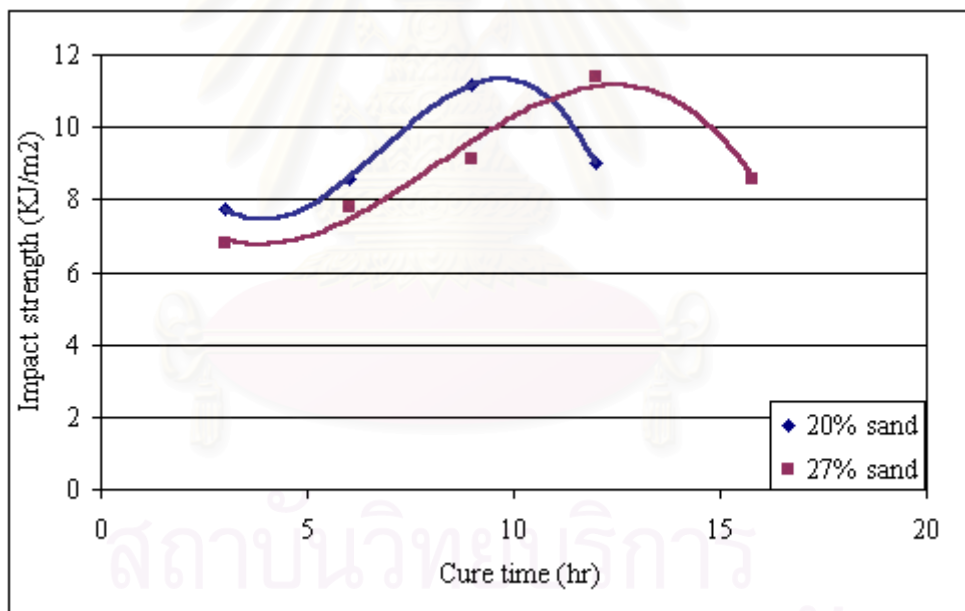


Figure 5.27 : Impact strength of the epoxy composite cured with 20% and 27% sand both were cured at 65°C.

5.4 IMPROVEMENT IN MECHANICAL PROPERTIES OF THE EPOXY COMPOSITES

From the experimental results in Section 5.3, it is obvious that the epoxy composite coat yields better mechanical properties than the neat epoxy. The order of improvement achieved in the mechanical properties of the epoxy composites is illustrated in Table 5.7 . It is obvious that glass fiber reinforcement increases the mechanical properties because it supports the applied load transferred from the epoxy resin. Moreover, the critical stress intensity factor and the fracture enhanced further by adding sand, which is a tough phase, to the epoxy composite. Though fracture properties of the glass fiber-reinforced epoxy composite are significantly elevated by adding sand, the compressive strength and the impact strength decreases slightly, but they are still higher than the neat epoxy. The reason for this is because the adhesion between the sand filler and the epoxy resin is not so good as between the glass fiber and the epoxy resin.

Table 5.7 : Improvement in mechanical properties of the epoxy composites cured at 65 °C for 36h.

Mechanical proprties	Improvement in properties (%)	
	Glass fiber-reinforced epoxy composite	27% sand filled glass fiber-reinforced epoxy composite
Compressive strength	11.9	9.9
Impact strength	86.4	22.8
Critical stress intensity factor	219	297
Fracture energy	832	1267

Results from the compression test in the epoxy composite coated concrete showed that the sequence of improvement in the coated concrete from the lowest to the highest compressive strength is the same as those observed in the epoxy composite coating material alone, as displayed in Table5.8 .

Table 5.8 : Improvement in compressive strength of the epoxy composites coated concrete cured at 65 °C for 36h.

Improvement in compressive strength (%)		
Concrete coated with neat epoxy	Concrete coated with glass fiber-reinforced epoxy composite	Concrete coated with 27% sand filled glass fiber-reinforced epoxy composite
3.5	16.9	16.6

The sequence of improvement in the impact strength of the epoxy composite coated on mortar is also the same as those in the epoxy composite coating material alone, as shown in Table 5.9 .

Table 5.9 : Improvement in mechanical properties of the epoxy composites coated mortar cured at 65 °C for 36h.

Improvement in the impact strength (%)		
Mortar coated with neat epoxy	Mortar coated with glass fiber-reinforced epoxy composite	Mortar coated with 27% sand filled glass fiber-reinforced epoxy composite
0.8	223	190

5.5 EFFECTS OF CURING FACTORS ON MECHANICAL PROPERTIES OF THE EPOXY COMPOSITES

Influences of the curing factors on the mechanical properties of the epoxy composites drawn from the experimental tests in Section 5.3 are summarized in from Tables 5.10 to 5.12 .

From Table 5.10, the cure temperature that gives the highest compressive strength in both the epoxy composite and the epoxy composite coated concrete is quite high. By extending the cure time, a more practical cure temperature

of 31°C, which is the lowest cure temperature in the range studied is recommended. High compressive strength can also be achieved by curing at this condition.

Table 5.10 : Effects of the cure temperature on mechanical properties of the epoxy composites.

Mechanical properties	Epoxy Composite	Concrete coated with epoxy composite	Mortar coated with epoxy composite
Compressive strength	Increasing cure temperature induces better compressive strength	Optimum at 67 °C	
Impact strength	Reducing cure temperature induces better impact strength		Reducing cure temperature induces better impact strength
Critical stress intensity factor (K_{Ic}) and Fracture energy (G_{Ic})	Reducing cure temperature induces better fracture properties		

Table 5.11 : Effects of the cure temperature on mechanical properties of the epoxy composites.

Mechanical properties	Epoxy Composite	Concrete coated with epoxy composite	Mortar coated with epoxy composite
Compressive strength	Increasing cure time induces better compressive strength	Optimum at 49 h	
Impact strength	Optimum at 12 h		Optimum at 29 h
Critical stress intensity factor (K_{Ic}) and Fracture energy (G_{Ic})	Increasing cure time induces better fracture properties		

Table 5.12 : Effects of the cure temperature on mechanical properties of the epoxy composites.

Mechanical properties	Epoxy Composite	Concrete coated with epoxy composite	Mortar coated with epoxy composite
Compressive strength	Reducing amount of sand induces better compressive strength	Optimum at 25%	
Impact strength	Optimum at 27%		Optimum at 29%
Critical stress intensity factor (K_{Ic}) and Fracture energy (G_{Ic})	Increasing amount of sand induces better compressive strength		

5.6 OPTIMUM CURE CONDITION

Curing the epoxy composite with an appropriate cure condition can enhance the mechanical properties of the epoxy coating composite material. Experimental results drawn from Section 5.3 illustrated how to cure the epoxy coating composite material to give the greatest mechanical properties, which are summarized in Table 5.13 .

Table 5.13 : The appropriate cure condition for each mechanical property.

Mechanical Properties	Cure temperature (°C)	Cure time (h)	Amount of sand filler (% vol)
Compressive strength	31	56.2	25
Impact strength	31	29	23
Critical stress intensity factor (K_{Ic}) and Fracture energy (G_{Ic})	31	15.8	38.77

Since the most suitable cure condition for adding each mechanical property at its best tend to vary, a compromise condition needs to be drawn. From the varying the curing factors in the response surface equations of the mechanical properties, the appropriate condition for curing the epoxy composite coat material is

at the cure temperature of 31 °C for 56.2 h with 29% sand. At this condition, reductions of mechanical properties from the highest values are compromised. The mechanical properties achieved at this recommended cure condition, as shown in Table 5.14, are still desirable and appropriate for industrial floor coating application.

Table 5.14 : The mechanical properties of the epoxy composites, the epoxy composite coated concrete and the mortar coated composites cured at 31 °C for 56.2 h. The amount of sand filler added is 29%.

Mechanical properties	Cure condition of 31°C for 56.2 h with 29% sand.	Decrease from the highest value achievable (%)
Epoxy composite		
Compressive strength (MPa)	89.04	24.2
Impact strength (KJ/m ²)	10.11	3.3
Critical stress intensity factor (MN/m ^{3/2})	4.943	18.8
G _{Ic} (J/m ²)	24,867	18.2
Concrete coated with epoxy composite		
Compressive strength (MPa)	46.96	9.7
Mortar coated with epoxy composite		
Impact strength (KJ/m ²)	4.915	3.6

5.7 MICROSCOPIC OBSERVATION

The studies of the fracture surface of epoxy composite coats are shown in their fractographs from Figures 5.28 to 5.42 .

Figures 5.28 to 5.32 show the micrographs of the fractured surface of epoxy composite failed by impact. A complete width depicting 5 individual layers of the fractured epoxy composite with glass fiber reinforced and sand filler appears in Figure 5.28 .

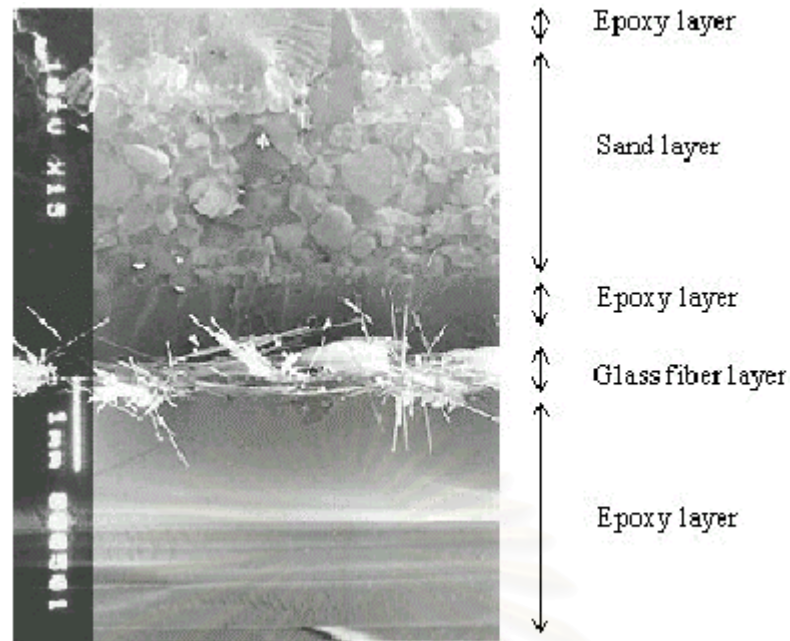


Figure 5.28 : Impact fracture surface of epoxy composite cured at 65 °C 36 h 27% sand.

Detailed analysis of the impact fractured surfaces from Figure 5.28 are shown in Figures 5.29 to 5.32 . Figure 5.29 displays the fracture in the epoxy layer at the bottom of the composite. Apparent on the fracture surface caused by local plastic deformation was the texture of river markings oriented in the direction of crack propagation [18, 48]. They were significant morphological clue for locating local crack propagation.

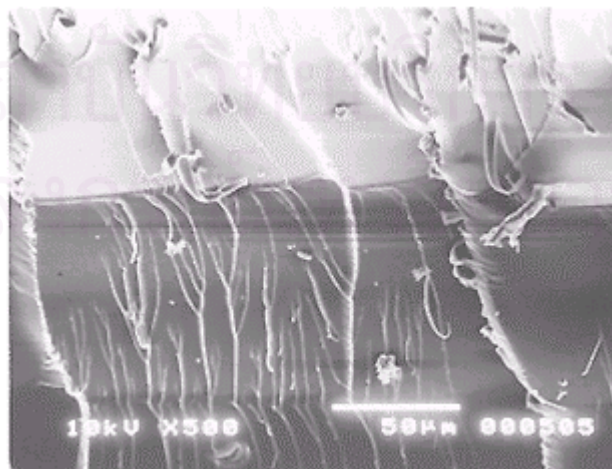


Figure 5.29 : Impact fracture surface in the epoxy layer of the epoxy composite cured at 65 °C for 36 h. The amount of sand added was 27%.



Figure 5.30 : Impact fracture surface in the epoxy layer of the epoxy composite cured at 65 °C for 36 h. The amount of sand added was 27%.

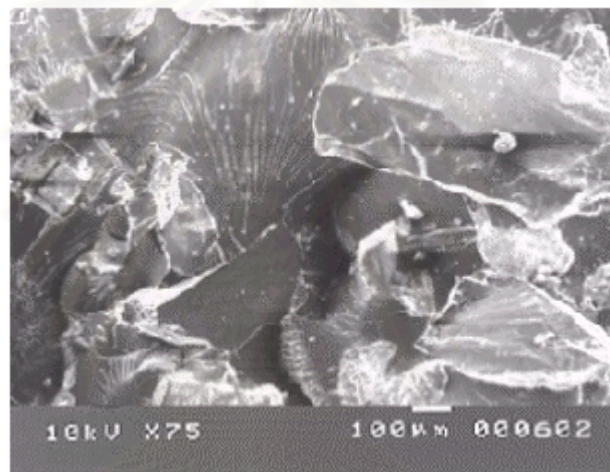


Figure 5.31 : The sand layer in the epoxy composite cured at 65 °C for 36 h. The amount of sand was 15.23%

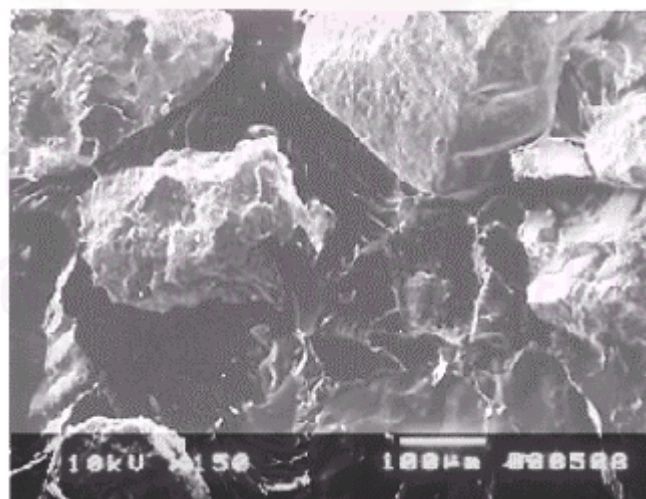


Figure 5.32 Adhesion between sand and epoxy resin in epoxy composite.

Figure 5.30 shows the sand layer in the epoxy composite cured at 65°C for 36 h. The amount of sand was 27%. The nature of local crack pattern in the sand filler layer is more apparent in Figure 5.31 where less amount of sand was present. Figure 5.32 shows adhesion between the sand filler and the epoxy matrix.

The fracture surfaces obtained from the double torsion test are shown in Figures 5.33 to 5.40 . It is obvious from the fractographs that the fracture behavior of the epoxy composites failed by double torsion differs from that failed by impact test. The fracture surface of epoxy composite, as shown in Figure 5.33, is quite rough, indication that it is quite a tough specimen. A section of the fracture area of the double torsion test specimen is displayed in Figure 5.34.



Figure 5.33 : Fracture surface of epoxy composite cured at 65°C 36 h 27% sand.

สถาบันวิทยบริการ
จุฬาลงกรณ์มหาวิทยาลัย

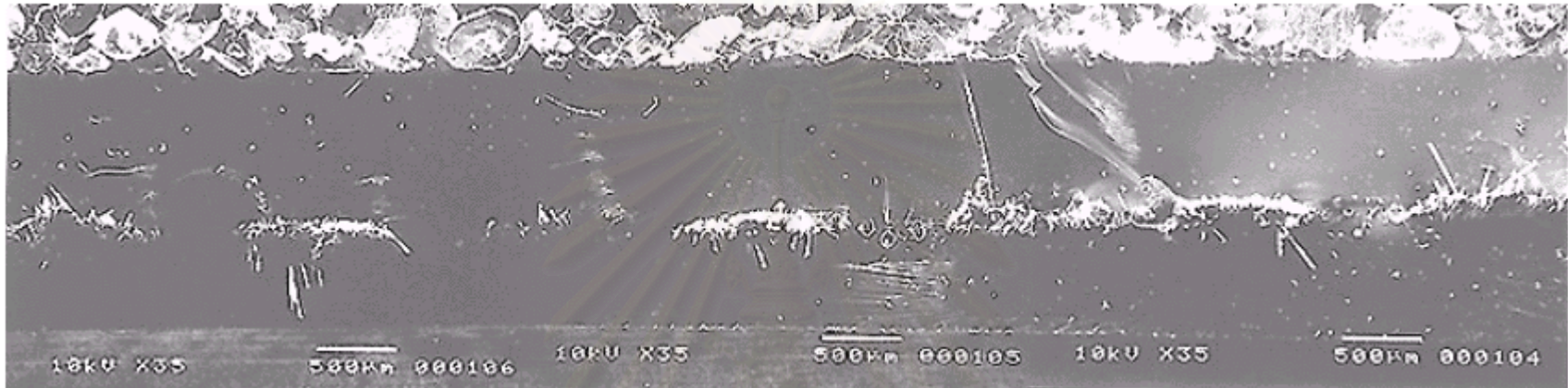


Figure 5.34 : Section of the fracture area of the epoxy composite cured °at 65 C for 36 h. The amount of sand added is 38.77%

สถาบันวิทยบริการ
จุฬาลงกรณ์มหาวิทยาลัย

A larger magnification of Figure 5.33 is shown in Figures 5.35 to 5.40. Figure 5.35 shows the river marking in the epoxy layer. Figure 5.36 shows the adhesion between the sand filler and the epoxy matrix, which is magnified in Figure 5.37. By comparing the surface shown in Figure 5.37 with that shown in Figure 5.31, it is apparent that the fracture in the sand layer of double torsion test and impact test occurred in different manners. Better adhesion between the sand filler and the epoxy resin is observed in the double torsion specimen as shown in Figure 5.37. This behavior is also the same in the adhesion between the glass fiber reinforcement and the epoxy matrix as shown in Figures 5.38 to 5.40, in which the resins is seen adhered to the pulled-out glass fibers.

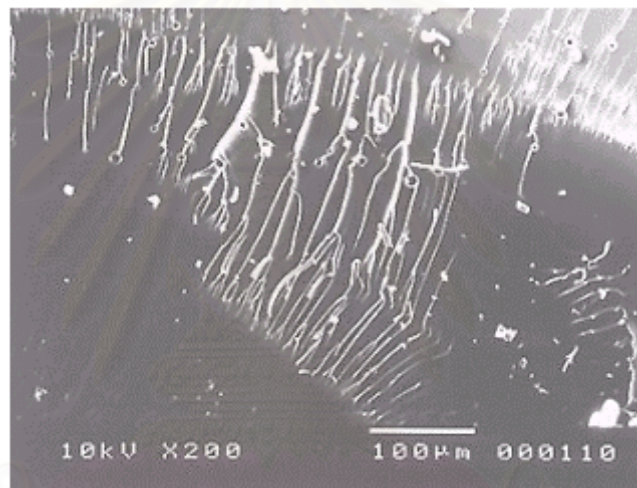


Figure 5.35 : River markings in the epoxy composite cured at 65°C for 36 h.

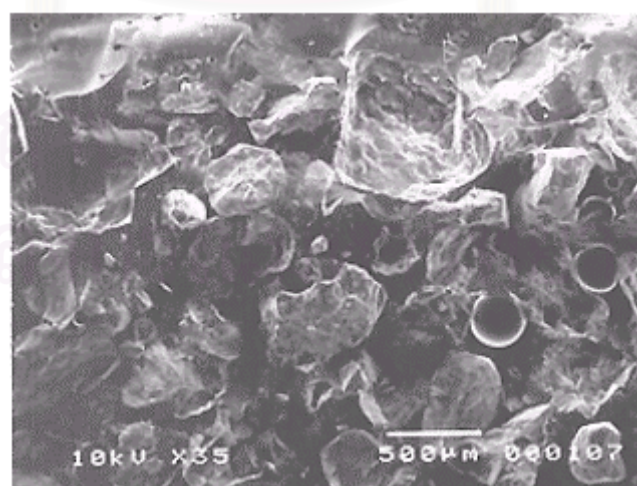


Figure 5.36 : The sand layer of the epoxy composite cured at 65°C for 36 h. The amount of sand added is 38.77%.

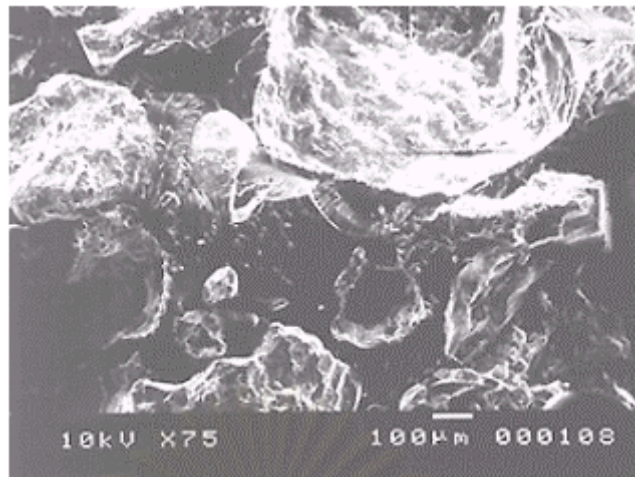


Figure 5.37 : Adhesion between the sand and the epoxy resin in epoxy composite cured at 65°C for 36 h. The amount of sand added is 38.77%.

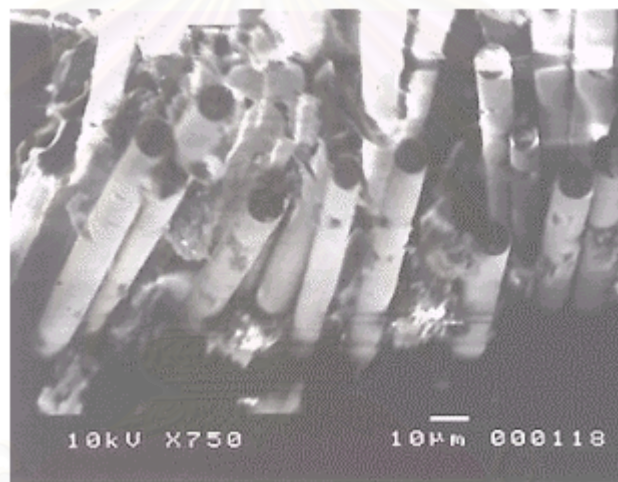


Figure 5.38 : Pulled-out glass fibers in the fracture surface of epoxy composite failed by double torsion test.

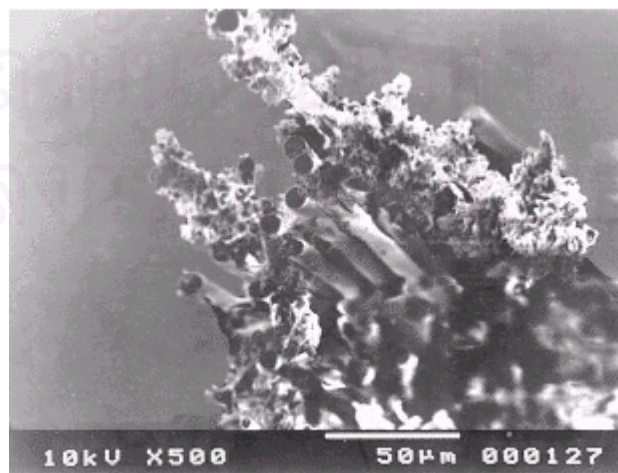


Figure 5.39 : Glass fibers and the epoxy resin adhered to them.

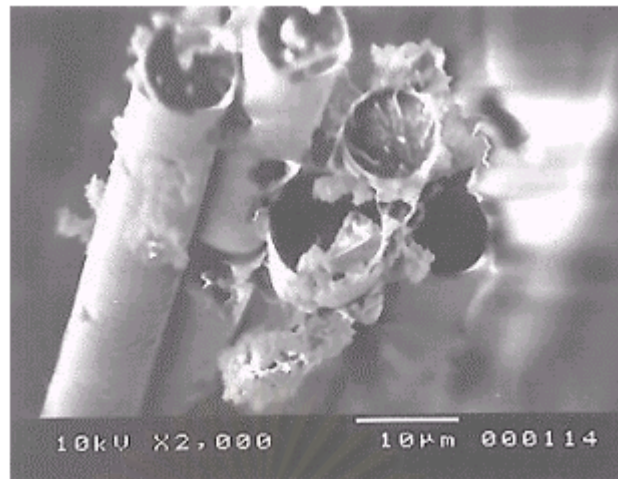


Figure 5.40 : Adhesion between glass fiber and epoxy resin.

Micrographs of the interface between the concrete substrate and the epoxy resin coated on the concrete are illustrated in Figure 5.41 and magnified in Figure 5.42, which exhibit adhesion between the concrete and the epoxy resin.

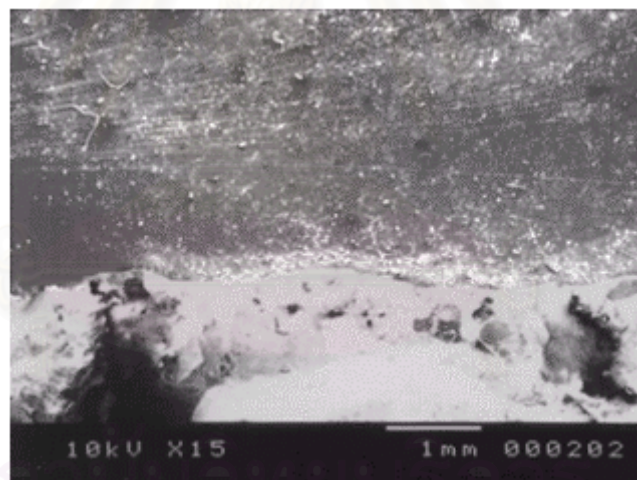


Figure 5.41 : Fracture surface of the concrete coated with the epoxy composite.

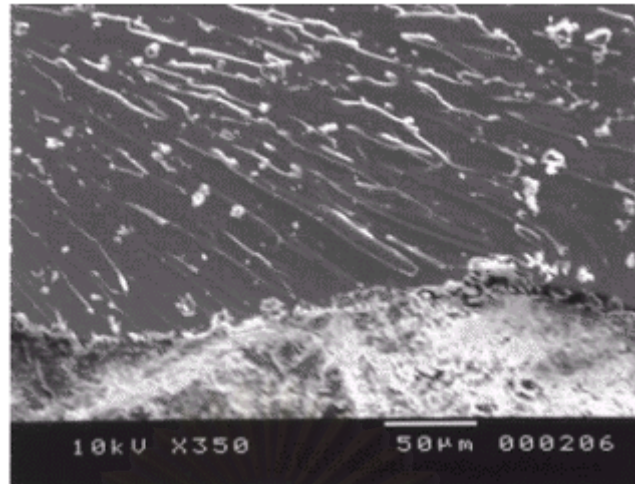


Figure 5.42 : Adhesion between the concrete and the epoxy composite.

5.8 SAMPLE CHARACTERIZATION

The Dynamic Mechanical Analysis (DMA) test is capable of measuring viscoelastic properties of polymers such as the storage modulus (G') and the loss tangent ($\tan \delta$). These properties are plotted against the temperature as shown in Figure 5.43 .

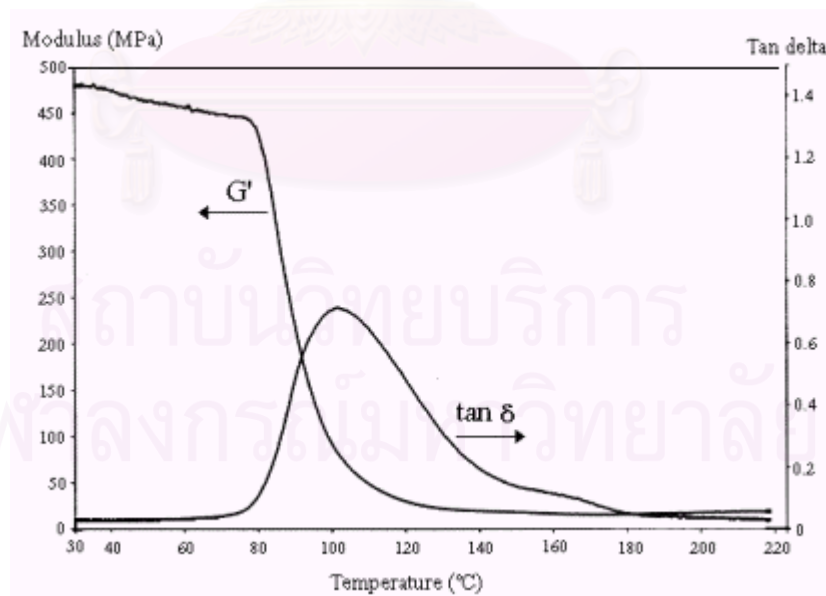


Figure 5.43 : The dynamic mechanical spectrum (storage modulus and loss tangent plotted against the temperature at the frequency of 1 Hz) of neat epoxy cured at 65 °C for 36 h.

The value of the glass transition temperature (T_g), the bending modulus in the rubbery state and the strand density or crosslink density of polymer can be evaluated from these property-temperature curves. The T_g can be detected at the peak of $\tan \delta$. An analysis on the crosslink density can be done by application of the statistical theory of rubber elasticity under the condition that makes the polymer elastic and rubber-like. The strand density of the epoxy resin can be derived from Equation 5.10 [19, 20].

$$\nu = \frac{G'}{K_B T} \quad 5.10$$

where ν is the strand density, which is defined as the number of crosslinking chains per unit volume. G' is the modulus at the temperature that epoxy is in a rubber-like state. K_B is the Boltzmann's constant, its value is 13.8×10^{-24} J/mol and T stands for the absolute temperature that induces the epoxy to be in its rubber-like state. The strand density implies whether the epoxy resin has low or high degree of crosslinks. High strand density is related to high degree of crosslinks while low strand density relates more to the softening of epoxy [19, 20]. The experimental results of the DMA test is tabulated in Table 5.15 .

Table 5.15 : Experimental results from dynamic mechanical analysis test for neat epoxy with different cure condition.

Cure temperature(°C)	Cure time (h)	Bending modulus (MPa)	Glass transition temperature(°C)	Strand density ($10^{27}/m^3$)
65	15.8	24.91	99.8	4.33
31	36	14.23	86	2.42
65	36	18.67	101.6	3.21
99	36	31.15	115.2	5.36
65	56.2	25.04	106.1	4.35

Experimental results drawn from table 5.15 illustrated that, at constant cure temperature, the T_g raised as the cure time was extended and at constant cure time, the T_g raised as the cure temperature was elevated. Table 5.15 also exhibited that, the strand density increases as the T_g increases.

CHAPTER VI

CONCLUSIONS AND RECOMMENDATIONS

6.1 CONCLUSIONS

The main objectives of the present study is to relate the curing factors with the mechanical properties of epoxy composite for industrial floor coating, and to find the optimum conditions for curing the coat. The mechanical properties of the epoxy composite coating layer and the simulated epoxy composite coated floor, which was epoxy composite coated on concrete/mortar substrate, were studied. Based on the experimental work conducted in this investigation, the results can be summarized as follows.

- 6.1.1 As floor coating material, glass fiber reinforced-epoxy composite exhibit better mechanical properties than neat epoxy resin. At the cure temperature of 65 °C for 36 h, the compressive strength of concrete coated with epoxy composite was enhanced by 16.9% while the neat epoxy did by 3.5%. The impact strength was increased by 190% in the glass fiber reinforced composite coated mortar due to the presence of the glass fiber. This is because of the superior properties of the glass fiber, which supports the applied load transferred from the epoxy resin matrix. Fracture toughness of epoxy composite is greater than that of neat epoxy by 832%.
- 6.1.2 Mechanical properties in terms of the compressive strength of the concrete-coated with epoxy composite and the impact strength of the mortar-coated with epoxy composite show the same trend as those found in the ones without any substrate. The compressive strength of uncoated concrete was raised by close to 17% upon coating with filled or unfilled epoxy composite, but in increase for those coated with neat epoxy was insignificant. The impact strength for mortar coated with unfilled epoxy composite was enhanced by 223% while the filled one led to a slightly lower raise of 190%. With the neat epoxy coat on mortar, the impact strength was relatively unchanged.

- 6.1.3 Cure temperature effects the impact strength and fracture toughness of the epoxy composite in the same manner, i.e. a lower cure temperature imparts better impact and fracture properties. For the range of cure temperature of 31 °C yields the greatest impact and fracture toughness. Greatest compressive strength was achieved when curing the epoxy composite and that coated in the concrete at 99 °C and 67 °C for 15.8 h and 29 h respectively. A raise in the cure temperature can be substituted by extended period of cure time at a lower cure temperature. A compressive strength of only 2.9% less than those at the optimum in the epoxy composite and 13.7% in the concrete coated with epoxy composite can be obtained by curing for extended period of 56.2 h at a lower cure temperature of 31 °C.
- 6.1.4 Influence of the cure time on the compressive strength and the fracture toughness of the epoxy composite are of the same manner. Extending the cure time tends to inferior these mechanical properties. The highest compressive strength and fracture toughness are attained upon curing the epoxy composite for 15.8 h. However, in curing the concrete coated with epoxy composite to give high compressive strength, the recommended cure time is for not less than 49 h. The optimum cure time, which gives the highest impact strength, found for both the epoxy composite and mortar coated with epoxy composite, were for the duration of 12 and 29 h respectively.
- 6.1.5 Filling sand with a higher amount increases both the fracture properties. Therefore, the epoxy composite with the highest fracture properties is achieved at the highest amount of sand, i.e. at 38.77%. An optimum amount of adding sand was discovered in the impact test of both the epoxy composite and the mortar coated with epoxy composite at 27% and 23% sand respectively. An optimum amount of adding sand is also found for the compressive strength of the concrete coated with epoxy composite at 25% sand while the compressive strength of the epoxy composite reduces as more amount of was added. Hence, the highest compressive strength is obtained from the lowest amount of 15.23% added sand.

6.1.6 An appropriate cure condition can improve the mechanical properties of the filled-epoxy composite coat. High temperature cure can be remedied by extended cure time. For optimum mechanical properties, the following cure conditions were found.

6.1.6.1 Epoxy composites with high compressive strength can be achieved by curing at 31°C for 56.2 h with the amount of sand filler of 25%.

6.1.6.2 Epoxy composites with high impact strength can be achieved by curing at 31°C for 29 h with the amount of sand filler of 23%.

6.1.6.3 Epoxy composites with high fracture toughness can be achieved by curing at 31°C with the shortest curing period and the highest amount of sand filler in this study, i.e. at 15.8 h and 38.77% respectively.

The optimum cure condition, which was compromised all mechanical properties, is at the cure temperature of 31 °C for 56.2 h with 29% sand. At this condition, the minimum reductions of mechanical properties from the highest value are obtained. The highest reduction at this condition is in the compressive strength of epoxy composite, which decreased by 24.2%.

6.1.7 At a constant cure temperature, the glass transition temperature of the neat epoxy was raised as the cure time was extended. At constant cure time, the glass transition temperature of epoxy increased as the cure temperature was elevated.

6.1.8 The glass transition temperature increased with the strand density of the neat epoxy.

6.1.9 Results from the regression analysis and the ANOVA test illustrated that the relationships between the curing factors and the mechanical properties are properly fitted by the response surface equations from the Central Composite Rotatable (CCR) technique and Response Surface Methodology (RSM). These equations are displayed in the Table 6.1 .

Table 6.1 : Interaction between cure temperature (T) and the coded variables of cure time (t), amount of added sand (x) and the mechanical property (y). All equations are valid when the epoxy composites are cured with the cure temperature from 45 to 85 °C, the cure time from 24 to 48 h and the amount of sand from 27 to 34%

Epoxy Composite Coating Material	
Compressive Strength (Mpa)	$y = 98.82 + 2.27T - 3.53t - 4.16x + 2.52tx$
Impact Strength (KJ/m ²)	$y = 7.801 - 0.985T + 0.229T^2 - 0.295x^2$
Fracture Toughness (MN/(m ^{3/2}))	$y = 3.972 - 0.413T - 0.208t + 0.175x + 0.197T^2$
Fracture Energy (J/m ²)	$y = 14,909 - 2,843T - 907t + 1,761x - 1,114Tx + 1,107T^2 + 850t^2$
Concrete Coated with Epoxy Composite	
Compressive Strength (Mpa)	$y = 51.23 - 4.09Tt - 5.42T^2 - 3.75x^2$
Mortar Coated with Epoxy Composite	
Impact Strength (KJ/m ²)	$y = 4.490 - 0.560T - 0.181t^2 - 0.169x^2$

6.2 RECOMMENDATIONS FOR FURTHER STUDY

- 6.2.1 Surface treatment of sand can be performed to promote better epoxy-sand adhesion.
- 6.2.2 An investigation on the effects of sand particle size can be studied.
- 6.2.3 A study on cure temperature profile is suggested to detect the actual temperature development during curing.
- 6.2.4 Deterioration due to environmental effects and physical aging of epoxy composite coat is an area still opened for investigation.
- 6.2.5 Hardness test of epoxy composite can be conducted.

REFERENCES

1. International coatings, Inc. Case Histories. Illinois : International coatings, Inc., 1998.
2. M. Gaschke and B. Dreher. Review of Solvent-Free Liquid Epoxy Coating Technology. Journal of Coating Technology 48, 671 (June 1976) : 46-51.
4. Marianne DiBenedetto. Multifunctional epoxy resins come of age. Journal of Coating Technology 52, 667 (August 1980) : 65-71.
5. In-Chul Choy and Donald J. Plazek. The Physical Properties of Bisphenol-Abased Epoxy Resins During and after Curing. Journal of Polymer Science: Part B: Polymer Physics 24 (1986) : 1303-1320.
6. J.C. Graham, et al. Effect of Temperature and Relative Humidity on Intercoat Adhesion Failure Of Aliphatic amine cured Epoxy Coatings. Journal of Coating Technology 60, 760 (May 1988) : 35-39.
7. Won Ho Jo and Kyoung Jin Ko. The effects of physical aging on the thermal and mechanical properties of an epoxy polymer. Polymer engineering and Science 31, 4 (February 1991) : 239-244.
8. Eliane Urbaczewski-Espuche, et al. Influence of chain flexibility and crosslink density on mechanical properties of epoxy/amine networks. Polymer engineering and Science 31, 22 (November 1991) : 1572-1580.

9. F. Fernandez-Nograro, et al. Dynamic and Mechanical Properties of DGEBA/Poly(propylene oxide) Amine Based Epoxy Resins as a Function of Stoichiometry. European Polymer Journal 32, 2 (1996) : 257-266.
10. L. Barral, et al. Effect of thermal degradation on the mechanical properties of a diglycidyl ether of bisphenol A/1,3-bisaminomethylcyclohexane (DGEBA/1,3-BAC) epoxy resin system. Journal of Applied Polymer Science 63 (1997) : 1841-1849.
11. Anthony E. Mayr, Wayne D. Cook, and Graham H. Edward. Yielding Behaviour in model epoxy thermosets-I. Effect of strain rate and composition. Polymer 39, 16 (1998) : 3719-3724.
12. Anthony E. Mayr, Wayne D. Cook, and Graham H. Edward. Yielding Behaviour in model epoxy thermosets-II. Temperature dependence. Polymer 39, 16 (1998) : 3725-3733.
13. F. Ellyin and C. Rohrbacher. Effect of aqueous environment and temperature on glass-fiber epoxy resin composites. Journal of Reinforced Plastics and Composites 19, 17 (2000) : 1405-1423.
14. M. Alagar, T. V. Thanikai Velan, and A. Ashok Kumar. Mechanical properties of E- glass fiber reinforced siliconized epoxy polymer composites. Polymer Composites 21, 5 (October 2000) : 739-744.
15. F. M. Zhao and N. Takeda. Effect of interfacial adhesion and statistical fiber strength on tensile strength of unidirectional glass fiber/epoxy composites. Part I: experiment results. Composites: Part A 31 (2000) : 1203-1214.
16. V.-T. Troung and B. C. Ennis. Effect of physical aging on the fracture behavior of crosslinked epoxies. Polymer Engineering and Science 31, 8 (April 1991) : 548-557.

17. B. Geisler and F. N. Kelley. Rubbery and rigid particle toughening of epoxy resins. Journal of Applied Polymer Science 54 (1994) : 177-189.
18. Seunghan Shin and Jyoungsik Jang. The effect of amine/epoxy ratio on the fracture toughness of tetrafunctional epoxy resin. Polymer Bullentin 39 (1997) : 353-359.
19. Wayne D. Cook, Mansour Mehrabi, and Graham H. Edward. Ageing and yielding in model epoxy thermosets. Polymer 40 (1999) : 1209-1218.
20. Jarun Chutmanop. Toughening of Epoxy by Rubber Particles. Master's Thesis, Department of Chemical Engineering, Chulalongkorn University, 1994.
21. Anawat Chansaksoong. Effects of Rubber Particles on Mechanical Properties of Epoxy Resin. Master's Thesis Department of Chemical Engineering, Chulalongkorn University, 1996.
22. S. Covavisaruch, R. E. Robertson and F. E. Filisko. The basic longitudinal texture in the brittle fracture of glassy polymers. Proceedings of the first Asean- Japan symposium on polymers, Indonesia, 1991.
23. อ.อรอุษา สรวารี. สารเคลือบผิว (สี วาร์นิช และแล็กเกอร์). กรุงเทพมหานคร : สำนักพิมพ์จุฬาลงกรณ์มหาวิทยาลัย, 2537.
24. Zeno W. Wicks, Jr., Frank N. Jones, S. Peter Pappas. Organic coatings : science and technology V.1 : film formation, components, and appearance. New York : Wiley, c1992.
25. Paul Oman. How and why to epoxy paint your concrete slab. New Hampshire : Paul Oman, 1997.

26. Peter C. Powell. Engineering with fibre-polymer laminates. London : Chapman & Hall, 1994.
27. Clayton A. May. Epoxy resins : chemistry and technology. 2nd edition, Revised and expanded. New York : Marcel Dekker, 1988.
28. Ronald F. Gibson. Principles of composite material mechanics. New York : McGraw-Hill, 1994.
29. Calvin E. Schildknecht with Irving Skeist. Polymerization processes. New York : Wiley, 1977.
30. Department of Polymer science, University of southern Mississippi. Macrogalleria directory. Southern Mississippi : Department of Polymer science, University of southern Mississippi, 1996.
31. Henery Lee and Kris Neville. Epoxy resins: Their applications and technology. New York : McGrawHill, 1957.
32. American Concrete Institute. Epoxies with concrete. Detroit : American Concrete Institute, 1968.
33. George Lubin. Handbook of fiberglass and advanced plastics composited. New York : Robert E. Krieger, 1969.
34. W. G. Potter. Epoxide resins. London : Iliffe, 1970.
35. Charles E. Watts. Anti-slip floor coating composition. United States Patent No. 5,431,960, 1995.
36. Witold Brostow and Roger D. Corneliussen. Failure of plastics. New York : Hanser Publishers, 1986.

37. Klaus Hinkelmann and Oscar Kempthorne. Design and analysis of experiments volume 1: introduction to experimental design. New York : John Wiley, 1994.
38. A. M. Dean and D. T. Voss. Design and analysis of experiments. New York : Springer, 1999.
39. George E. P. Box and Norman R. Draper. Empirical model-building and response surfaces Part I. New York : John Wiley, 1987.
40. George Earl Troxell, Harmer E. Davis, and Joe w. Kelly. Composition and properties of concrete. 2nd edition New York : McGraw-Hill, 1995.
41. Arthur H. Nilson and George Winter. Design of concrete structures. 11th edition. New York : McGraw-Hill, 1991.
42. ชัชวาลย์ เศรษฐบุตตร. คอนกรีตเทคโนโลยี. พิมพ์ครั้งที่ 4 กรุงเทพมหานคร : เดอะพรีนซ์ อินเทอร์เน็ตชั่นแนล, 2539.
43. วินิต ช่อวิเชียร. คอนกรีตเทคโนโลยี. พิมพ์ครั้งที่ 7 กรุงเทพมหานคร : สำนักพิมพ์จุฬาลงกรณ์มหาวิทยาลัย, 2529.
44. Kenneth Leet. Reinforced concrete design. 2nd edition New York : McGraw-Hill, 1991.
45. ประณต กุลประสูต. เทคนิคงานปูน-คอนกรีต. พิมพ์ครั้งที่ 4 กรุงเทพมหานคร : อัมรินทร์พริ้นติ้งแอนด์พับลิชชิ่ง, 2536.
46. Gougeon Brothers. West system technical manual and product guide. Michigan : Gougeon Brothers, 1994.
47. Robert J. Young and Peter W. R. Beaumont. Time-dependent failure of poly (methacrylate). Polymer 17 (August 1976) : 717-722.



APPENDICES

สถาบันวิทยบริการ
จุฬาลงกรณ์มหาวิทยาลัย

APPENDIX A

Results of Mechanical Properties from the Experimental Tests

Appendix A-1 :The compressive strength of epoxy composites.

Run	Cure Temperature (°C)	Cure Time (h)	Sand (% vol.)	Compressive Strength (MPa)
1	45	24	20	108.50
2	85	24	20	112.82
3	45	48	20	94.59
4	85	48	20	99.71
5	45	24	34	94.80
6	85	24	34	98.39
7	45	48	34	89.34
8	85	48	34	97.00
9	31	36	27	94.29
10	99	36	27	100.45
11	65	15.8	27	100.50
12	65	56.2	27	92.00
13	65	36	15.23	99.19
14	65	36	38.77	86.87
15	65	36	27	101.53
16	65	36	27	98.50
17	65	36	27	97.50
18	65	36	27	99.83
19	65	36	27	97.47
20	65	36	27	98.88

Appendix A-2 : The impact strength of epoxy composites.

Run	Cure Temperature (°C)	Cure Time (h)	Sand (% vol.)	Impact Strength (J/m)	Impact Strength (KJ/m²)
1	45	24	20	52.63	8.771
2	85	24	20	41.91	6.984
3	45	48	20	52.48	8.747
4	85	48	20	42.85	7.142
5	45	24	34	50.90	8.483
6	85	24	34	42.67	7.112
7	45	48	34	53.22	8.869
8	85	48	34	41.06	6.843
9	31	36	27	62.55	10.425
10	99	36	27	38.76	6.461
11	65	15.8	27	50.43	8.405
12	65	56.2	27	46.26	7.709
13	65	36	15.23	43.09	7.181
14	65	36	38.77	41.66	6.943
15	65	36	27	46.86	7.810
16	65	36	27	48.07	8.012
17	65	36	27	47.26	7.876
18	65	36	27	46.80	7.800
19	65	36	27	47.17	7.862
20	65	36	27	44.70	7.449

สถาบันวิทยบริการ
จุฬาลงกรณ์มหาวิทยาลัย

Appendix A-3 : The critical stress intensity factor and the fracture energy of epoxy composites.

Run	Cure Temperature (°C)	Cure Time (hr)	Sand (% vol.)	K_{Ic} (NM/m ^{3/2})	G_{Ic} (J/m ²)
1	45	24	20	4.590	15,114
2	85	24	20	4.001	12,532
3	45	48	20	4.302	16,143
4	85	48	20	3.669	13,248
5	45	24	34	5.103	22,330
6	85	24	34	3.917	13,640
7	45	48	34	4.470	18,395
8	85	48	34	3.850	12,699
9	31	36	27	5.202	23,502
10	99	36	27	3.650	12,227
11	65	15.8	27	4.178	15,079
12	65	56.2	27	3.275	9,576
13	65	36	15.23	3.524	11,195
14	65	36	38.77	4.486	19,532
15	65	36	27	4.026	15,376
16	65	36	27	3.827	14,287
17	65	36	27	3.803	14,462
18	65	36	27	3.929	13,250
19	65	36	27	4.022	15,645
20	65	36	27	4.262	16,493

สถาบันวิทยบริการ
จุฬาลงกรณ์มหาวิทยาลัย

Appendix A-4 : The compressive strength of concrete coated with epoxy composites.

Run	Cure Temperature (°C)	Cure Time (hr)	Sand (% vol.)	Compressive Strength (MPa)
1	45	24	20	35.79
2	85	24	20	44.00
3	45	48	20	48.48
4	85	48	20	42.54
5	45	24	34	28.71
6	85	24	34	43.83
7	45	48	34	44.44
8	85	48	34	40.97
9	31	36	27	33.67
10	99	36	27	37.21
11	65	15.8	27	47.84
12	65	56.2	27	46.42
13	65	36	15.23	42.59
14	65	36	38.77	37.77
15	65	36	27	52.44
16	65	36	27	52.26
17	65	36	27	52.18
18	65	36	27	50.93
19	65	36	27	46.85
20	65	36	27	50.06

สถาบันวิทยบริการ
จุฬาลงกรณ์มหาวิทยาลัย

Appendix A-5 : Impact strength of mortar coated with epoxy composites.

Run	Cure Temperature (°C)	Cure Time (hr)	Sand (% vol.)	Impact Strength (J)	Impact Strength (KJ/m ²)
1	45	24	20	3.866	4.989
2	85	24	20	2.739	3.534
3	45	48	20	3.449	4.451
4	85	48	20	2.900	3.742
5	45	24	34	3.423	4.417
6	85	24	34	2.789	3.599
7	45	48	34	3.464	4.469
8	85	48	34	2.900	3.742
9	31	36	27	3.907	5.041
10	99	36	27	2.094	2.702
11	65	15.8	27	2.819	3.638
12	65	56.2	27	3.061	3.949
13	65	36	15.23	3.027	3.906
14	65	36	38.77	2.905	3.749
15	65	36	27	3.664	4.727
16	65	36	27	3.623	4.675
17	65	36	27	3.423	4.417
18	65	36	27	3.377	4.357
19	65	36	27	3.377	4.357
20	65	36	27	3.464	4.469

สถาบันวิทยบริการ
จุฬาลงกรณ์มหาวิทยาลัย

APPENDIX B

Calculation Method

Experimental design and statistical analysis for impact strength of epoxy composite is exemplified in this section. Other mechanical properties can also be analyzed by the same approach.

1. Calculation of coded independent variable in central composite rotatable design

In central composite rotatable design, independent variables are represented by codes ± 1 , 0, and $\pm\alpha$. The code α for three independent variables is calculated by from the following equation

$$\alpha = 2^{k/4} = 2^{3/4} = 1.682$$

the actual numerical measures will be converted to coded variables by using Equation 2.9

$$x = \frac{X - X_0}{t} \quad 2.9$$

where X is the variables to standardized (or coded), x is variables, X_0 is the center of the region and t is the current region of interest for X .

In this study, temperature will be varied from 31 to 99 °C, which gives the center point (X_0) at 65 °C. The coded variable for the highest temperature 99 °C is 1.682, so t can be calculated from

$$t = (X - X_0)/\alpha = (99 - 65)/1.682 = 20 \quad B-1$$

At coded variable 1, experimental test temperature is

$$X = xt + 65 = (1)(20) + 65 = 85^\circ\text{C} \quad B-2$$

Other test condition can also be derived from the same calculation giving the following curing condition

Table 4.2 : Test Condition at center point, cube point and star point.

Independent Variable	Star Point (-1.682)	Cube Point (-1)	Center Point (0)	Cube Point (1)	Star Point (1.682)
Cure Temperature (°C)	31	45	65	85	99
Cure Time (h)	15.8	24	36	48	56.2
Sand Filler (% by volume)	15.23	20	27	34	38.77

2. Estimation of multiple linear regression coefficients

The study of response surface methodology in all mechanical properties are carried out by creating mathematical model with second order polynomial equation as shown in Equation B-3

$$Y = b_0 + b_1X_1 + b_2X_2 + b_3X_3 + b_{11}X_1^2 + b_{22}X_2^2 + b_{33}X_3^2 + b_{12}X_1X_2 + b_{13}X_1X_3 + b_{23}X_2X_3$$

B-3

The estimation of coefficients in the above equation can be done by matrix calculation using in multiple linear regression analysis. The result of impact strength of epoxy composite in Table 4.1 can be written in matrix as follows.

สถาบันวิทยบริการ
จุฬาลงกรณ์มหาวิทยาลัย

$$(X'X)^{-1} = \begin{bmatrix} 0.166 & 0 & 0 & 0 & -0.057 & -0.057 & -0.057 & 0 & 0 & 0 \\ 0 & 0.073 & 0 & 0 & 0 & 0 & 0 & 0 & 0 & 0 \\ 0 & 0 & 0.073 & 0 & 0 & 0 & 0 & 0 & 0 & 0 \\ 0 & 0 & 0 & 0.0732 & 0 & 0 & 0 & 0 & 0 & 0 \\ -0.06 & 0 & 0 & 0 & 0.0694 & 0.0069 & 0.0069 & 0 & 0 & 0 \\ -0.06 & 0 & 0 & 0 & 0.0069 & 0.0694 & 0.0069 & 0 & 0 & 0 \\ -0.06 & 0 & 0 & 0 & 0.0069 & 0.0069 & 0.0694 & 0 & 0 & 0 \\ 0 & 0 & 0 & 0 & 0 & 0 & 0 & 0.125 & 0 & 0 \\ 0 & 0 & 0 & 0 & 0 & 0 & 0 & 0 & 0.125 & 0 \\ 0 & 0 & 0 & 0 & 0 & 0 & 0 & 0 & 0 & 0.125 \end{bmatrix}$$

$$X'Y = \begin{bmatrix} 0y \\ 1y \\ 2y \\ 3y \\ 11y \\ 22y \\ 33y \\ 12y \\ 13y \\ 23y \end{bmatrix} = \begin{bmatrix} 156.88 \\ -13.46 \\ -0.92 \\ -0.737 \\ 110.72 \\ 108.54 \\ 102.91 \\ -0.473 \\ -0.005 \\ -0.017 \end{bmatrix}$$

Therefore, multiple linear regression coefficients can be estimated from

$$b = (X'X)^{-1}(X'Y) = \begin{bmatrix} b_0 \\ b_1 \\ b_2 \\ b_3 \\ b_{11} \\ b_{22} \\ b_{33} \\ b_{12} \\ b_{13} \\ b_{23} \end{bmatrix} = \begin{bmatrix} 7.801 \\ -0.985 \\ -0.067 \\ -0.054 \\ 0.2294 \\ 0.0929 \\ -0.259 \\ -0.059 \\ -7E-04 \\ -0.002 \end{bmatrix}$$

Hence, the response surface equation can be written in second order polynomial equation showing the relationship between curing factors and imp strength of epoxy composite as Equation 5.2

$$y = 7.801 - 0.985x_1 - 0.067x_2 - 0.054x_3 - 0.059x_1x_2 - 0.001x_1x_3 - 0.002x_2x_3 + 0.229x_1^2 + 0.093x_2^2 - 0.295x_3^2 \quad 5.2$$

For other responses, regression analysis can also be calculated for this method.

3. Analysis of Variance

The total sum of square of responses y is calculated from Equation 2.28 .

$$\begin{aligned}
 SS_T &= \sum_{i=1}^n y_i^2 - \frac{G^2}{n} & 2.28 \\
 &= (8.77^2 + 6.98^2 + \dots + 7.45^2) - (8.77 + 6.98 + \dots + 7.45)^2/20 \\
 &= 17.095
 \end{aligned}$$

Regression sum of square is calculated from Equation 2.30 or Equation B-4 as follows.

$$SS_R = b'X'Y - \frac{G^2}{n} \quad 2.30$$

$$SS_R = SS_{R1} + SS_{R2} \quad B-4$$

The first order term of regression sum of square is calculated from Equation 2.31

$$\begin{aligned}
 SS_{R1} &= \sum_{i=1}^n b_i(iy) & 2.31 \\
 &= (-0.985)(-13.46) + (-0.067)(-0.92) + (-0.054)(-0.737) \\
 &= 13.36
 \end{aligned}$$

Mean square of coefficient of the first order term is

$$MS_1 = (SS_{R1})/k = 13.36/3 = 4.453$$

The first order term of regression sum of square is calculated from Equation 2.32

$$\begin{aligned}
 SS_{R2} &= b_0(0y) + \sum_{i=1}^k \sum_{j=1}^k b_{ij}(ijy) - \frac{G^2}{n} & 2.32 \\
 &= (7.801)(156.88) + [(0.229)(110.72) + (0.093)(108.54) + \dots + \\
 &\quad (-0.02)(-0.017)] - (8.77 + 6.98 + \dots + 7.45)^2/20 \\
 &= 1223.8 + 8.852 - 1225 \\
 &= 7.717
 \end{aligned}$$

Mean square of coefficient of the second order term is

$$MS_2 = \frac{SS_{R2}}{k(k+1)} = 7.717/6 = 1.286$$

Therefore, regression sum of square calculated from Equation B-4 is

$$SS_R = 13.36 + 7.717 = 21.077$$

Mean square of coefficient of the regression is

$$MS_R = \frac{SS_R}{k(k+3)} = 21.077/9 = 2.342$$

Error sum of square is calculated from Equation 2.34 by replacing information from Table 5.2 as follows

$$\begin{aligned} SS_E &= \sum_{i=1}^n (y_i - \hat{y}_i)^2 && 2.34 \\ &= (8.771-8.909)^2 + (6.984-7.062)^2 + \dots + (7.449-7.801)^2 \\ &= 0.817 \end{aligned}$$

Mean square of coefficient of the error sum of square is

$$MS_E = \frac{SS_E}{n-1} = \frac{0.816}{10} = 0.0816$$

Pure error sum of square is calculated from Equation 2.37

$$SS_{PE} = \sum_{u=1}^n (y_{1u} - \bar{y}_1)^2 \quad 2.37$$

\bar{y} is the average of center responses, which is equal to

$$\begin{aligned} \bar{y} &= (7.810+8.012+7.876+7.800+7.862+7.449)/6 \\ &= 7.801 \end{aligned}$$

So, SS_{PE} is

$$SS_{PE} = (7.810-7.801)^2 + (8.012-7.801)^2 + \dots + (7.449-7.801)^2 = 0.178$$

Mean square of coefficient of the pure error sum of square is

$$MS_{PE} = SS_{PE} / (n_1 - 1) = 0.178 / (6-1) = 0.036$$

Hence,

$$SS_{LOF} = SS_E - SS_{PE} = 0.817 - 0.178 = 0.639$$

$$MS_{LOF} = \frac{SS_{LOF}}{n_2 - \frac{k(k+3)}{2}} = 0.128$$

4. Calculation of statistical F_0

Statistical value F_0 of the regression analysis is calculated from Equation 2.40

$$F_0 = \frac{\frac{SS_R}{k(k+3)}}{\frac{SS_E}{n_1 - \frac{k(k+3)}{2}}} = \frac{MS_R}{MS_E} \quad 2.40$$

$$= 2.342 / 0.082 = 28.67$$

F_0 of SS_{R1} and SS_{R2} is also calculated from the same method

F_0 of error is calculated from Equation 2.41

$$F_0 = \frac{\frac{SS_{LOF}}{k(k+3)}}{\frac{SS_{PE}}{n_1 - 1}} = \frac{MS_{LOF}}{MS_{PE}} \quad 2.41$$

$$= 0.128 / 0.0356 = 3.6$$

5. Calculation of statistical t_0

Statistical value t_0 of each regression coefficient is calculated from Equation 2.44

$$t_0 = \frac{b_i}{\sqrt{MS_{E C_{ii}}}} \quad 2.44$$

For Example, t_0 of b_0 is

$$t_0 = \frac{7.801}{\sqrt{(0.082)(0.1663)}} = 66.95$$

6. Coefficient of determination

Coefficient of determination of regression analysis is calculated from Equation 2.45

$$R^2 = \frac{SS_R}{SS_T} = 1 - \frac{SS_E}{SS_T} \quad 2.45$$

$$= 1 - (0.817/17.095) = 0.949$$

สถาบันวิทยบริการ
จุฬาลงกรณ์มหาวิทยาลัย

APPENDIX C

ANOVA Table and Regression Coefficients

Appendix C-1 : ANOVA table for the multiple regression analysis of the interactions of cure temperature, cure time, and amount of sand on the compressive strength of epoxy composites.

Source of Variation	Sum of Square	DF	Mean Square	F ₀
Regression	556.04	9	61.78	7.76
First order terms	476.82	3	158.94	19.97
Secondary order terms	79.22	6	13.20	1.66
Error	79.56	10	7.96	
Lack of fit	67.63	5	13.53	5.67
Pure error	11.93	5	2.39	
Total	635.29	19	R² =	0.875

Appendix C-2 : Statistic-t₀ test of coefficients testing for interactions of cure temperature, cure time, and amount of sand on the compressive strength of epoxy composites.

Regression Coefficients		t ₀	Hypothesis test (t _{0.025/2,10} = 2.228)
b ₀	98.821	85.90	Significance
b ₁	2.274	2.98	Significance
b ₂	-3.527	-4.62	Significance
b ₃	-4.160	-5.45	Significance
b ₁₂	0.609	0.61	Not significance
b ₁₃	0.226	0.23	Not significance
b ₂₃	2.521	2.53	Significance
b ₁₁	0.296	0.40	Not significance
b ₂₂	-0.101	-0.14	Not significance
b ₃₃	-1.239	-1.67	Not significance

Appendix C-3 : ANOVA table for the multiple regression analysis of the interactions of cure temperature, cure time, and amount of sand on the impact strength of epoxy composites.

Source of Variation	Sum of Square	DF	Mean Square	F ₀
Regression	21.077	9	2.342	28.67
First order terms	13.360	3	4.453	54.55
Secondary order terms	7.717	6	1.286	15.76
Error	0.817	10	0.082	
Lack of fit	0.639	5	0.128	3.6
Pure error	0.178	5	0.036	
Total	16.251	19	R² =	0.949

Appendix C-4 : Statistic-t₀ test of coefficients testing for interactions of cure temperature, cure time, and amount of sand on the impact strength of epoxy composites.

Regression Coefficients		t ₀	Hypothesis test (t _{0.025/2,10} = 2.228)
b ₀	7.801	66.95	Significance
b ₁	-0.985	-12.74	Significance
b ₂	-0.067	-0.97	Not significance
b ₃	-0.054	-0.70	Not significance
b ₁₂	-0.059	-0.58	Not significance
b ₁₃	-0.001	-0.01	Not significance
b ₂₃	-0.002	-0.02	Not significance
b ₁₁	0.229	3.05	Significance
b ₂₂	0.093	1.23	Not significance
b ₃₃	-0.259	-3.44	Significance

Appendix C-5 : ANOVA table for the multiple regression analysis of the interactions of cure temperature, cure time, and amount of sand on the critical stress intensity factor of epoxy composites.

Source of Variation	Sum of Square	DF	Mean Square	F ₀
Regression	4.068	9	0.452	9.65
First order terms	3.339	3	1.113	23.75
Secondary order terms	0.729	6	0.121	2.59
Error	0.469	10	0.047	
Lack of fit	0.378	5	0.066	2.33
Pure error	0.141	5	0.028	
Total	7.743	19	R² =	0.897

Appendix C-6 : Statistic-t₀ test of coefficients testing for interactions of cure temperature, cure time, and amount of sand on the critical stress intensity factor of epoxy composites.

Regression Coefficients		t ₀	Hypothesis test (t _{0.025/2,10} = 2.228)
b ₀	3.972	44.96	Significance
b ₁	-0.413	-7.05	Significance
b ₂	-0.208	-3.55	Significance
b ₃	0.175	2.99	Significance
b ₁₂	0.065	0.85	Not significance
b ₁₃	-0.073	-0.95	Not significance
b ₂₃	-0.010	-0.13	Not significance
b ₁₁	0.196	3.45	Significance
b ₂₂	-0.051	-0.89	Not significance
b ₃₃	0.048	0.84	Not significance

Appendix C-7 : ANOVA table for the multiple regression analysis of the interactions of cure temperature, cure time, and amount of sand on the fracture energy of epoxy composites.

Source of Variation	Sum of Square	DF	Mean Square	F ₀
Regression	212*10 ⁶	9	23.55*10 ⁶	11.27
First order terms	164*10 ⁶	3	54.66*10 ⁶	26.16
Secondary order terms	48*10 ⁶	6	8*10 ⁶	3.83
Error	23.28*10 ⁶	10	2.33*10 ⁶	
Lack of fit	14.29*10 ⁶	5	2.86*10 ⁶	2.16
Pure error	6.61*10 ⁶	5	1.32*10 ⁶	
Total	233*10 ⁶	19	R² =	0.91

Appendix C-8 : Statistic-t₀ test of coefficients testing for interactions of cure temperature, cure time, and amount of sand on the fracture energy of epoxy composites.

Regression Coefficients		t ₀	Hypothesis test (t _{0.025/2,10} = 2.228)
b ₀	14,909	25.29	Significance
b ₁	-2,843	-7.27	Significance
b ₂	-907	-2.32	Significance
b ₃	1,761	4.50	Significance
b ₁₂	335	0.66	Not significance
b ₁₃	-1,114	-2.27	Significance
b ₂₃	-828	-1.62	Not significance
b ₁₁	1,107	2.91	Significance
b ₂₂	-850	-2.23	Significance
b ₃₃	223	0.59	Not significance

Appendix C-9 : ANOVA table for the multiple regression analysis of the interactions of cure temperature, cure time, and amount of sand on the compressive strength of concrete coated with epoxy composites.

Source of Variation	Sum of Square	DF	Mean Square	F ₀
Regression	386.42	9	42.93	6.19
First order terms	117.51	3	39.17	5.75
Secondary order terms	268.91	6	44.82	6.46
Error	79.559	10	7.956	
Lack of fit	45.296	5	9.059	1.78
Pure error	25.420	5	5.084	
Total	888.223	19	R² =	0.92

Appendix C-10 : Statistic-t₀ test of coefficients testing for interactions of cure temperature, cure time, and amount of sand on the compressive strength of concrete coated with epoxy composites.

Regression Coefficients		t ₀	Hypothesis test (t _{0.025/2,10} = 2.228)
b ₀	51.231	47.70	Significance
b ₁	1.455	2.02	Not significance
b ₂	1.590	2.21	Not significance
b ₃	-1.535	-2.13	Not significance
b ₁₂	-4.093	-4.35	Significance
b ₁₃	1.173	1.25	Not significance
b ₂₃	0.205	0.22	Not significance
b ₁₁	-5.422	-7.74	Significance
b ₂₂	-1.289	-1.84	Not significance
b ₃₃	-3.746	-5.35	Significance

Appendix C-11 : ANOVA table for the multiple regression analysis of the interactions of cure temperature, cure time, and amount of sand on the impact strength of mortar coated with epoxy composites.

Source of Variation	Sum of Square	DF	Mean Square	F ₀
Regression	5.520	9	0.613	8.23
First order terms	4.330	3	4.453	1.443
Secondary order terms	1.190	6	0.198	2.66
Error	0.7457	10	0.075	
Lack of fit	0.6148	5	0.123	3.6
Pure error	0.1310	5	0.026	
Total	6.264	19	R² =	0.881

Appendix C-12 : Statistic-t₀ test of coefficients testing for interactions of cure temperature, cure time, and amount of sand on the impact strength of mortar coated with epoxy composites.

Regression Coefficients		t ₀	Hypothesis test (t _{0.025/2,10} = 2.228)
b ₀	4.490	40.33	Significance
b ₁	-0.560	-7.57	Significance
b ₂	0.028	0.38	Not significance
b ₃	-0.055	-0.75	Not significance
b ₁₂	0.105	1.08	Not significance
b ₁₃	0.077	0.80	Not significance
b ₂₃	0.066	0.68	Not significance
b ₁₁	-0.153	-2.13	Not significance
b ₂₂	-0.181	-2.51	Significance
b ₃₃	-0.169	-2.35	Significance



APPENDIX D

Table of Statistical t and F Distribution

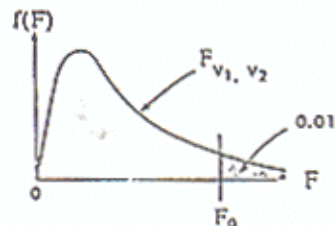
สถาบันวิทยบริการ
จุฬาลงกรณ์มหาวิทยาลัย

Appendix D-1 : The critical value of t-distribution



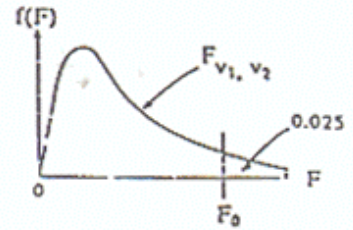
ν \ α	.10	.25	.10	.05	.025	.01	.005	.0025	.001	.0005
1	.325	1.000	3.078	6.314	12.706	31.821	63.657	127.32	318.31	636.62
2	.289	.816	1.566	2.920	4.303	6.965	7.925	14.069	23.326	31.598
3	.277	.765	1.538	2.353	3.182	4.541	5.841	7.453	10.213	12.924
4	.271	.741	1.533	2.132	2.776	3.747	4.604	5.598	7.173	8.610
5	.267	.727	1.474	2.015	2.571	3.365	4.032	4.773	5.893	6.369
6	.265	.718	1.440	1.943	2.447	3.143	3.707	4.317	5.208	5.959
7	.263	.711	1.415	1.895	2.345	2.998	3.499	4.029	4.785	5.402
8	.262	.706	1.397	1.860	2.306	2.894	3.355	3.833	4.501	5.041
9	.261	.703	1.383	1.833	2.282	2.821	3.250	3.690	4.297	4.781
10	.260	.700	1.372	1.812	2.228	2.764	3.169	3.581	4.144	4.587
11	.260	.697	1.363	1.796	2.201	2.718	3.106	3.497	4.025	4.437
12	.259	.695	1.356	1.782	2.179	2.681	3.055	3.428	3.930	4.318
13	.259	.694	1.350	1.771	2.160	2.650	3.012	3.372	3.852	4.221
14	.258	.692	1.345	1.761	2.145	2.624	2.977	3.326	3.787	4.140
15	.258	.691	1.341	1.753	2.131	2.602	2.947	3.286	3.733	4.073
16	.258	.690	1.337	1.746	2.210	2.583	2.921	3.252	3.686	4.015
17	.257	.689	1.333	1.740	2.110	2.567	2.898	3.222	3.644	3.965
18	.257	.688	1.330	1.734	2.101	2.552	2.878	3.197	3.610	3.922
19	.257	.688	1.328	1.729	2.093	2.539	2.861	3.174	3.579	3.883
20	.257	.687	1.325	1.725	2.084	2.528	2.845	3.153	3.552	3.850
21	.257	.686	1.321	1.721	2.080	2.518	2.831	3.135	3.527	3.819
22	.256	.686	1.321	1.717	2.074	2.508	2.819	3.119	3.505	3.792
23	.256	.685	1.319	1.714	2.069	2.500	2.807	3.104	3.485	3.767
24	.256	.685	1.318	1.711	2.064	2.492	2.797	3.091	3.467	3.745
25	.256	.684	1.316	1.708	2.060	2.485	2.787	3.078	3.450	3.725
26	.256	.684	1.315	1.706	2.056	2.479	2.779	3.067	3.435	3.707
27	.256	.684	1.314	1.703	2.052	2.473	2.771	3.057	3.421	3.690
28	.256	.683	1.313	1.701	2.048	2.467	2.763	3.047	3.408	3.674
29	.256	.683	1.311	1.699	2.045	2.462	2.756	3.038	3.396	3.659
30	.256	.683	1.310	1.697	2.042	2.457	2.750	3.030	3.385	3.644
40	.255	.681	1.303	1.684	2.021	2.423	2.704	2.971	3.307	3.551
60	.254	.679	1.296	1.671	2.000	2.390	2.660	2.915	3.232	3.460
120	.254	.677	1.289	1.658	1.980	2.358	2.617	2.860	3.160	3.371
∞	.253	.674	1.282	1.645	1.960	2.326	2.574	2.807	3.090	3.291

Appendix D-2 : The critical value of F-distribution at the level of significant of 0.01.



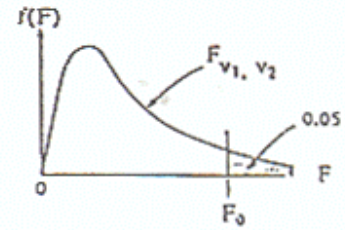
$v_1 \backslash v_2$	1	2	3	4	5	6	7	8	9	10	12	15	20	24	30	40	60	120	∞
1	4052	4999.5	5463	5625	5744	5859	5928	5982	6022	6056	6106	6157	6209	6235	6261	6267	6313	6339	6366
2	98.50	99.00	99.17	99.25	99.30	99.33	99.36	99.37	99.39	99.40	99.42	99.43	99.45	99.46	99.47	99.47	99.48	99.49	99.50
3	34.12	30.82	29.46	28.71	28.24	27.91	27.67	27.49	27.35	27.23	27.05	26.87	26.69	26.00	26.50	26.41	26.32	26.22	26.13
4	21.20	18.00	16.69	15.98	15.52	15.21	14.98	14.80	14.66	14.55	14.37	14.20	14.02	13.93	13.84	13.75	13.65	13.56	13.45
5	16.26	13.27	12.06	11.39	10.97	10.67	10.46	10.29	10.16	10.05	9.89	9.72	9.55	9.47	9.38	9.29	9.20	9.11	9.02
6	13.75	10.92	9.78	9.15	8.75	8.47	8.26	8.10	7.98	7.87	7.72	7.56	7.40	7.31	7.23	7.14	7.06	6.97	6.88
7	12.25	9.55	8.45	7.85	7.46	7.19	6.99	6.84	6.72	6.62	6.47	6.31	6.16	6.07	5.99	5.91	5.82	5.74	5.65
8	11.26	8.65	7.59	7.01	6.63	6.37	6.18	6.03	5.91	5.81	5.67	5.52	5.36	5.23	5.20	5.12	5.03	4.95	4.86
9	10.56	8.02	6.99	6.42	6.06	5.80	5.61	5.47	5.35	5.26	5.11	4.96	4.81	4.73	4.65	4.57	4.48	4.40	4.31
10	10.04	7.56	6.55	5.99	5.64	5.39	5.20	5.06	4.94	4.85	4.71	4.56	4.41	4.33	4.25	4.17	4.08	4.00	3.91
11	9.65	7.21	6.22	5.67	5.32	5.07	4.89	4.74	4.63	4.54	4.40	4.25	4.10	4.02	3.94	3.86	3.78	3.69	3.60
12	9.33	6.98	5.95	5.41	5.06	4.82	4.64	4.50	4.39	4.30	4.16	4.01	3.86	3.78	3.70	3.62	3.54	3.45	3.36
13	9.07	6.70	5.74	5.21	4.86	4.62	4.44	4.30	4.19	4.10	3.96	3.82	3.66	3.59	3.51	3.43	3.34	3.25	3.17
14	8.86	6.51	5.56	5.04	4.69	4.46	4.28	4.14	4.03	3.94	3.80	3.66	3.51	3.43	3.35	3.27	3.18	3.09	3.00
15	8.68	6.36	5.43	4.89	4.54	4.32	4.14	4.00	3.89	3.80	3.67	3.52	3.37	3.29	3.21	3.13	3.05	2.96	2.87
16	8.53	6.23	5.29	4.77	4.41	4.20	4.03	3.89	3.78	3.69	3.55	3.41	3.26	3.18	3.10	3.02	2.93	2.84	2.75
17	8.40	6.11	5.18	4.67	4.31	4.10	3.93	3.79	3.68	3.59	3.46	3.31	3.16	3.08	3.00	2.92	2.83	2.75	2.65
18	8.29	6.01	5.09	4.58	4.25	4.01	3.84	3.71	3.60	3.51	3.37	3.23	3.08	3.00	2.92	2.84	2.75	2.66	2.57
19	8.18	5.93	5.01	4.50	4.17	3.94	3.77	3.63	3.52	3.43	3.30	3.15	3.00	2.92	2.84	2.76	2.67	2.58	2.49
20	8.10	5.85	4.94	4.43	4.10	3.87	3.70	3.56	3.46	3.37	3.23	3.09	2.94	2.86	2.78	2.69	2.61	2.52	2.42
21	8.02	5.78	4.87	4.37	4.04	3.81	3.64	3.51	3.40	3.31	3.17	3.03	2.88	2.80	2.72	2.64	2.55	2.46	2.36
22	7.95	5.72	4.82	4.31	3.99	3.76	3.59	3.45	3.35	3.26	3.12	2.98	2.83	2.75	2.67	2.58	2.50	2.40	2.31
23	7.88	5.66	4.76	4.26	3.94	3.71	3.54	3.41	3.30	3.21	3.07	2.93	2.78	2.70	2.62	2.54	2.45	2.35	2.26
24	7.82	5.61	4.72	4.22	3.90	3.67	3.50	3.36	3.26	3.17	3.03	2.89	2.74	2.66	2.58	2.49	2.40	2.31	2.21
25	7.77	5.57	4.68	4.18	3.85	3.63	3.46	3.32	3.22	3.13	2.99	2.85	2.70	2.62	2.54	2.45	2.36	2.27	2.17
26	7.72	5.53	4.64	4.14	3.82	3.59	3.42	3.29	3.18	3.09	2.96	2.81	2.66	2.58	2.50	2.42	2.33	2.23	2.13
27	7.68	5.49	4.60	4.11	3.78	3.56	3.39	3.26	3.15	3.06	2.93	2.78	2.63	2.55	2.47	2.38	2.29	2.20	2.10
28	7.64	5.45	4.57	4.07	3.75	3.53	3.36	3.23	3.12	3.03	2.90	2.75	2.60	2.52	2.44	2.35	2.26	2.17	2.06
29	7.60	5.42	4.54	4.04	3.73	3.50	3.33	3.20	3.09	3.00	2.87	2.73	2.57	2.49	2.41	2.33	2.23	2.14	2.03
30	7.56	5.39	4.51	4.02	3.70	3.47	3.30	3.17	3.07	2.98	2.84	2.70	2.55	2.47	2.39	2.30	2.21	2.11	2.01
40	7.31	5.18	4.31	3.83	3.51	3.29	3.12	2.99	2.89	2.80	2.66	2.52	2.37	2.29	2.20	2.11	2.02	1.92	1.80
60	7.08	4.98	4.13	3.65	3.34	3.12	2.95	2.82	2.72	2.63	2.50	2.35	2.20	2.12	2.03	1.94	1.84	1.73	1.60
120	6.85	4.79	3.95	3.48	3.17	2.96	2.79	2.66	2.56	2.47	2.34	2.19	2.03	1.95	1.86	1.76	1.66	1.53	1.38
∞	6.43	4.61	3.78	3.32	3.02	2.80	2.64	2.51	2.41	2.32	2.18	2.04	1.88	1.79	1.70	1.59	1.47	1.32	1.00

Appendix D-3 : The critical value of F-distribution at the level of significant of 0.025.



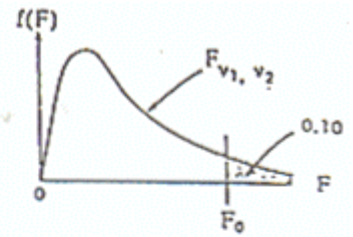
$v_1 \backslash v_2$	1	2	3	4	5	6	7	8	9	10	12	15	20	24	30	40	60	120	∞				
1	647.8	799.5	864.2	899.6	921.8	937.1	948.2	956.7	963.3	968.6	972.7	976.9	980.9	984.9	989.1	993.1	997.2	1001	1006	1010	1014	1018	
2	38.51	39.00	39.17	39.25	39.30	39.33	39.36	39.37	39.39	39.40	39.41	39.43	39.45	39.46	39.46	39.47	39.48	39.49	39.50				
3	17.44	18.04	18.44	18.70	18.91	19.07	19.20	19.31	19.40	19.47	19.53	19.58	19.62	19.65	19.68	19.70	19.72	19.74	19.75	19.76	19.77	19.78	19.79
4	12.22	12.65	12.98	13.20	13.36	13.49	13.60	13.69	13.76	13.82	13.87	13.91	13.94	13.96	13.98	13.99	14.00	14.01	14.02	14.02	14.03	14.03	14.04
5	10.01	10.43	10.76	10.98	11.15	11.29	11.41	11.50	11.57	11.63	11.67	11.70	11.72	11.74	11.75	11.76	11.77	11.78	11.78	11.79	11.79	11.80	11.80
6	8.41	8.82	9.15	9.37	9.54	9.68	9.79	9.88	9.95	10.00	10.04	10.07	10.09	10.10	10.11	10.12	10.12	10.13	10.13	10.13	10.14	10.14	10.14
7	7.47	7.87	8.20	8.42	8.59	8.73	8.84	8.93	9.00	9.05	9.08	9.11	9.13	9.14	9.15	9.16	9.16	9.17	9.17	9.17	9.18	9.18	9.18
8	6.77	7.16	7.49	7.71	7.88	8.02	8.13	8.22	8.29	8.34	8.37	8.40	8.42	8.43	8.44	8.45	8.45	8.46	8.46	8.46	8.47	8.47	8.47
9	6.21	6.59	6.92	7.14	7.31	7.45	7.56	7.65	7.72	7.77	7.80	7.82	7.84	7.85	7.85	7.86	7.86	7.87	7.87	7.87	7.88	7.88	7.88
10	5.79	6.16	6.49	6.71	6.88	7.02	7.13	7.22	7.29	7.34	7.37	7.40	7.42	7.43	7.44	7.44	7.45	7.45	7.45	7.46	7.46	7.46	7.46
11	5.44	5.81	6.14	6.36	6.53	6.67	6.78	6.87	6.94	6.99	7.02	7.05	7.07	7.08	7.09	7.09	7.10	7.10	7.10	7.11	7.11	7.11	7.11
12	5.14	5.51	5.84	6.06	6.23	6.37	6.48	6.57	6.64	6.69	6.72	6.75	6.77	6.78	6.79	6.80	6.80	6.81	6.81	6.81	6.82	6.82	6.82
13	4.89	5.26	5.59	5.81	5.98	6.12	6.23	6.32	6.39	6.44	6.47	6.50	6.52	6.53	6.54	6.55	6.55	6.56	6.56	6.56	6.57	6.57	6.57
14	4.67	5.04	5.37	5.59	5.76	5.90	6.01	6.10	6.17	6.22	6.25	6.28	6.30	6.31	6.32	6.33	6.33	6.34	6.34	6.34	6.35	6.35	6.35
15	4.48	4.85	5.18	5.40	5.57	5.71	5.82	5.91	5.98	6.03	6.06	6.09	6.11	6.12	6.13	6.14	6.14	6.15	6.15	6.15	6.16	6.16	6.16
16	4.31	4.68	5.01	5.23	5.40	5.54	5.65	5.74	5.81	5.86	5.89	5.92	5.94	5.95	5.96	5.97	5.97	5.98	5.98	5.98	5.99	5.99	5.99
17	4.16	4.53	4.86	5.08	5.25	5.39	5.50	5.59	5.66	5.71	5.74	5.77	5.79	5.80	5.81	5.82	5.82	5.83	5.83	5.83	5.84	5.84	5.84
18	4.02	4.39	4.72	4.94	5.11	5.25	5.36	5.45	5.52	5.57	5.60	5.63	5.65	5.66	5.67	5.68	5.68	5.69	5.69	5.69	5.70	5.70	5.70
19	3.89	4.26	4.59	4.81	4.98	5.12	5.23	5.32	5.39	5.44	5.47	5.50	5.52	5.53	5.54	5.55	5.55	5.56	5.56	5.56	5.57	5.57	5.57
20	3.77	4.14	4.47	4.69	4.86	4.99	5.10	5.19	5.26	5.31	5.34	5.37	5.39	5.40	5.41	5.42	5.42	5.43	5.43	5.43	5.44	5.44	5.44
21	3.66	4.03	4.36	4.58	4.75	4.88	4.99	5.08	5.15	5.20	5.23	5.26	5.28	5.29	5.30	5.31	5.31	5.32	5.32	5.32	5.33	5.33	5.33
22	3.56	3.93	4.26	4.48	4.65	4.78	4.89	4.98	5.05	5.10	5.13	5.16	5.18	5.19	5.20	5.21	5.21	5.22	5.22	5.22	5.23	5.23	5.23
23	3.47	3.84	4.17	4.39	4.56	4.69	4.80	4.89	4.96	5.01	5.04	5.07	5.09	5.10	5.11	5.12	5.12	5.13	5.13	5.13	5.14	5.14	5.14
24	3.39	3.76	4.09	4.31	4.48	4.61	4.72	4.81	4.88	4.93	4.96	4.99	5.01	5.02	5.03	5.04	5.04	5.05	5.05	5.05	5.06	5.06	5.06
25	3.31	3.68	4.01	4.23	4.40	4.53	4.64	4.73	4.80	4.85	4.88	4.91	4.93	4.94	4.95	4.96	4.96	4.97	4.97	4.97	4.98	4.98	4.98
26	3.24	3.61	3.94	4.16	4.33	4.46	4.57	4.66	4.73	4.78	4.81	4.84	4.86	4.87	4.88	4.89	4.89	4.90	4.90	4.90	4.91	4.91	4.91
27	3.17	3.54	3.87	4.09	4.26	4.39	4.50	4.59	4.66	4.71	4.74	4.77	4.79	4.80	4.81	4.82	4.82	4.83	4.83	4.83	4.84	4.84	4.84
28	3.11	3.48	3.81	4.03	4.20	4.33	4.44	4.53	4.60	4.65	4.68	4.71	4.73	4.74	4.75	4.76	4.76	4.77	4.77	4.77	4.78	4.78	4.78
29	3.05	3.42	3.75	3.97	4.14	4.27	4.38	4.47	4.54	4.59	4.62	4.65	4.67	4.68	4.69	4.70	4.70	4.71	4.71	4.71	4.72	4.72	4.72
30	3.00	3.37	3.70	3.92	4.09	4.22	4.33	4.42	4.49	4.54	4.57	4.60	4.62	4.63	4.64	4.65	4.65	4.66	4.66	4.66	4.67	4.67	4.67
40	2.87	3.24	3.57	3.79	3.96	4.09	4.20	4.29	4.36	4.41	4.44	4.47	4.49	4.50	4.51	4.52	4.52	4.53	4.53	4.53	4.54	4.54	4.54
60	2.75	3.12	3.45	3.67	3.84	3.97	4.08	4.17	4.24	4.29	4.32	4.35	4.37	4.38	4.39	4.40	4.40	4.41	4.41	4.41	4.42	4.42	4.42
120	2.64	3.01	3.34	3.56	3.73	3.86	3.97	4.06	4.13	4.18	4.21	4.24	4.26	4.27	4.28	4.29	4.29	4.30	4.30	4.30	4.31	4.31	4.31
∞	2.55	2.92	3.25	3.47	3.64	3.77	3.88	3.97	4.04	4.09	4.12	4.15	4.17	4.18	4.19	4.20	4.20	4.21	4.21	4.21	4.22	4.22	4.22

Appendix D-4 : The critical value of F-distribution at the level of significant of 0.05.



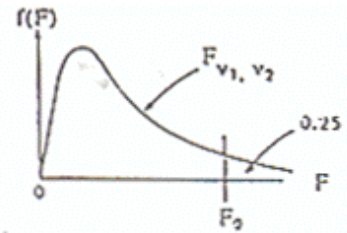
$v_1 \backslash v_2$	1	2	3	4	5	6	7	8	9	10	12	15	20	24	30	40	50	120	∞
1	161.4	199.5	213.7	224.6	230.2	234.0	236.8	238.9	240.5	241.9	243.9	245.9	248.0	249.3	250.1	251.1	252.2	253.3	254.3
2	18.51	19.00	19.16	19.25	19.30	19.33	19.35	19.37	19.38	19.40	19.41	19.43	19.45	19.45	19.46	19.47	19.48	19.49	19.50
3	10.13	9.55	9.28	9.12	9.01	8.94	8.89	8.85	8.81	8.79	8.74	8.70	8.66	8.64	8.62	8.59	8.57	8.55	8.53
4	7.71	6.94	6.59	6.39	6.26	6.16	6.09	6.04	6.00	5.94	5.91	5.86	5.80	5.77	5.75	5.72	5.69	5.66	5.63
5	6.61	5.79	5.41	5.19	5.05	4.95	4.88	4.82	4.77	4.74	4.68	4.62	4.56	4.53	4.50	4.46	4.43	4.40	4.36
6	5.99	5.14	4.76	4.53	4.39	4.28	4.21	4.15	4.10	4.06	4.00	3.94	3.87	3.84	3.81	3.77	3.74	3.70	3.67
7	5.59	4.74	4.35	4.12	3.97	3.87	3.79	3.73	3.68	3.64	3.57	3.51	3.44	3.41	3.38	3.34	3.30	3.27	3.23
8	5.32	4.46	4.07	3.84	3.69	3.58	3.50	3.44	3.39	3.35	3.28	3.22	3.15	3.12	3.08	3.04	3.01	2.97	2.93
9	5.12	4.26	3.86	3.63	3.48	3.37	3.29	3.23	3.18	3.14	3.07	3.01	2.94	2.90	2.86	2.83	2.79	2.75	2.71
10	4.96	4.10	3.71	3.48	3.33	3.22	3.14	3.07	3.02	2.98	2.91	2.85	2.77	2.74	2.70	2.66	2.62	2.58	2.54
11	4.84	3.98	3.59	3.36	3.20	3.09	3.01	2.95	2.90	2.85	2.79	2.72	2.65	2.61	2.57	2.53	2.49	2.45	2.40
12	4.75	3.89	3.49	3.26	3.11	3.00	2.91	2.85	2.80	2.75	2.69	2.62	2.54	2.51	2.47	2.43	2.38	2.34	2.30
13	4.67	3.81	3.41	3.18	3.03	2.92	2.83	2.77	2.71	2.67	2.60	2.53	2.46	2.42	2.38	2.34	2.30	2.25	2.21
14	4.60	3.74	3.34	3.11	2.96	2.85	2.76	2.70	2.65	2.60	2.53	2.46	2.39	2.35	2.31	2.27	2.22	2.18	2.13
15	4.54	3.68	3.29	3.06	2.90	2.79	2.71	2.64	2.59	2.54	2.48	2.40	2.33	2.29	2.25	2.20	2.16	2.11	2.07
16	4.49	3.63	3.24	3.01	2.85	2.74	2.66	2.59	2.54	2.49	2.42	2.35	2.28	2.24	2.19	2.15	2.11	2.06	2.01
17	4.45	3.59	3.20	2.96	2.81	2.70	2.61	2.55	2.49	2.45	2.38	2.31	2.23	2.19	2.15	2.10	2.06	2.01	1.96
18	4.41	3.55	3.16	2.93	2.77	2.66	2.58	2.51	2.46	2.41	2.34	2.27	2.19	2.15	2.11	2.06	2.02	1.97	1.92
19	4.38	3.52	3.13	2.90	2.74	2.63	2.54	2.48	2.42	2.38	2.31	2.23	2.16	2.11	2.07	2.03	1.98	1.93	1.88
20	4.35	3.49	3.10	2.87	2.71	2.60	2.51	2.45	2.39	2.35	2.28	2.20	2.12	2.08	2.04	1.99	1.95	1.90	1.84
21	4.32	3.47	3.07	2.84	2.68	2.57	2.49	2.42	2.37	2.32	2.25	2.18	2.10	2.05	2.01	1.96	1.92	1.87	1.81
22	4.30	3.44	3.05	2.82	2.66	2.55	2.46	2.40	2.34	2.30	2.23	2.15	2.07	2.03	1.98	1.94	1.89	1.84	1.78
23	4.28	3.42	3.03	2.80	2.64	2.53	2.44	2.37	2.32	2.27	2.20	2.13	2.05	2.01	1.96	1.91	1.86	1.81	1.76
24	4.26	3.40	3.01	2.78	2.62	2.51	2.42	2.36	2.30	2.25	2.18	2.11	2.03	1.98	1.94	1.89	1.84	1.79	1.73
25	4.24	3.39	2.99	2.76	2.60	2.49	2.40	2.34	2.28	2.24	2.16	2.09	2.01	1.96	1.92	1.87	1.82	1.77	1.71
26	4.23	3.37	2.98	2.74	2.59	2.47	2.39	2.32	2.27	2.22	2.15	2.07	1.99	1.95	1.90	1.85	1.80	1.75	1.69
27	4.21	3.35	2.96	2.73	2.57	2.46	2.37	2.31	2.25	2.20	2.13	2.06	1.97	1.93	1.88	1.84	1.79	1.73	1.67
28	4.20	3.34	2.95	2.71	2.54	2.45	2.36	2.29	2.24	2.19	2.12	2.04	1.96	1.91	1.87	1.82	1.77	1.71	1.65
29	4.18	3.33	2.93	2.70	2.55	2.43	2.35	2.28	2.22	2.18	2.10	2.03	1.94	1.90	1.85	1.81	1.75	1.70	1.64
30	4.17	3.32	2.92	2.69	2.53	2.42	2.33	2.27	2.21	2.16	2.09	2.01	1.93	1.89	1.84	1.79	1.74	1.68	1.62
40	4.08	3.23	2.84	2.61	2.45	2.34	2.25	2.18	2.12	2.08	2.00	1.92	1.84	1.79	1.74	1.69	1.64	1.58	1.51
60	4.00	3.15	2.76	2.53	2.37	2.25	2.17	2.10	2.04	1.99	1.92	1.84	1.75	1.70	1.65	1.59	1.53	1.47	1.39
120	3.92	3.07	2.68	2.45	2.29	2.17	2.09	2.02	1.96	1.91	1.83	1.75	1.66	1.61	1.55	1.50	1.43	1.35	1.25
∞	3.84	3.00	2.60	2.37	2.21	2.10	2.01	1.94	1.88	1.83	1.75	1.67	1.57	1.52	1.46	1.39	1.32	1.22	1.00

Appendix D-5 : The critical value of F-distribution at the level of significant of 0.10.



$v_1 \backslash v_2$	1	2	3	4	5	6	7	8	9	10	12	15	20	24	30	40	50	120	∞	
1	39.84	49.50	53.57	55.83	57.24	58.29	58.71	59.11	59.44	59.86	60.19	60.71	61.22	61.74	62.00	62.26	62.53	62.79	63.03	63.33
2	8.53	9.00	9.16	9.24	9.29	9.33	9.35	9.37	9.38	9.39	9.41	9.42	9.44	9.44	9.45	9.46	9.47	9.47	9.48	9.49
3	5.54	5.44	5.39	5.34	5.31	5.28	5.27	5.25	5.24	5.23	5.22	5.20	5.18	5.18	5.17	5.16	5.16	5.15	5.14	5.13
4	4.54	4.32	4.19	4.11	4.05	4.01	3.98	3.95	3.94	3.94	3.92	3.90	3.87	3.84	3.83	3.82	3.80	3.79	3.78	3.76
5	4.06	3.78	3.62	3.52	3.45	3.40	3.37	3.34	3.32	3.30	3.27	3.24	3.21	3.19	3.17	3.16	3.14	3.12	3.10	3.08
6	3.75	3.46	3.29	3.18	3.11	3.05	3.01	2.98	2.96	2.94	2.90	2.87	2.84	2.82	2.80	2.78	2.76	2.74	2.72	2.70
7	3.59	3.26	3.07	2.96	2.88	2.83	2.78	2.75	2.72	2.70	2.67	2.63	2.59	2.58	2.56	2.54	2.51	2.49	2.47	2.45
8	3.46	3.11	2.92	2.81	2.73	2.67	2.62	2.59	2.56	2.54	2.50	2.46	2.42	2.40	2.38	2.36	2.34	2.32	2.29	2.27
9	3.34	3.01	2.81	2.69	2.61	2.55	2.51	2.47	2.44	2.42	2.38	2.34	2.29	2.28	2.25	2.23	2.21	2.18	2.16	2.14
10	3.27	2.92	2.73	2.61	2.52	2.46	2.41	2.38	2.35	2.32	2.28	2.24	2.20	2.18	2.16	2.13	2.11	2.08	2.06	2.04
11	3.23	2.86	2.66	2.54	2.45	2.39	2.34	2.30	2.27	2.25	2.21	2.17	2.12	2.10	2.08	2.05	2.03	2.00	1.97	1.95
12	3.18	2.81	2.61	2.48	2.39	2.33	2.28	2.24	2.21	2.19	2.15	2.10	2.06	2.04	2.01	1.99	1.96	1.93	1.90	1.88
13	3.14	2.76	2.56	2.43	2.35	2.28	2.23	2.20	2.16	2.14	2.10	2.05	2.01	1.99	1.96	1.93	1.90	1.88	1.85	1.83
14	3.10	2.73	2.52	2.39	2.31	2.24	2.19	2.15	2.12	2.10	2.05	2.01	1.96	1.94	1.91	1.89	1.86	1.83	1.80	1.78
15	3.07	2.70	2.49	2.36	2.27	2.21	2.16	2.12	2.09	2.06	2.02	1.97	1.92	1.90	1.87	1.85	1.82	1.79	1.76	1.74
16	3.05	2.67	2.46	2.33	2.24	2.18	2.13	2.09	2.06	2.03	1.99	1.94	1.89	1.87	1.84	1.81	1.78	1.75	1.72	1.70
17	3.03	2.64	2.44	2.31	2.22	2.15	2.10	2.06	2.03	2.00	1.96	1.91	1.86	1.84	1.81	1.78	1.75	1.72	1.69	1.67
18	3.01	2.62	2.42	2.29	2.20	2.13	2.08	2.04	2.00	1.98	1.93	1.89	1.84	1.81	1.78	1.75	1.72	1.69	1.66	1.64
19	2.99	2.61	2.40	2.27	2.18	2.11	2.06	2.02	1.98	1.96	1.91	1.86	1.81	1.79	1.76	1.73	1.70	1.67	1.63	1.61
20	2.97	2.59	2.38	2.25	2.16	2.09	2.04	2.00	1.96	1.94	1.89	1.84	1.79	1.77	1.74	1.71	1.68	1.64	1.61	1.59
21	2.96	2.57	2.36	2.23	2.14	2.07	2.02	1.98	1.95	1.92	1.87	1.83	1.78	1.75	1.72	1.69	1.66	1.62	1.59	1.57
22	2.95	2.56	2.35	2.22	2.13	2.06	2.01	1.97	1.93	1.90	1.86	1.81	1.76	1.73	1.70	1.67	1.64	1.60	1.57	1.55
23	2.94	2.55	2.34	2.21	2.11	2.05	1.99	1.95	1.92	1.89	1.84	1.80	1.74	1.72	1.69	1.66	1.62	1.59	1.55	1.53
24	2.93	2.54	2.33	2.19	2.10	2.04	1.98	1.94	1.91	1.88	1.83	1.78	1.73	1.70	1.67	1.64	1.61	1.57	1.53	1.51
25	2.92	2.53	2.32	2.18	2.09	2.02	1.97	1.93	1.89	1.87	1.82	1.77	1.72	1.69	1.66	1.63	1.59	1.56	1.52	1.50
26	2.91	2.52	2.31	2.17	2.08	2.01	1.96	1.92	1.88	1.86	1.81	1.76	1.71	1.68	1.65	1.61	1.58	1.54	1.50	1.48
27	2.90	2.51	2.30	2.17	2.07	2.00	1.95	1.91	1.87	1.85	1.80	1.75	1.70	1.67	1.64	1.60	1.57	1.53	1.49	1.47
28	2.89	2.50	2.29	2.16	2.06	2.00	1.94	1.90	1.87	1.84	1.79	1.74	1.69	1.66	1.63	1.59	1.56	1.52	1.48	1.46
29	2.89	2.50	2.28	2.15	2.06	1.99	1.93	1.89	1.86	1.83	1.78	1.73	1.68	1.65	1.62	1.58	1.55	1.51	1.47	1.45
30	2.88	2.49	2.28	2.14	2.05	1.98	1.93	1.89	1.85	1.82	1.77	1.72	1.67	1.64	1.61	1.57	1.54	1.50	1.46	1.44
40	2.84	2.44	2.23	2.09	2.00	1.93	1.87	1.83	1.79	1.76	1.71	1.66	1.61	1.57	1.54	1.51	1.47	1.42	1.38	1.36
60	2.77	2.39	2.18	2.04	1.95	1.87	1.82	1.77	1.74	1.71	1.66	1.60	1.54	1.51	1.48	1.44	1.40	1.35	1.29	1.27
120	2.75	2.35	2.13	1.99	1.90	1.82	1.77	1.72	1.68	1.65	1.60	1.55	1.48	1.45	1.41	1.37	1.32	1.26	1.19	1.17
∞	2.71	2.30	2.08	1.94	1.85	1.77	1.72	1.67	1.63	1.60	1.55	1.49	1.42	1.38	1.34	1.29	1.24	1.17	1.10	1.08

Appendix D-6 : The critical value of F-distribution at the level of significant of 0.25.



$v_1 \backslash v_2$	1	2	3	4	5	6	7	8	9	10	12	15	20	24	30	40	50	120	∞	
1	5.03	7.50	8.20	8.58	8.82	8.98	9.10	9.19	9.26	9.32	9.37	9.41	9.44	9.47	9.50	9.53	9.55	9.57	9.58	9.59
2	2.57	3.00	3.15	3.23	3.28	3.31	3.34	3.35	3.37	3.38	3.39	3.41	3.43	3.43	3.44	3.45	3.46	3.47	3.47	3.48
3	2.02	2.25	2.36	2.39	2.41	2.42	2.43	2.44	2.44	2.44	2.45	2.46	2.46	2.46	2.47	2.47	2.47	2.47	2.47	2.47
4	1.81	2.00	2.05	2.06	2.07	2.08	2.08	2.08	2.08	2.08	2.08	2.08	2.08	2.08	2.08	2.08	2.08	2.08	2.08	2.08
5	1.69	1.85	1.88	1.89	1.89	1.89	1.89	1.89	1.89	1.89	1.89	1.89	1.89	1.89	1.89	1.89	1.89	1.89	1.89	1.89
6	1.62	1.76	1.78	1.79	1.79	1.78	1.78	1.78	1.77	1.77	1.77	1.76	1.76	1.75	1.75	1.75	1.74	1.74	1.74	1.74
7	1.57	1.70	1.72	1.72	1.71	1.71	1.70	1.70	1.70	1.69	1.68	1.68	1.67	1.67	1.66	1.66	1.65	1.65	1.65	1.65
8	1.54	1.66	1.67	1.66	1.66	1.65	1.64	1.64	1.63	1.63	1.62	1.62	1.61	1.60	1.60	1.59	1.59	1.58	1.58	1.58
9	1.51	1.62	1.63	1.63	1.62	1.61	1.60	1.60	1.59	1.59	1.58	1.57	1.56	1.56	1.55	1.54	1.54	1.53	1.53	1.53
10	1.49	1.60	1.60	1.59	1.59	1.58	1.57	1.56	1.56	1.55	1.54	1.53	1.52	1.52	1.51	1.51	1.50	1.49	1.48	1.48
11	1.47	1.58	1.58	1.57	1.56	1.55	1.54	1.53	1.53	1.52	1.51	1.50	1.49	1.47	1.48	1.47	1.47	1.46	1.45	1.45
12	1.46	1.56	1.56	1.55	1.54	1.53	1.52	1.51	1.51	1.50	1.49	1.48	1.47	1.46	1.45	1.45	1.44	1.43	1.42	1.42
13	1.45	1.55	1.55	1.53	1.52	1.51	1.50	1.49	1.49	1.48	1.47	1.46	1.45	1.44	1.43	1.42	1.42	1.41	1.40	1.40
14	1.44	1.53	1.53	1.52	1.51	1.50	1.49	1.48	1.47	1.46	1.45	1.44	1.43	1.42	1.41	1.41	1.40	1.39	1.38	1.38
15	1.43	1.52	1.52	1.51	1.49	1.48	1.47	1.46	1.46	1.45	1.44	1.43	1.41	1.41	1.40	1.39	1.38	1.37	1.36	1.36
16	1.42	1.51	1.51	1.50	1.48	1.47	1.46	1.45	1.44	1.44	1.43	1.41	1.40	1.39	1.38	1.37	1.36	1.35	1.34	1.34
17	1.42	1.51	1.50	1.49	1.47	1.46	1.45	1.44	1.43	1.43	1.41	1.40	1.39	1.38	1.37	1.36	1.35	1.34	1.33	1.33
18	1.41	1.50	1.49	1.48	1.46	1.45	1.44	1.43	1.42	1.42	1.40	1.39	1.38	1.37	1.36	1.35	1.34	1.33	1.32	1.32
19	1.41	1.49	1.49	1.47	1.46	1.44	1.43	1.42	1.41	1.41	1.40	1.38	1.37	1.36	1.35	1.34	1.33	1.32	1.31	1.31
20	1.40	1.49	1.48	1.47	1.45	1.44	1.43	1.42	1.41	1.40	1.39	1.37	1.36	1.35	1.34	1.33	1.32	1.31	1.29	1.29
21	1.40	1.48	1.48	1.46	1.44	1.43	1.42	1.41	1.40	1.39	1.38	1.37	1.35	1.34	1.33	1.32	1.31	1.30	1.28	1.28
22	1.40	1.48	1.47	1.45	1.44	1.42	1.41	1.40	1.39	1.39	1.37	1.36	1.34	1.33	1.32	1.31	1.30	1.29	1.28	1.28
23	1.39	1.47	1.47	1.45	1.43	1.42	1.41	1.40	1.39	1.38	1.37	1.35	1.34	1.33	1.32	1.31	1.30	1.28	1.27	1.27
24	1.39	1.47	1.46	1.44	1.43	1.41	1.40	1.39	1.38	1.38	1.36	1.35	1.33	1.32	1.31	1.30	1.29	1.28	1.26	1.26
25	1.39	1.47	1.46	1.44	1.42	1.41	1.40	1.39	1.38	1.37	1.36	1.34	1.33	1.32	1.31	1.29	1.28	1.27	1.25	1.25
26	1.38	1.46	1.45	1.44	1.42	1.41	1.39	1.38	1.37	1.37	1.35	1.34	1.32	1.31	1.30	1.29	1.28	1.26	1.25	1.25
27	1.38	1.46	1.45	1.43	1.42	1.40	1.39	1.38	1.37	1.36	1.35	1.33	1.32	1.31	1.30	1.28	1.27	1.26	1.24	1.24
28	1.38	1.46	1.45	1.43	1.41	1.40	1.39	1.38	1.37	1.36	1.34	1.33	1.31	1.30	1.29	1.28	1.27	1.25	1.24	1.24
29	1.38	1.45	1.45	1.43	1.41	1.40	1.38	1.37	1.36	1.35	1.34	1.32	1.31	1.30	1.29	1.27	1.26	1.25	1.23	1.23
30	1.38	1.45	1.44	1.42	1.41	1.39	1.38	1.37	1.36	1.35	1.34	1.32	1.30	1.29	1.28	1.27	1.26	1.24	1.23	1.23
40	1.36	1.44	1.42	1.40	1.39	1.37	1.36	1.35	1.34	1.33	1.31	1.30	1.28	1.26	1.25	1.24	1.22	1.21	1.19	1.19
60	1.35	1.42	1.41	1.38	1.37	1.35	1.33	1.32	1.31	1.30	1.29	1.27	1.25	1.24	1.22	1.21	1.19	1.17	1.15	1.15
120	1.34	1.40	1.39	1.37	1.35	1.33	1.31	1.30	1.29	1.28	1.26	1.24	1.22	1.21	1.19	1.18	1.16	1.13	1.10	1.10
∞	1.32	1.39	1.37	1.35	1.33	1.31	1.29	1.28	1.27	1.25	1.24	1.22	1.19	1.18	1.16	1.14	1.12	1.08	1.00	1.00

VITA

Miss Vichaya Vichayapai Bunnag was born in Bangkok, Thailand on May 27, 1976. She graduated at secondary school level from St. Joseph Convent School in 1992 and high school level from Triam Udom Suksa School in 1994. In 1998, she received a Bachelor Degree of Chemical Engineering from Chulalongkorn University. After graduation, she immediately pursues her graduate study for a Master's Degree in Chemical Engineering at the Department of Chemical Engineering, Faculty of Engineering, Chulalongkorn University.



สถาบันวิทยบริการ
จุฬาลงกรณ์มหาวิทยาลัย